Comprehensive Progress Report

MASTER

Contract AT(11-1)3380

U. S. Department of Energy
Division of Biology and Medicine
Washington 25, D. C.

Project Title:	The Tumorigenic Action of Beta, Proton, Alpha and Electron Radiation on the Rat Skin
Institution:	Department of Environmental Medicine The New York University College of Medicine 550 First Avenue New York, N.Y. 10016
Principal Investigator:	Fredric J. Burns, Ph.D.
Co-Investigator:	Roy E. Albert, M.D.
Period Covered by Proposal:	August 1, 1976 through January 31, 1980

DISCLAIMER

Technical Scope Summary

Rat skin is being utilized as a model system for studying dose and time related aspects of the oncogenic action of ionizing radiation, ultraviolet light and polycyclic aromatic hydrocarbons. Molecular lesions in the DNA of the epidermis, including, strand breaks and thymine dimers, are being measured and compared to the temporal and dose related aspects of tumor induction. The induction and repair kinetics of molecular lesions are being compared to split dose recovery as modified by sensitizers and type of radiation of oncogenic damage.

Summary

Tumor induction is being studied in rat skin exposed to various types, doses, and dose rates of ionizing radiation and different doses and wavelengths of ultraviolet light. Molecular lesions, such as, strand breaks and thymine dimers, in the epidermal DNA will be measured and related to the radiation dose. The ability of the cells to repair or remove the molecular damage to the DNA will be compared to the ability to remove oncogenic damage to split dose experiments. Skin will be exposed to argon-40 ions so that a determination can be made whether breaks induced in epidermal DNA by high linear energy transfer (LET) radiation are repaired differently than breaks induced in the same tissue by low LET radiation. A theory of how the temporal and dose related aspects of tumor induction by single doses of radiation can be utilized to predict the outcome of long term chronic exposure will be tested by giving multiple daily or weekly exposures to electrons. Sensitizers that interact with DNA in specific ways or modify split dose recovery for endpoints other than tumor induction will be utilized in an attempt to determine whether molecular lesions in DNA are good indicators of radiation dose relevant to oncogenesis, and whether split dose recovery for cell lethality

has the same dose and temperature dependence as split dose recovery for tumor induction. The induction and removal of pyrimidine dimers in epidermal DNA is to be related to the carcinogenic action of ultraviolet light. The repair of DNA strand breaks will be measured in the epidermis of rats and related to age and proliferation rate of the basal cells.

Comprehensive Progress Report

Rat skin has proved to be a remarkably sensitive and reproducible model for studying the mechanism of radiation carcinogenesis and for formulating ideas that could lead to improved estimates of risk in radiation protection calculations. Studies of the shape of the dose-response curve (1), the effect of spatial distribution of dose (2, 3, 4), the effect of the time pattern (5, 6), and the importance of the density of energy deposition (7, 8) on the induction of skin tumors has led to important insights into radiation carcinogenesis. Whether tumor incidence is proportional to the amount of tissue irradiated was studied by irradiating rat skin in grid and sieve patterns of various pore sizes with electrons, protons and low energy X-rays. A consistent finding was the localized dose patterns were less oncogenic than uniform patterns for low linear energy transfer (LET) radiation, electrons (2) and X-rays (4), but not for high LET protons (9). It was estimated from geometrical considerations that the interaction distance between irradiated and unirradiated tissue was approximately 170 microns and mice are less sensitive than rats (10).

It was found that tumor yield was not dependent on the growth phase of hair follicles at the time of irradiation, although the growing follicle consisted of about ten times as

many cells as the resting follicle (14). When radiation penetrated sufficiently to reach the entire growing phase follicle, the number of tumors produced was not significantly greater than that observed in resting-phase skin. It was shown that radiation must penetrate to a depth of about 0.3 mm into the skin in order to induce tumors (3). The follicular stem cells may be the primary targets for oncogenesis, however, selective irradiation at 0.3 mm, the position of the stem cells, did not produce tumors. Secondary factors, such as gross tissue injury or epidermal depopulation may be required for full expression of the potential to induce cancer (11).

Skin is capable of repairing much of the radiation induced damage that leads to the formation of tumors (5, 6). Recovery of oncogenic damage from electron radiation occurred within 24 hours as demonstrated with split dose irradiation (5, 6). Our recent experiments indicate that the halftime of recovery or repair is between 2 and 3 hours (12, 13). A comparable degree of recovery was found for the carcinogenic effect of protons despite the fact that protons are more oncogenic than electrons (RBE about 2.0-2.4) (8).

The temporal aspects of tumor induction in rat skin are well documented (3). Tumors begin to appear after a latent period of about 20 weeks, and they continue to appear at a reasonably constant rate for up to 90 weeks which is a

substantial portion of lifetime. The guarantee time or minimum latent period does not depend significantly on dose except possibly at very high doses.

Growth and Induction Kinetics of Radiation-Induced Rat Skin Tumors

Following a single dose of ionizing radiation to rat skin tumors first begin to appear between 15 and 40 weeks and continue to appear for periods up to 80 weeks which represents a significant fraction of the rat's lifespan (Figure 1). There are two general possibilities to explain this pattern. Either the late appearing tumors began growing long after the irradiation or the late tumors were slowly growing tumors which began to grow at the time of irradiation. If the radiation-induced tumors were growing so slowly that a significant portion of the rat's lifespan was necessary for them to grow from onset to a detectable size, then the growth process itself must be taken into account when assessing the carcinogenic potency of a given radiation dose. The present study was undertaken to determine the growth patterns of radiation-induced tumors in rat skin and to assess the effect of growth rate on the appearance kinetics.

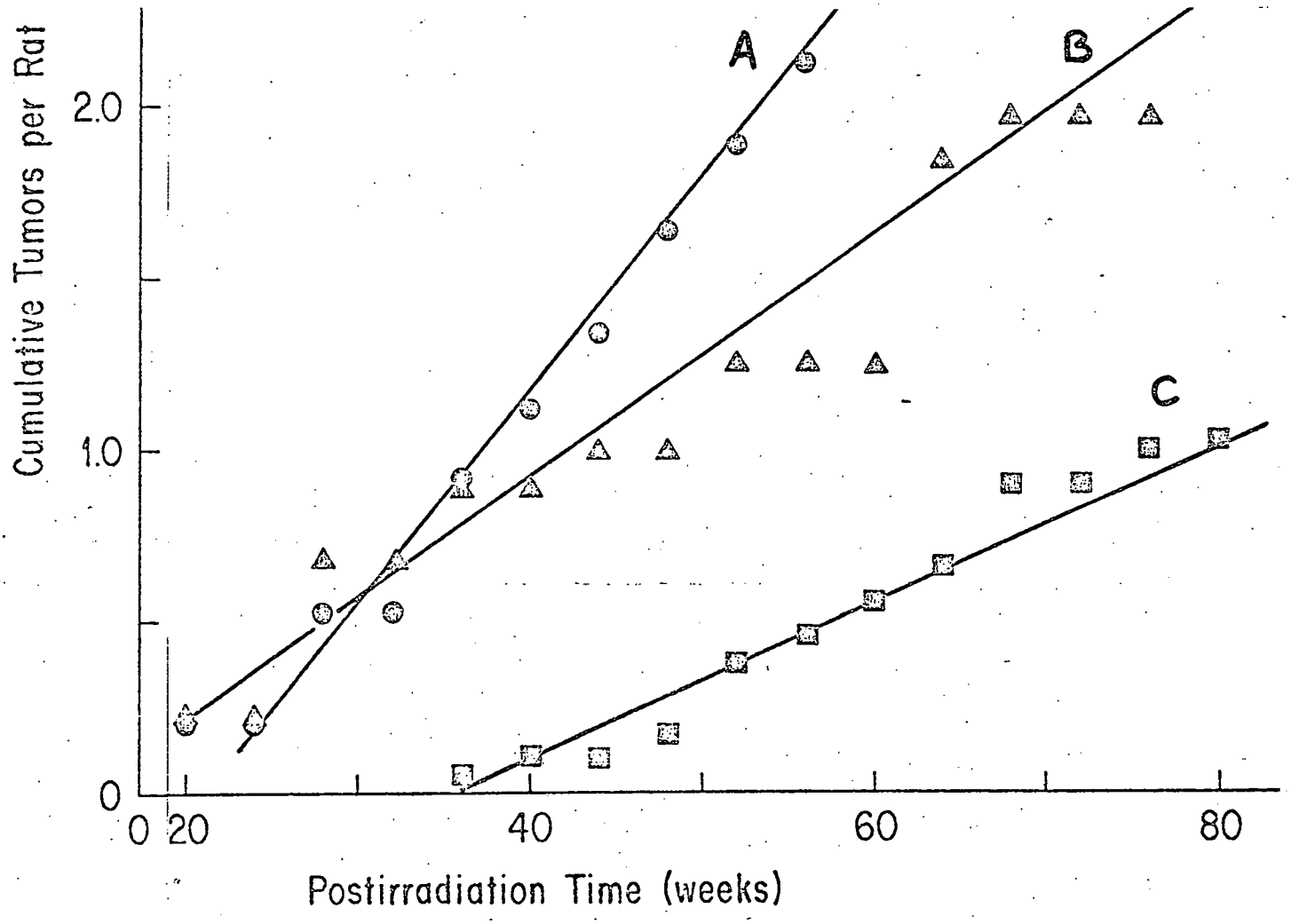

Figure 1. The yield of tumors in rat skin as a function of elapsed time after electron radiation. A, B and C refer to high dose (2200 rads), intermediate dose (1500 rads) and low dose (1100 rads) respectively.

Results and Discussion of the Model

A scorable tumor must be visible to the naked eye which means it must be on the order of 1.0 mm in diameter. A sphere 1.0 mm in diameter could contain as many as 10^6 cells and if

the tumors start as a single cell many doubling times must transpire between the initial cell and the scorable tumor. Tumors were induced with single electron doses from 1500 rads to 6000 rads. Tumor diameters were measured from photographs made every 4 weeks. A computerized least squares procedure was devised which allowed Gompertz functions to be fitted to the experimental growth data.

The growth curves of 153 tumors were analyzed. The Gompertz function was chosen from several functions that might fit the growth data because it has been used in several tumor growth systems (15, 16). The Gompertz function is generated by assuming that the specific growth rate decreases exponentially with an exponential constant that is referred to as the retardation constant.

The Gompertz function requires the evaluation of 3 independent parameters and is therefore sufficiently flexible that any growth curve where the specific growth rate is decreasing in a regular manner can be fitted reasonably well (17). Some examples of the fit of Gompertz functions to experimental growth data are shown in Figure 2. All but 6 of the tumors had growth curves that could be described reasonably well with the Gompertz function. The 6 nonfitting tumors either showed regression, size reduction, or a sudden increase in growth rate.

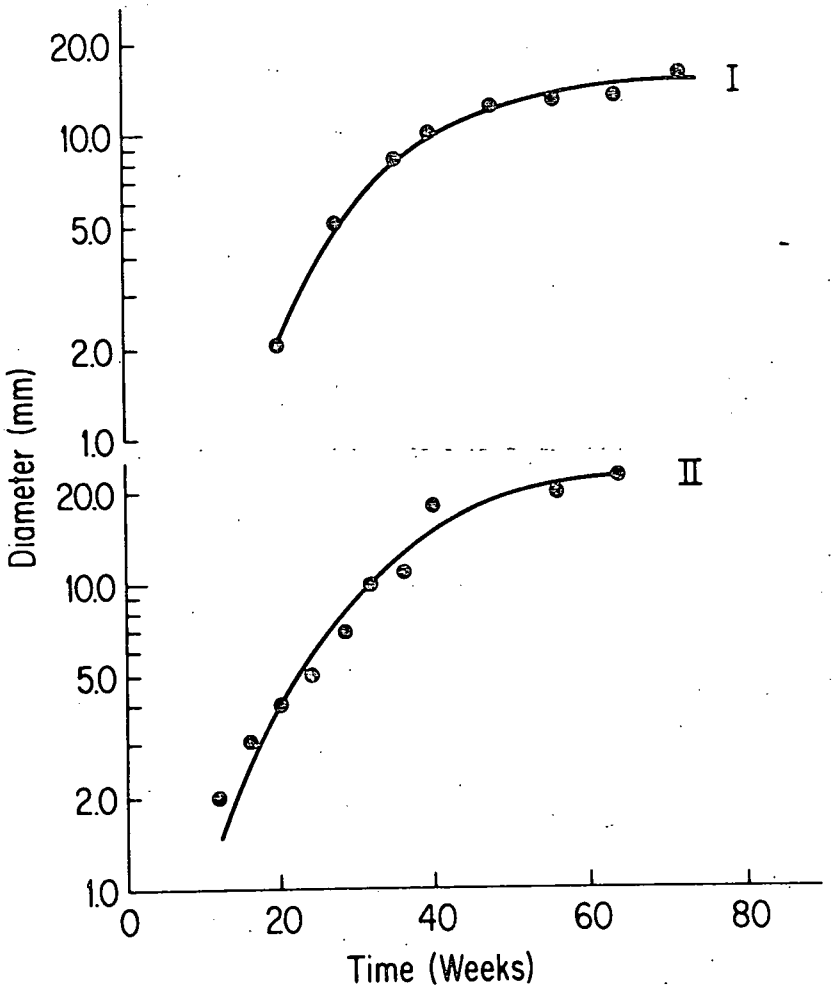

Figure 2. Typical growth curves of radiation-induced rat skin tumors.

The three parameters required for each growth curve are: (1) A, the growth rate at a diameter of 1.0 mm, (2) α, the retardation constant and (3) V_o, the initial tumor size. For simplicity the latter was assumed to be one cell. Values for A and α were determined for each tumor. The results for A are shown in Figure 3. All analyses were made in terms of tumor diameter.

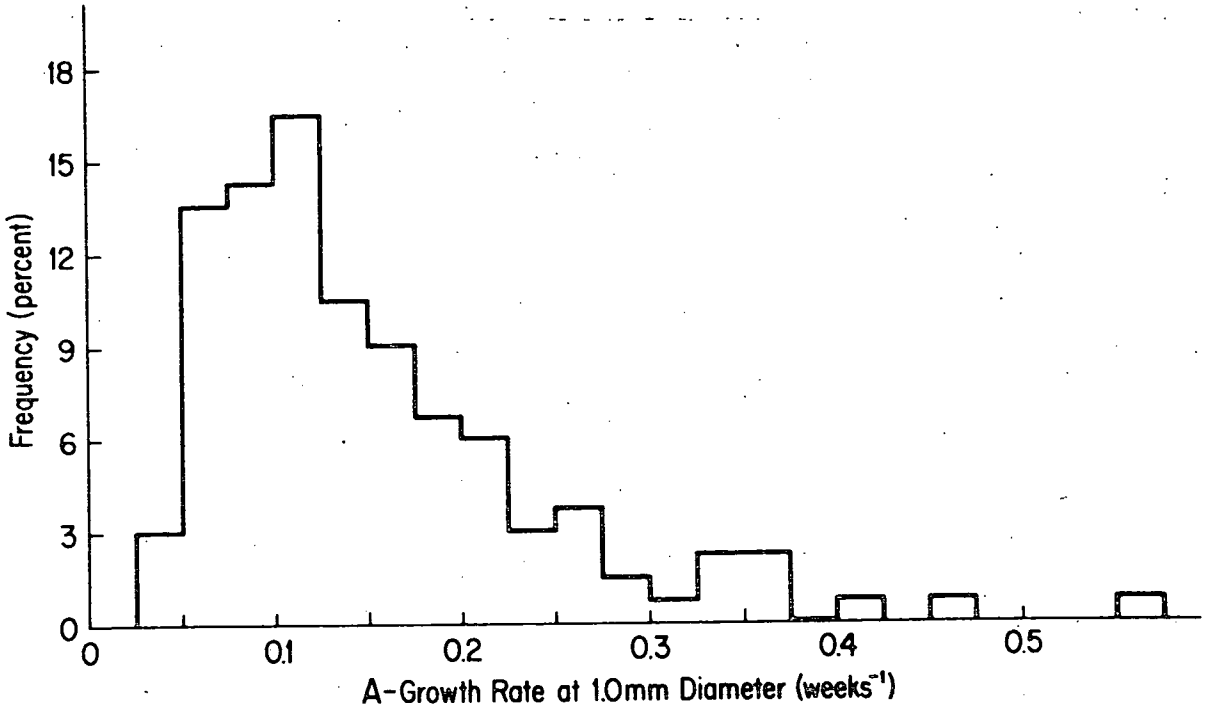

Figure 3. Frequency distribution of growth rates of radiation-induced rat skin tumors.

The lack of tumors with growth rates less than 0.025 $weeks^{-1}$ is probably an artifact because below that value even in the absence of retardation there would be insufficient time in the experiment for growth to a detectable size. Only 5% of the tumors have an A value greater than 0.3 $week^{-1}$ which represents a diameter doubling time of 2.3 week and volume doubling time, assuming a spherical shape, of about 6 days. The median value of A was 0.15 per week with a standard deviation of 0.12 $week^{-1}$.

Figure 4 shows the retardation constants. Approximately

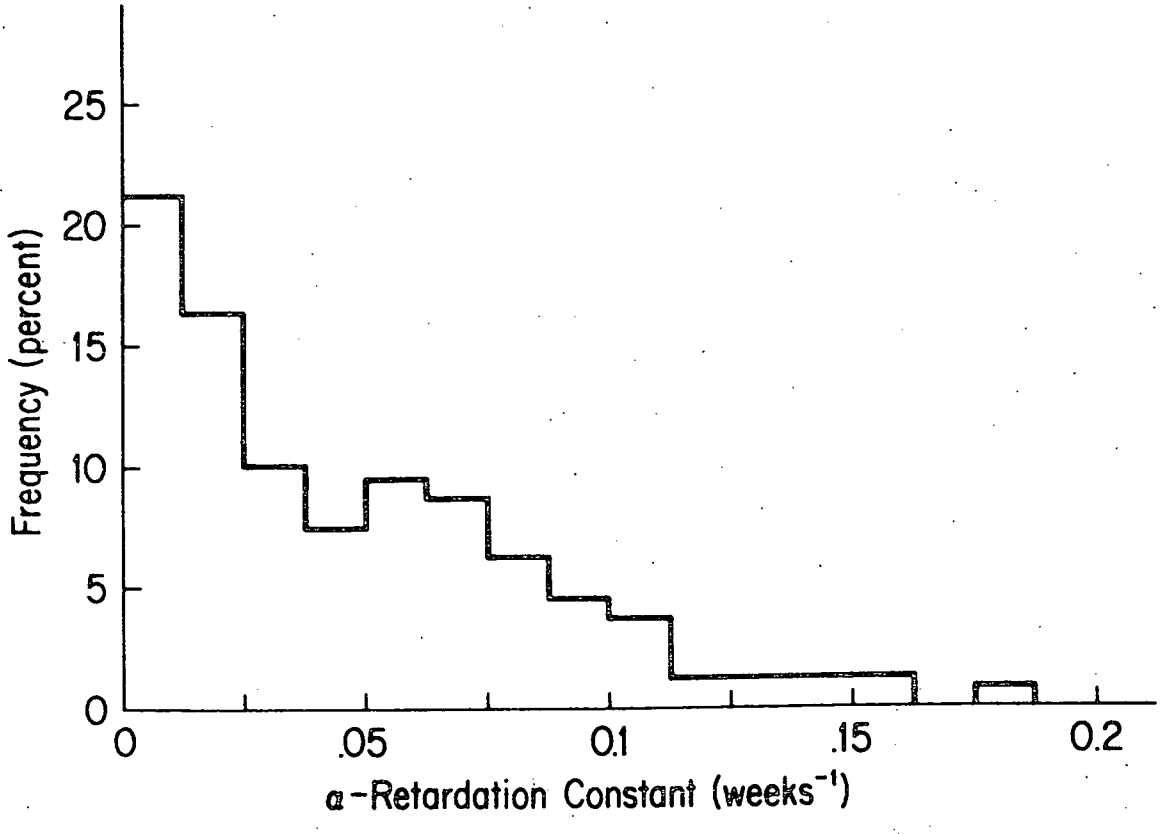

Figure 4. Frequency distribution of Gompertz retardation constants for radiation-induced rat skin tumors.

22% of the tumors have α values below 0.013 week^{-1}. Such tumors are essentially unretarded and growing exponentially. More than 50% of the tumors show significant retardation, i.e., α values greater than 0.025 week^{-1}.

Figure 5 shows a plot of A vs. α for all the tumors.

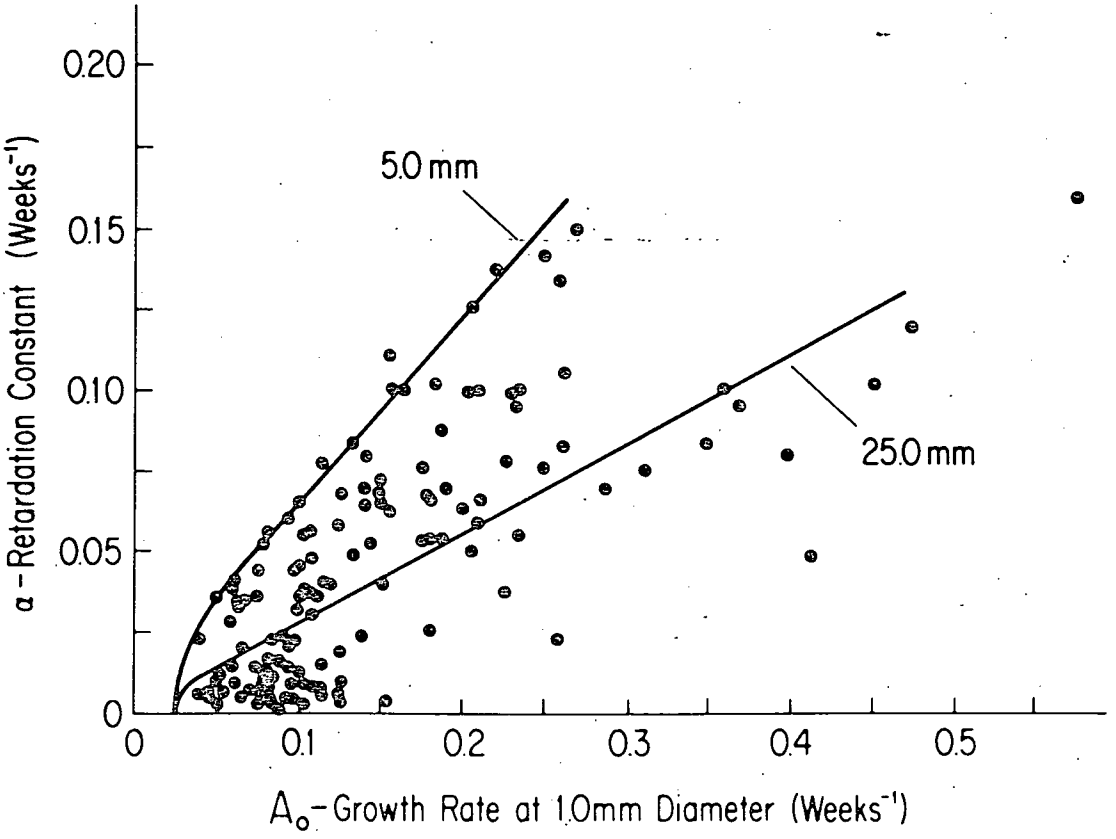

Figure 5. Scatter diagram of growth rate and retardation constant for 153 radiation-induced rat skin tumors. Curves show combination of α and A that will produce tumors with asymptotic diameters as indicated.

Asymptotic size is well defined mathematically although its biological significance is less clear. A number of tumors actually reached measurable asymptotes mostly less than 10.0 mm. The lines on the left and right represent A and α values for an asymptotic sizes of 5.0 mm and 25.0 mm, respectively. The absence of points in the region less than 5.0 mm is probably an experimental artifact since growth curves are difficult to measure for small tumors close to their asymptote. While the scatter of points in Figure 5 is substantial, there is clearly an absence of tumors with rapid exponential growth, i.e., A values greater than 0.15 $week^{-1}$. Large α values tend to be associated with large A values.

With the tumor growth characteristics as described, a model was constructed to determine how growth rate of tumors would be expressed in the time-incidence curves. Experimentally, the cumulative tumors per rat data can be represented by a linear function with a slope equal to the rate of tumor appearance and a time intercept that varies slowly with dose.

Figure 6 shows the time intercepts from a number of experiments as a function to dose. The time intercept has a value of about 40 weeks at doses less than 2500 rads. At higher doses, the time intercept decreases to about 20 weeks.

In contrast to the time-intercept, the slope was extremely dose-dependent. As shown in Figure 7, a log plot of slope versus

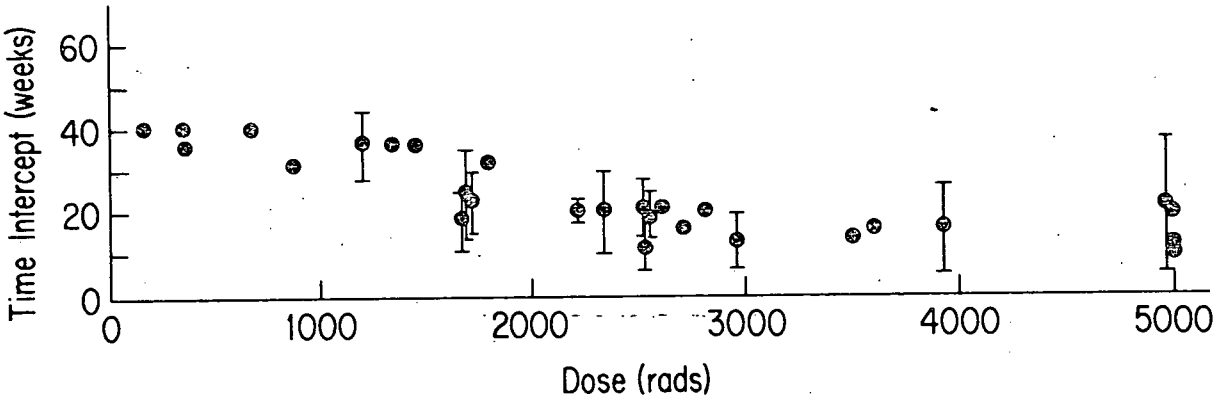

Figure 6. Extrapolation values of the temporal onset curves for tumors induced by ionizing radiation as a function of dose.

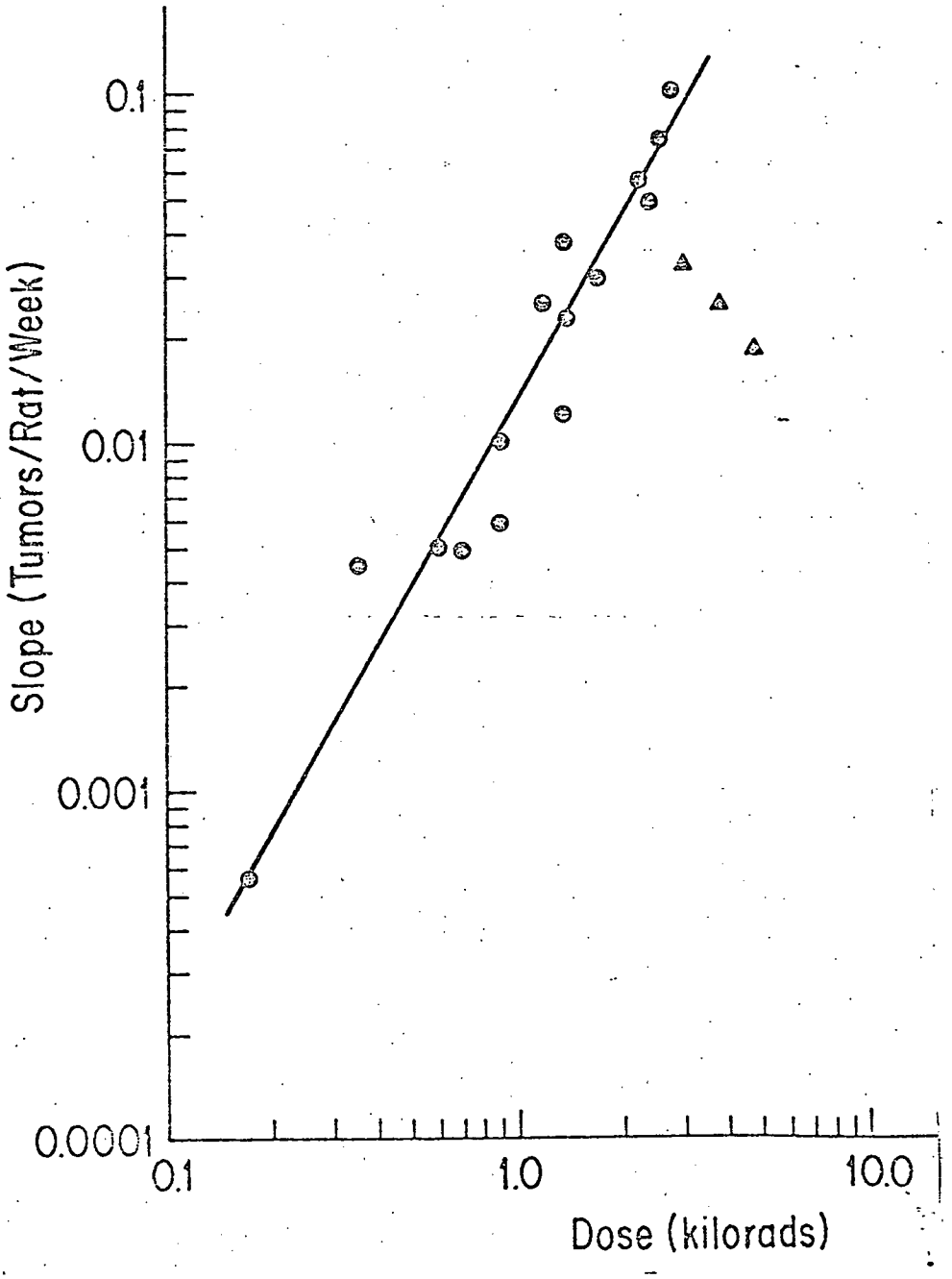

Figure 7. A log-log plot of rate of tumor appearance on rat skin as a function of dose of electron radiation.

dose, the slope increased as about the 1.7th power of dose up to about 3000 rads. Above 3000 rads the slope decreased, presumably, as a result of the lethal effect of the radiation.

The tumor growth data is not sufficiently precise to permit a calculation of the true one cell inception times of the tumors. Let us assume for the moment that all the tumors actually began to grow at the time of irradiation. This assumption is not contradicted by the growth data in the present experiment, however, its proof will require growth data at much earlier stages of tumor development.

It is convenient to define the concept of growth time as the time required for a tumor to grow from its initial inception (assumed to be one cell) to a detectable size. Based on the relatively broad distributions found for A and α, it can be assumed that the growth time distribution would be an extremely broad function.

If all the tumors start growing at time zero, it can be shown that the slope of the tumors per rat versus time function equals the value of the growth time function at the corresponding point in time. If the slope of the tumors per rat curve is in fact a constant, the growth time function must be rectangular with a low time cut off at the time intercept which must represent the time for the fastest growing tumor to reach detectability. The existence of an upper time cut off has not

been established experimentally up through 80 weeks. No upper cut off suggests there may be many slowly growing microtumors in the skin. The height of the rectangular growth time function could be used as a measure of the magnitude of the tumor response. If an upper cut off exists, the height is proportional to the total number of tumors, whereas if there is no upper cut off, i.e., lifespan is the effective upper cut off, then the height is proportional to number of tumors per lifespan.

Age-Dependence of the Oncogenicity of Ionizing Radiation in Rat Skin

Evidence obtained from surveys of the atomic bomb survivors indicate that those people irradiated early in life (< 14 years) have a higher relative risk of leukemia and tumor induction than those irradiated later in life (18, 19). The relation of age to the life-shortening effects of radiation (much of which has been attributed to the induction of neoplasms) has been investigated in rodents (20) and, in general, susceptibility to life-shortening declines with increasing age at irradiation. The experiment at induction of neoplasms is likewise affected by age at irradiation. While some exceptions exist, resistance to radiation-induced tumors is usually greater in adult than in juvenile rodents (21).

Age dependent changes in tumor induction after administration of chemical carcinogens by several routes has been studied in a number of strains of mice (22, 23, 24). In

one series of experiments (25, 26, 27), skin from young and old syngeneic donors were grafted onto young recipients and then treated with a chemical carcinogen. Results showed that susceptibility to the carcinogen decreased from young to middle ages but increased in senescent animals. Other age dependent changes in the studies on the induction of skin tumors after chemical carcinogens are conflicting, demonstrating either a decreased carcinogenic susceptibility with age (28, 29) or no change (30). Because age sensitivity at the time of exposure is of practical importance in formulating age related exposure limits and because age-related differences in sensitivity may provide clues as to the nature of the target for oncogenesis, without the conflicting effect of changing of drug metabolizing enzyme activity with age (31), we have investigated the age dependence of tumor induction in the rat skin system (32) with x-radiation.

Male albino rats, CD strain from the Charles River Breeding Farms, Brookline, Massachusetts, were irradiated at 0 (newborns), 28, 57, or 99 days of age. All animals were selected in the resting phase of the hair growth cycle.

Newborn animals were irradiated with surface doses of 500, 1000, 1500, 2250 and 3000 rads of a 20 KVP Grenz ray at a dose rate of 880 R/min. At this operating voltage the half value layer in aluminum was 25 μm. The 28, 57, and 99 day

old animals were irradiated with surface doses of 1000, 2000, 3000, 4000 and 5000 rads of a 35 KVP Grenz ray at a dose rate of 265 R/min. At this operating voltage the half value layer in aluminum was 38 μm. Dose measurements were made with a parallel plate ionization chamber.

Irradiations were carried out by anesthetizing the animals with an I.P. injection of 25 mg/kg sodium pentobarbital. The animals were placed in a box and the dorsal skin surface was exposed through an opening in a metal plate. In order to ensure that an equivalent number of hair follicles were irradiated in the different age groups, the area irradiated was increased in proportion to the growth of the animals' skin. The growth of the skin was estimated by calculating the 2/3 power of the ratio of the weight at sacrifice to the weight of irradiation. The maximum area of dorsal skin which could be irradiated in the newborn age group was 25% of the area irradiated in the other age groups. Newborn animals also have a 2.5 times greater follicle density than the other age group animals. Therefore, the tumor incidences were multiplied by a factor of 1.52 in order to take into account these differences.

After irradiation the rats were observed weekly for 4 weeks in order to follow the initial progress of the acute skin damage. Thereafter, the rats were observed for both acute skin damage and tumor formation every 6 weeks for 70 weeks.

At death, or at the end of the experiment, each lesion was examined histologically.

The acute response of animals to X-ray radiation consisted of blanching of the skin, suppression of hair growth and desquamation, followed by ulceration in the higher dose groups. The maximum percentage of animals showing ulceration after irradiation (11-21 days) as a function of surface dose is shown in Figure 8.

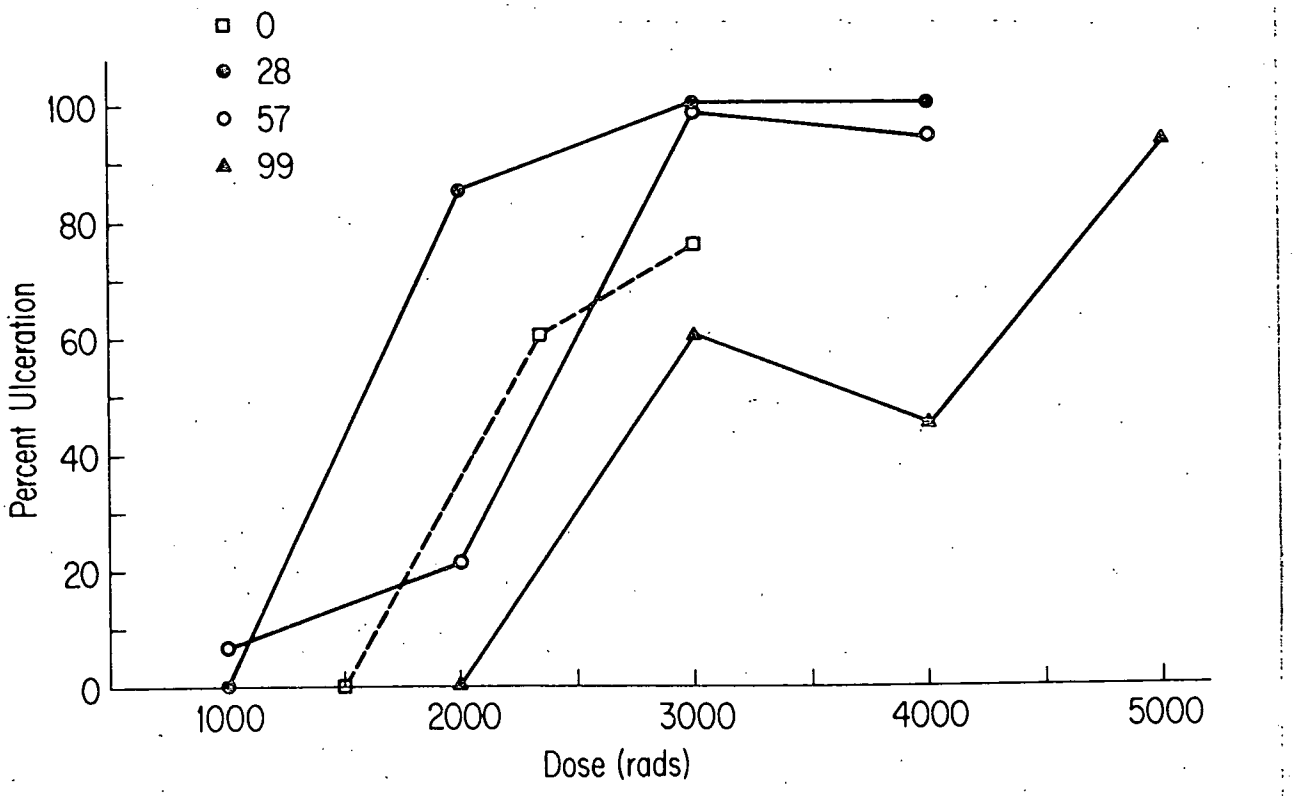

Figure 8. The greatest amount of skin ulceration in rats expressed as percentage of the irradiated skin involved as a function of radiation dose for various ages in days 0, 28, 57, or 99 as indicated.

The 28 day old animals were most sensitive and the 99 day old animals were most resistant to the radiation. Newborn and 57 day old animals showed an intermediate response.

The maximum percentage of animals with ulceration after 3000 rads of radiation as a function of postirradiation time is shown in Figure 9.

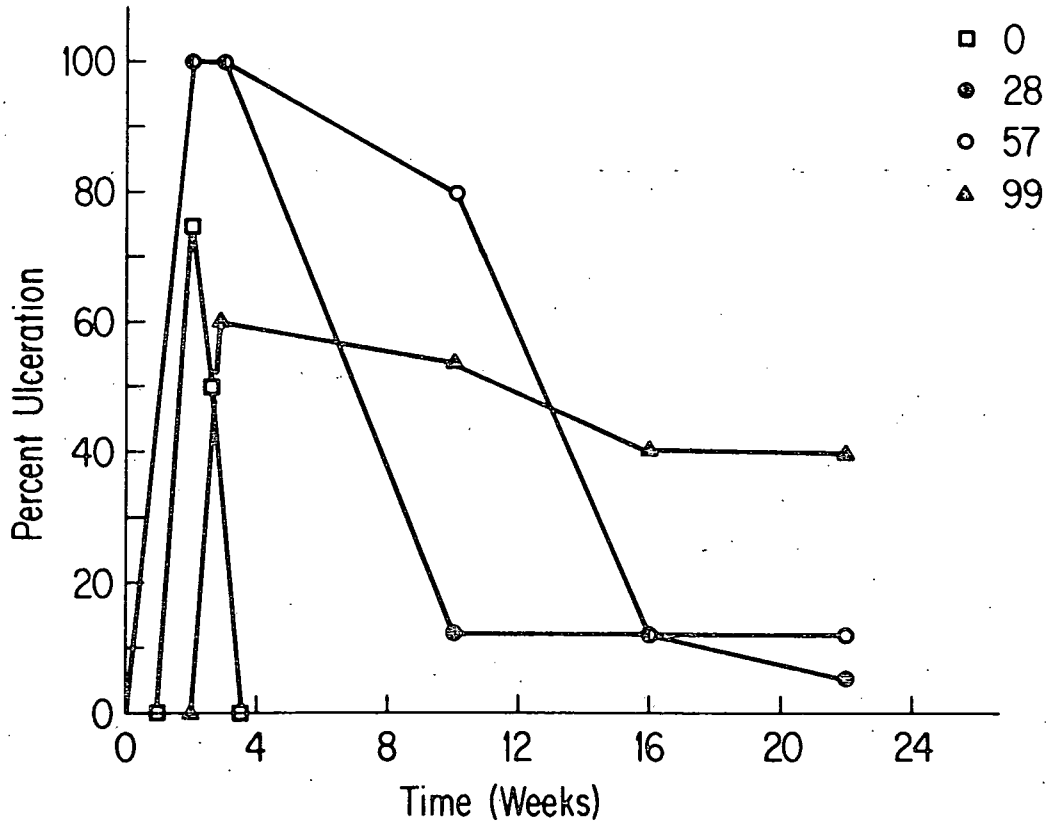

Figure 9. The amount of skin ulceration in rats as a function of time after 3000 R of x-irradiation for various ages in days 0, 28, 57, or 99 as indicated.

The time required for the disappearance of ulceration was shortest in the newborns and increased dramatically with increasing age. This is also seen in Figure 10, which shows that the time to heal

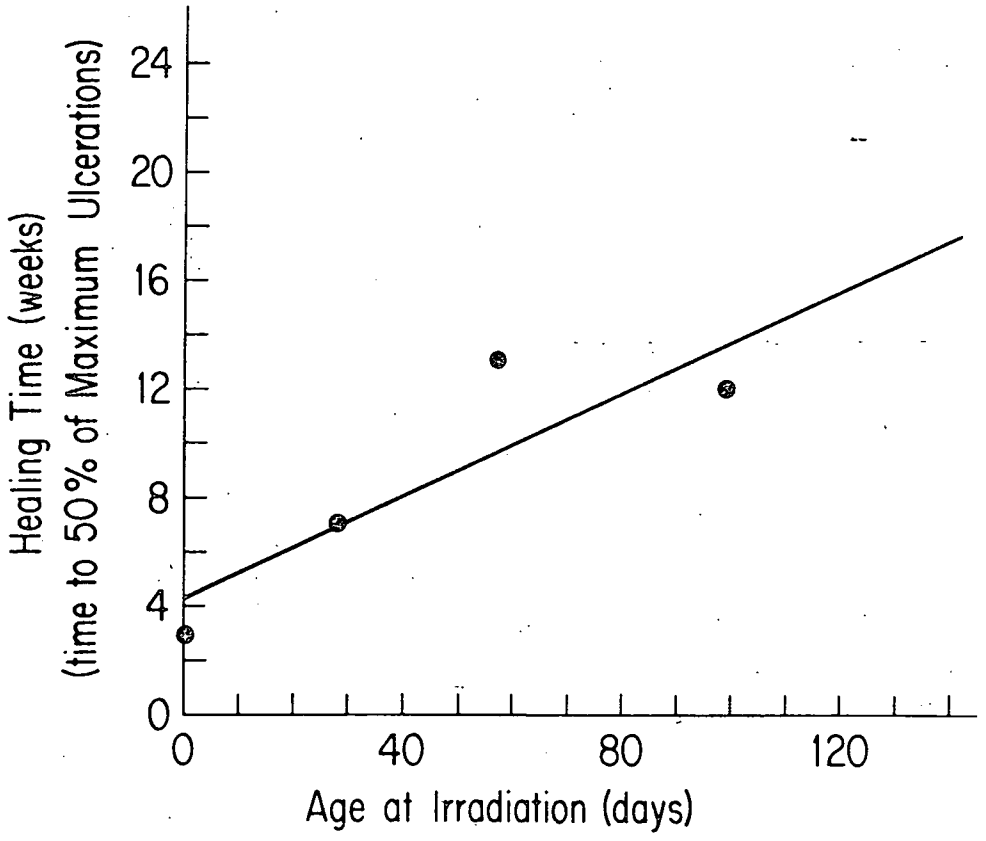

Figure 10. The healing rate of skin ulceration for a x-radiation dose of 3000 R as a function of age at time of irradiation.

50% of the maximum percent ulceration increases in proportion to age at the time of irradiation. Thus, while older animals

were able to withstand a larger radiation dose before skin breakdown, once ulceration had occurred, their capacity for wound healing was limited.

The tumor yield as a function of time is shown in Figure 11 for each of the age groups after exposure to

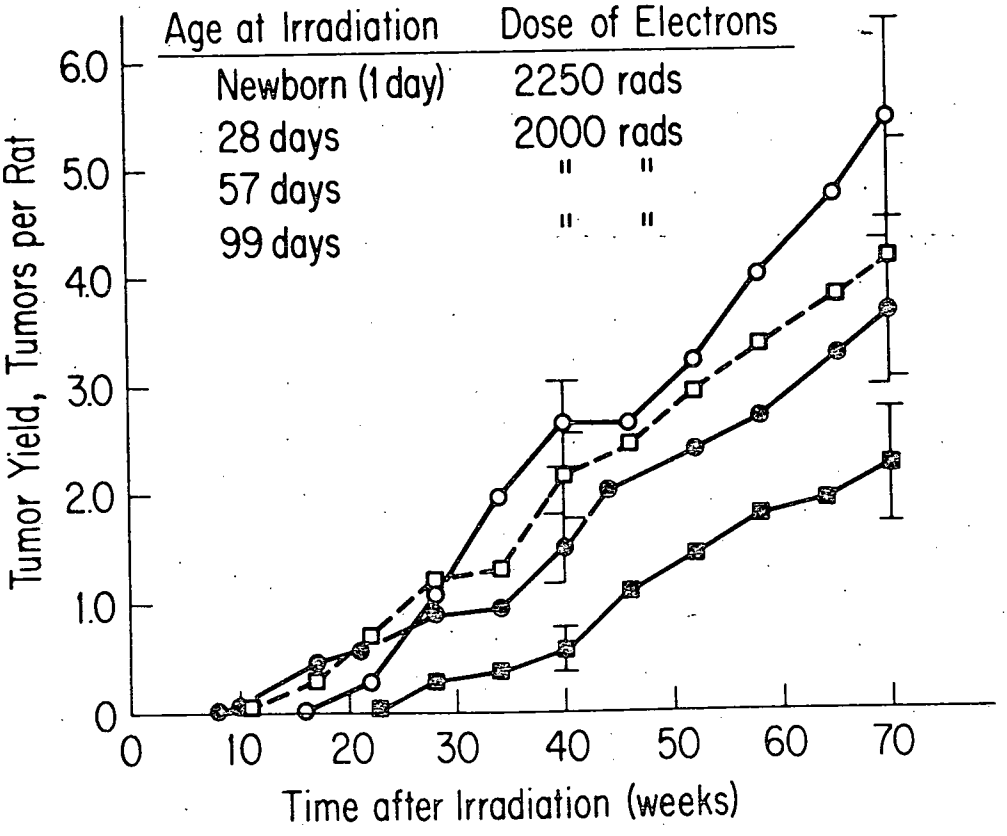

Figure 11. The yield of tumors in rat skin as a function of time after various doses of x-irradiation as indicated.

2000 rads of X-ray radiation. The newborn animals were the most sensitive and the 99 day old animals were the least sensitive with a general trend of decreasing carcinogenic susceptibility with increasing age. The time to the appearance of first tumor was between 10 and 40 weeks, was independent of age, but decreased with increasing dose of radiation.

Figure 12 shows the tumor yield at 70 weeks

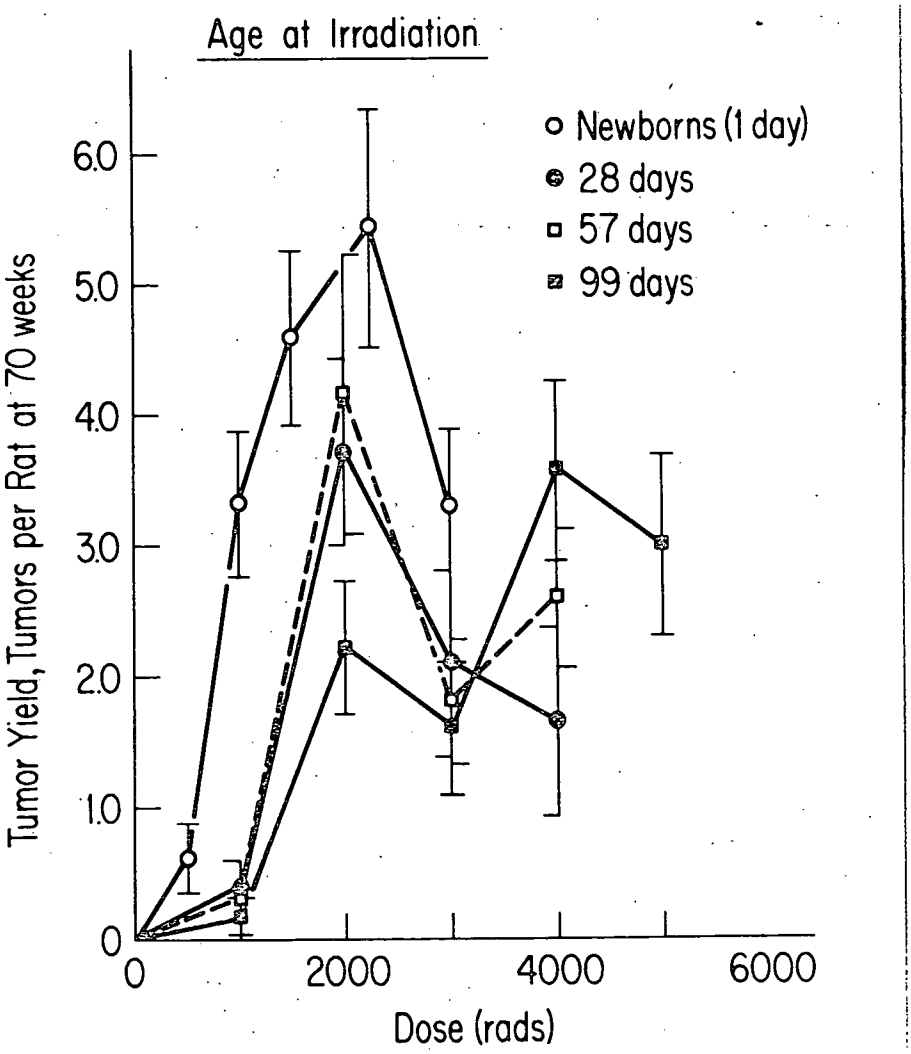

Figure 12. The yield of rat skin tumors at 70 weeks after x-irradiation as a function of dose for various ages at the time of irradiation as indicated.

as a function of dose for each of the age groups. The ascent to peak tumor yield is most rapid in newborn animals and declines with increasing age. The height of the tumor yield peak decreases with age between newborns and 99 day old animals. The tumor yield also appears to shift to higher doses with increasing age.

We have observed a general increase in radio-resistance with age for both the acute and oncogenic responses, consistent with the atomic bomb survival data, and also with data on the experimental induction of tumors. Concomitantly, the ability to heal radiation-induced ulceration declines with increasing age. This also agrees with observations, in skin and tissues, that the capacity for wound healing declines with age (33).

By examining age related susceptibility to x-radiation over abroad range of doses, we have eliminated several of the problems previously associated with studies of these types. First, possible differences in carcinogen metabolism with age are not a problem in our system. In light of the fact that the ability to initiate adaptive changes in tissue enzyme levels after environmental insults declines with age for many enzyme systems (31), it remains to be shown whether tissue levels of carcinogen metabolizing enzymes, i.e., aryl hydrocarbon hydroxylase, change with age. Secondly, by studying the age

related effect over a range of doses, we have eliminated the possibility that an arbitrary choice of a single dose might detect different effects which could be similarly associated with age. As can be seen in Figure 12 at 2000 rads, the trend is towards decreasing carcinogenic susceptibility with age, while at 4000 rads, the opposite trend could be inferred. Finally, our results cannot be explained by differences in effective dose to the hair follicle (2, 3) as adjustments were made for age related changes in follicle density, and no detectable differences in follicle depth could be detected between the newborns and 200 day old animals.

Induction of Skin Tumors in the Rat by Single Exposure to Ultraviolet Radiation

Attempts to study the mechanism of UV oncogenesis experimentally have been hampered somewhat by the lack of a model in which tumors could be induced with a single exposure. The induction of tumors in mouse skin usually requires multiple doses large enough to produce tissue damage (34, 35). The sarcoma is the most common tumor type observed in the mouse when the UV penetrates sufficiently to irradiate dermal cells, whereas squamous cell carcinomas and mixed tumors of epidermal origin occur more frequently when the exposure is limited mostly to the epidermis (36). The hairless mouse was utilized for studies of UV oncogenesis (37), 38) because of its thin stratum corneum

and absence of hair. In this animal 280-320 nm UV induced predominately squamous cell carcinomas rather than sarcomas. Malignant melanomas have also been induced by UV irradiation of chemically induced benign lesions in pigmented hairless mice (39). Ultraviolet radiation can act to initiate tumors that are brought out by promotion with a chemical, such as, croton oil (40, 41).

The oncogenic wavelengths have been determined to be between 280 nm and 320 nm, with the 280 to 320 nm range being most effective (42, 40). Recent evidence suggests that UV can act as a complete carcinogen following exposure to a single ulcerating exposure in the wavelength range 275-375 nm (43).

Previous experience in our laboratory has shown that rat skin is a sensitive system for tumor induction studies with ionizing radiation. This information prompted us to investigate the oncogenic dose-response relationship for exposure of rat skin to UV.

Male CD-1 rats obtained from Charles River Company, Brookline, Massachusetts, were housed two per cage and fed Purina Lab Chow and water ad libitum. The rats were irradiated unanesthetized at 28 days of age in the telogen phase of hair growth after the hair was removed with electric clippers from 15 cm^2 of dorsal skin.

The 275-375 nm UV source was a series of four Westinghouse FS20 fluorescent sun lamps with a spectral range of 275-375 nm and peak output at 313 nm. The exposure rate was 5.0-5.8 J/m^2/sec. at 25 cm measured with an International Light IL570 photometer and PT171C vacuum photodiode detector with NB297 interference filter. The source of 254 nm UV was four Westinghouse G36T6L Sterilamps (medium pressure mercury lamps) emitting only negligible amounts of UV at wavelengths other than 254 nm. The exposure rate was 15.6 J/m^2/sec. at 30 cm measured with the above described photometer and detector with NB254 interference filter.

The protocol was designed to define the dose response relation for single exposures to 275-375 nm UV source in the dose range 0.80×10^4 J/m^2 to 25.2×10^4 J/m^2, and to 254 nm UV in the dose range of 0.08×10^4 J/m^2 to 26.0×10^4 J/m^2. Two groups of animals were exposed to multiple weekly exposures to the 275-375 nm UV to investigate the effect of fractionation. One of these groups received 0.42×10^4 J/m^2 per week for a 20 week period for a total dose of 8.4×10^4 J/m^2 and the other received 2.1×10^4 J/m^2 per week for a 12 week period for a total dose of 25.2×10^4 J/m^2.

Observations

The skin was observed every six weeks and photographs were taken of each lesion when it was first observed and periodically

thereafter. The tumor yield in each observation interval was calculated as the average incidence rate of new tumors in the interval. In any given six week interval, if there were L animals at the start of the interval, N new tumors occurred, and D animals died during the time interval, then the tumor appearance rate was calculated as N/(L-D/2). The cumulative yield at a given time after irradiation was the sum of the rates in all preceding intervals. Sketches of tumor location were made from the photographs so that each tumor could be identified, assigned a time of appearance, and examined histologically at the time of death.

The experiments were terminated at 70 weeks postirradiation and all surviving rats were sacrificed for histological samples and to obtain skin samples from which epithelial whole mounts could be prepared by overnight incubation in 0.5% crude trypsin at $4^{o}C$. After incubation the epidermis and hair follicles were removed from the dermis, fixed in formalin, and stained with hematoxylin and eosin, as described previously (3). The mean number of surviving hair follicles per cm^2 was then determined microscopically.

The transmission of UV through the rat epidermis was measured in order to estimate the fraction of the incident radiation that reached the basal cell layer. The epidermis was removed by means of the hot-cold separation technique of Marrs

and Voorhees (44). The procedure consisted of immersing the depilated, surgically removed dorsal skin in 55°C water followed immediately by an ice water bath. The epidermis was separated from the dermis and an epidermal sheet 3 cm^2 was transferred carefully with a blunt scalpel onto a sheet of Parafilm. The epidermal sheet was suspended over an opening in a lucite holder that was inserted into a quartz cuvette. The transmission spectrum of the epidermis was determined between 240 nm and 400 nm with a Gilford 250 spectrophotometer.

Erythema was observed 24 to 48 hours after irradiation and desquamation occurred at 5 days after irradiation. Ulceration became apparent at 8 days in the two highest exposure groups (12.6×10^4 and 25.2×10^4 J/m^2) of the 275-375 nm UV. The ulcers subsequently healed and formed scar tissue. The 254 nm UV produced a less severe reaction than the 275-375 nm UV for the same exposure. For 254 nm UV ulceration did not occur and erythema and desquamation were observed only at the highest exposure (26×10^4 J/m^2).

The cumulative tumor yield as a function of time post-irradiation is shown in Figure 13 for 254 nm UV (UVC) and in Figure 14 for 275-375 nm UV (UVAB). After a tumor free latent period of 10 to 30 weeks the tumor yield (tumors/rat) increased steadily throughout the experiment (70 weeks). A small percentage ($\sim$ 5%) of the tumors regressed spontaneously for both types of

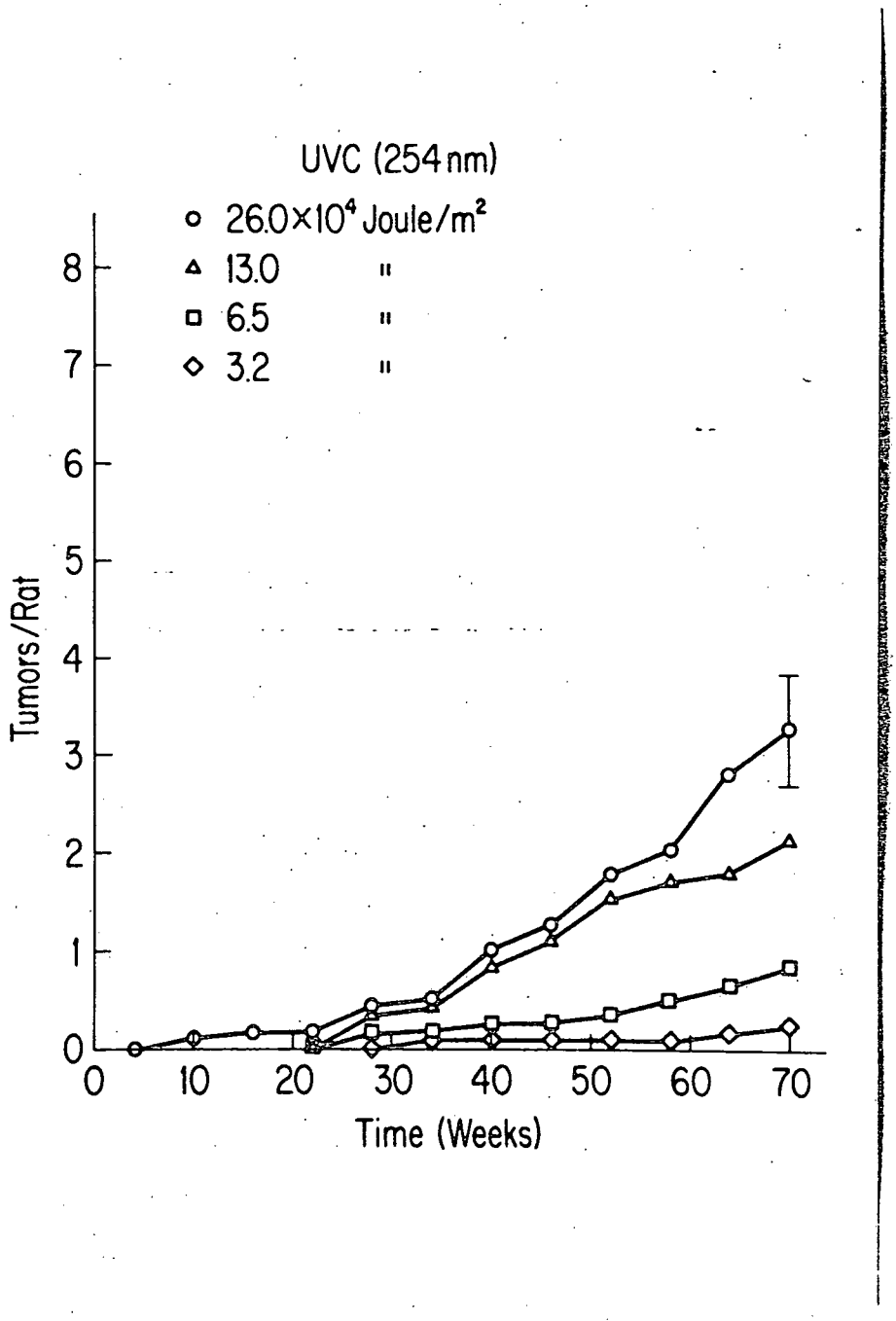

Figure 13. Cumulative tumor yield versus time after doses of UVC (254 nm) radiation as indicated.

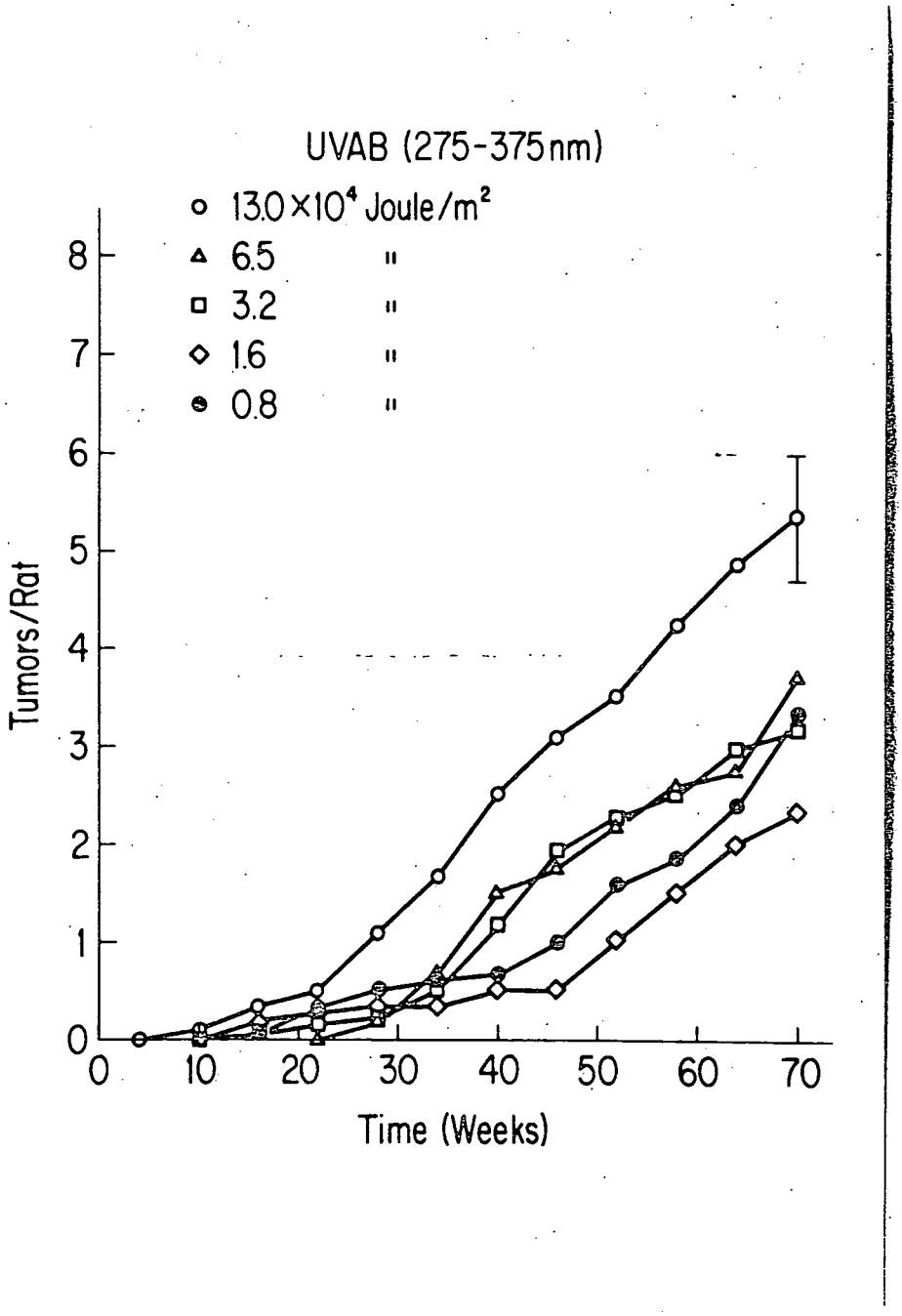

Figure 14. Cumulative tumor yield versus time after doses of UVAB radiation as indicated

UV exposure. The tumors were distributed among the rats as a Poisson distribution which is expected if multiple tumors on the same animal are independent of one another. The survival at the end of the experiment was 87% and varied between 75% and 92% for separate experimental groups.

The cumulative tumor yield at 70 weeks as a function of surface dose is shown in Figure 15 for both types of UV. The error bars represent standard deviations estimated from the square root of the total number of tumors observed in each group. The 275-375 nm UV tumor yield was about 3 tumors/rat at the lowest dose administered and remained within a relatively narrow range (2.4-5.4) throughout the entire dose range covering a factor of 30. The 254 nm UV produced a tumor yield that was approximately proportional to dose throughout the dose range 0.65×10^4 to 26×10^4 J/m^2, although no tumors were observed at 0.32×10^4 J/m^2 and lower. Therefore, the dose-response curves for the two types of UV were distinctly different in shape.

When the 275-375 nm UV was fractionated into 12 weekly fractions of 2.1×10^4 J/m^2 each (total - 25.2×10^4 J/m^2), the tumor yield was equivalent to that produced when the dose was administered in a single exposure of 25.2×10^4 J/m^2. However, when the 275-375 nm UV was fractionated into 20 weekly fractions of 0.42×10^4 J/m^2 (total - 8.4×10^4 J/m^2), the tumor yield

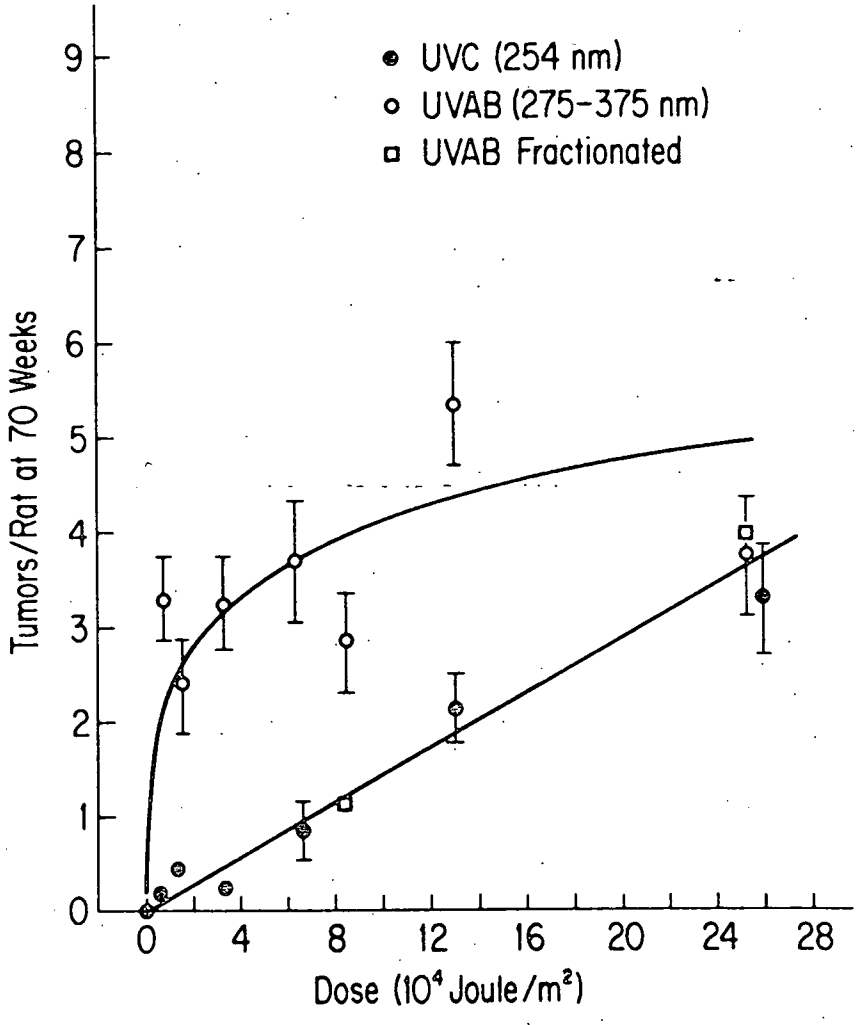

Figure 15. Cumulative tumor yield at 70 weeks after UV irradiation ± standard deviation versus dose. the fractionated exposures were performed with UVAB (275-375 nm). The curves shown were drawn by eye to represent the trend of the data.

was about 50% of that produced by a single exposure to 8.4 x 10^4 J/m^2. Thus, fractionation reduced the oncogenic effectiveness at the lower dose, but not at the higher dose.

The lesions observed in this study were composed of multilayered squamous epithelium usually surrounding a central noncellular keratotic plug. In later stages of growth, the lesions became large and crateriform and were similar, though not identical, to keratoacanthomas found in human skin. In early stages of growth, the lesions resembled epidermoid cysts but differed from cysts in that the epithelial lining was multilayered and irregular. Further, the lesions progressed to a stage of partial involution and in some cases exuded their contents. A nearly identical lesion induced in hamster skin by UV exposure (45) has been designated keratoacanthoma. While this term is descriptively accurate its use may be confusing because it is often used to refer to a human tumor with similar characteristics. To avoid this problem, we prefer to designate the lesions observed in the present study keratoacanthoma-like tumors or keratoacanthomatoids.

Follicle survival at 70 weeks following exposure to 275-375 nm UV is shown in Figure 16 as a function of dose. The standard errors of the mean of five to seven animals are shown. Control values were 24.5 $\pm$ 1.6 follicles/mm^2. A consistent

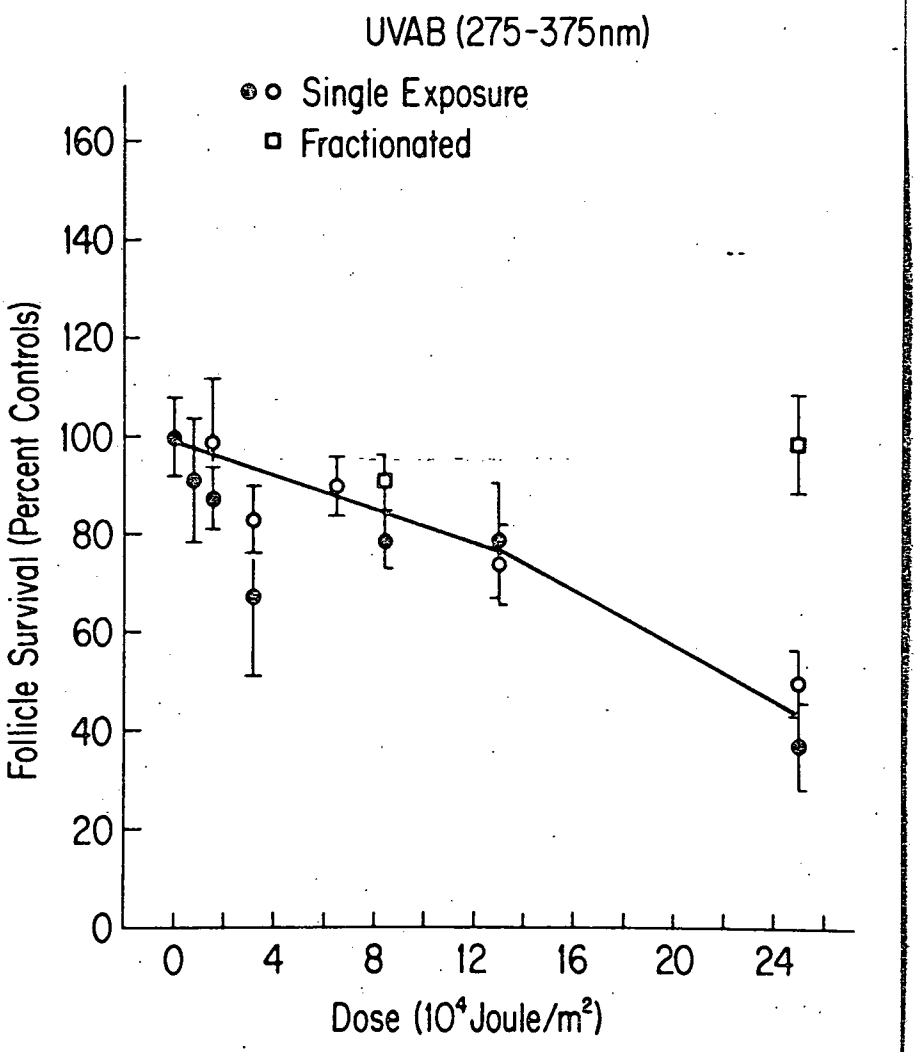

Figure 16. Follicle survival at 70 weeks after UVAB irradiation ± standard error versus dose. Open and closed circles represent two separate experiments. The curve shown was drawn by eye to represent the trend of the data.

decrease in follicle survival was observed with increasing dose over the dose range investigated. At the highest dose of 25 x $10^4 J/m^2$, follicle survival was 40% of controls. A curve for fractionated 275-375 nm UV is also shown in Figure 16, and no decrease in survival was observed in these dose groups, even at the highest dose tested. Follicle survival following exposure to 275 nm UV was also measured, and no decrease in survival was observed over the dose range tested (0 to 25 x 10^5 J/m^2).

The average UV transmission spectrum determined spectrophotometrically for five samples of rat skin epidermis is shown in Figure 17. The low level of transmission in the 240 to 280 nm range is presumably caused by nucleic acid and protein absorption at these wavelengths. Above 280 nm the transmission increased steadily with wavelength and at 300 nm the UV transmission to the basal cell layer was 15%; whereas at 254 nm the transmission was 3% of surface dose.

Discussion

These experiments demonstrate quantitative tumor dose-response relationships for single UV exposures on rat skin. The oncogenic response to 275-375 nm UV confirms previously reported evidence in mouse skin (43) that these wavelengths can cause skin tumors following a single exposure. The experiments reported here also demonstrate that 254 nm UV causes skin tumors following a single exposure.

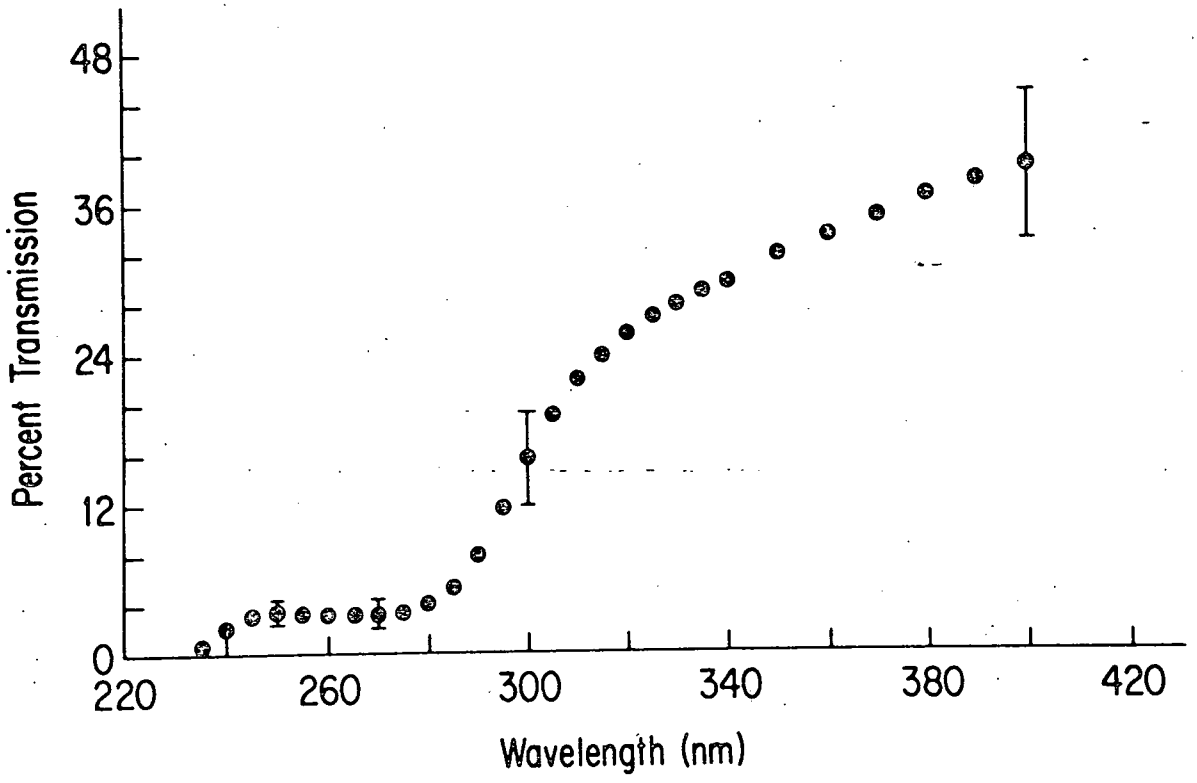

Figure 17. Average UVR transmission spectrum for five samples of rat skin epidermis (± standard error) expressed as percentage of incident UVR dose.

Tumors occurred at subulcerating doses following either 275-375 nm UV or 254 UV in contrast to the previous report which suggests that the dose must be great enough to produce significant tissue damage (43). Our study demonstrates that tumor induction can occur following a dose of UV that produced only erythema as an acute response. In the present study, new tumors continued to appear throughout the life of the animals also in contrast to the previous observation (43) that the appearance rate of new tumors declined after 28 weeks.

The shape of the 275-375 nm UV dose response curve is of interest because it implies that oncogenesis and cell lethality may be in competition. The abrupt increase in tumor yield at low doses and the relatively constant yield for a broad range of higher doses could mean that opposing tendencies are nearly in balance (44). If cell killing is occurring throughout a broad dose range, the resulting cell survival curve would decline slowly as is suggested by the follicle survival data presented in Figure 16 (40% of controls at 25×10^4 J/m^2). Cell survival curves of this type would be expected to produce a tumor dose response curve that remains constant if the tumors are produced initially in proportion to dose. When the follicle survival data are used to approximate UV induced tissue destruction, a follicle-corrected tumor dose response relation is generated as shown in Figure 18. In performing the

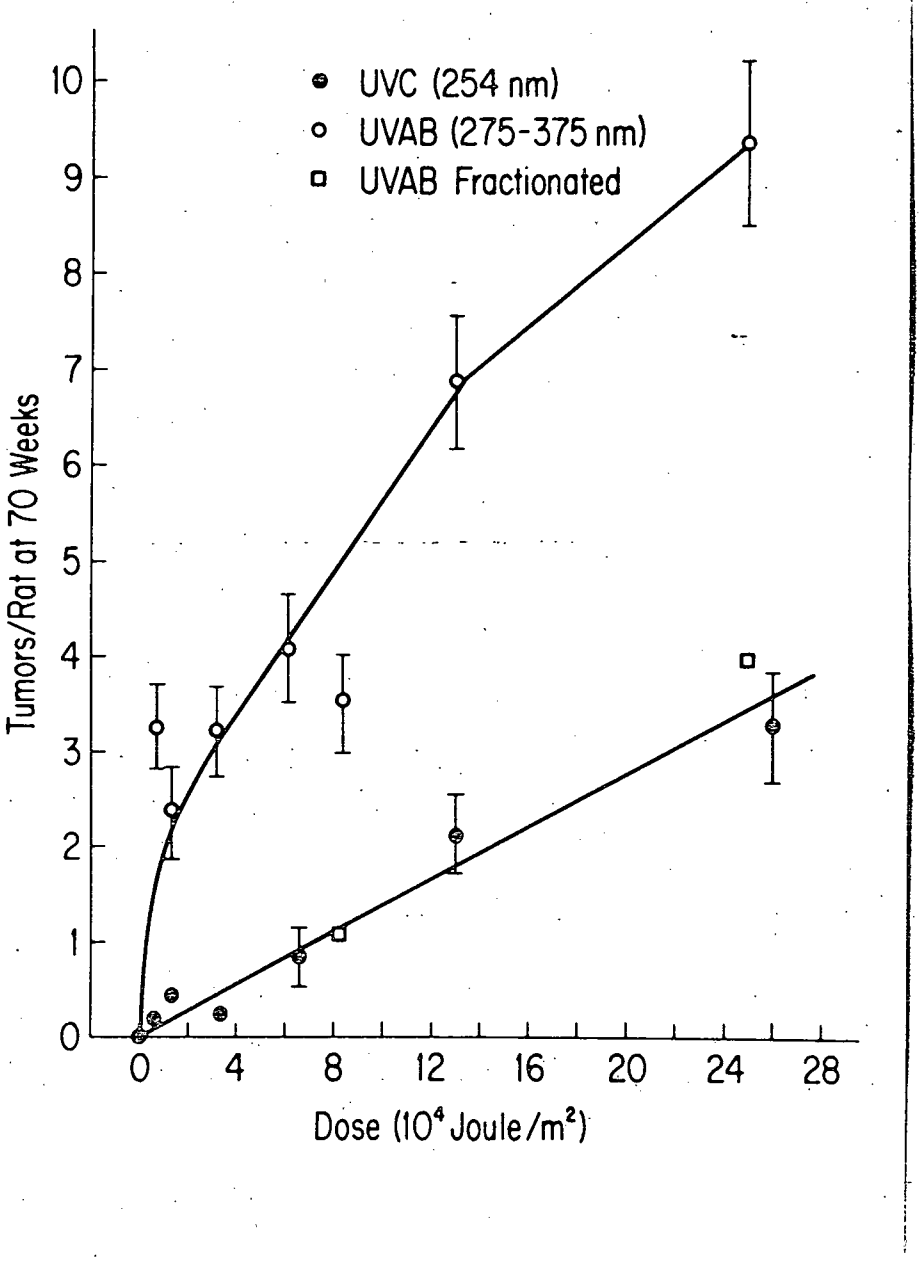

Figure 18. Follicle corrected tumor yield at 70 weeks after UV irradiation versus surface dose. The actual tumor yield was divided by the fraction of follicles surviving. The fractionated exposures were performed with UVAB (275-375 nm). The curves shown were drawn by eye to represent the trend of the data.

correction, the tumor yield was divided by the fraction of follicles surviving. The tumor yields at the four highest UVAB doses (6.3×10^4 to 25.2×10^4 J/m^2) increased as a result of the follicle correction. All other points remain unchanged because no follicle killing was observed at these doses. Although the follicle survival correction is a rough approximation of tissue damage, the resulting dose response relation is more nearly linear with dose over the dose range tested. The effects of fractionation can now be seen at the high (25.2×10^4) fractionated dose as well as at the lower (8.4×10^4) dose.

The dose-response data can be further corrected for the amount of UV reaching the basal layer of the epidermis by neglecting wavelengths above 320 nm (about 50% of the 275-375 nm UV dose) and applying the transmission factors for rat epidermis. When these corrections are made the dose response curves for 275-375 nm and 254 nm become nearly coincident.

Dose Dependence of Pyrimidine Dimers Induced in Rat Epidermal DNA by Ultraviolet Light

Pyrimidine dimers are one of the principal lesions produced in DNA when cells are irradiated with ultraviolet light, but their possible role in skin carcinogenesis is not clear (45). These dimers have been linked to oncogenesis in fish where it was shown that specific removal of the dimers by enzymatic photoreactivation greatly reduced the number of tumors (46). The clinical syndrome, xeroderma pigmentosum, is

characterized by hypersensitivity to solar radiation and a high incidence of multiple carcinomas. The cells from these individuals are more sensitive to UVR in vitro than normal cells and lack the ability to excise pyrimidine dimers (47).

Rat skin which has been studied extensively as a model for carcinogenesis by ionizing radiation was recently shown to be susceptible to tumor induction by 254 nm UV and 275-375 nm UV (48). The suggestion that dimers might be involved in oncogenesis requires further study in tissues where dimers and tumors can be determined separately. Additionally, the quantitation of dimers could be useful dosimetrically, because wavelength-dependent absorbtion in the keratin and outer cell layers of epidermis makes it difficult to determine the dose to the epidermal basal cells (49). The methodology described here is ideally suited to measure 'dose,' because the measurement of dimers is limited to basal cell nuclei. Such a 'dose' measurement may be more useful than fluence for studying the oncogenicity of ultraviolet light if dimers are important as initial lesions in tumor induction.

Materials and Methods

The procedure used to measure pyrimidine dimers is a modification of Pathak's (50) procedure using the Marmour DNA extraction method. Solvents and chemicals used were reagent grade and were used without further purification unless otherwise

stated (Methyl-^{3}H)thymidine (20 Ci/mmole) was obtained from Schwartz BioResearch, Orangeburg, New York. Whatman ion-exchange chromatography paper (grade WA-2) loaded with IRC-50 resin was obtained from Reeve Angel, Clifton, New Jersey. RNase (bovine pancreas) Type I-A was from Sigma Chemical Co.

Twenty-four hours prior to irradiation, 28 day old male CD-1 (Charles River Farms, Inc., Wilmington, Mass.) rats were depilated with a commercial wax over the entire back. ^{3}H-TdR was applied topically, 250 µCi per animal in 1.5 ml of 65% ethanol. The dorsal skin was then covered with a sheet of polyethylene until irradiation. The animals were restrained and irradiated without anesthesia. The dorsal skin was removed surgically from the sacrificed animals and the epidermis was isolated by the stretch method of Freedberg and Baden (51).

The DNA solution was assayed for specific activity by counting in a toluene based scintillation cocktail and measuring DNA fluorometrically (DABA assay). DNA yields were 14-21% with this extraction procedure and specific activity was approximately 150 dpm/µg DNA (52).

The solution of DNA was mixed and centrifuged (5 min. at 200 g). The DNA solution was precipitated and washed with 95% ethanol, ethanol-ether (3:1 v/v), and ether; and dried in an oven (1 hr. at 50^{o}C). The dry DNA was hydrolyzed in 50 µl 70% perchloric acid for 1 hr. at 85^{o}C. Distilled H_2O (100 µl) and

45% KOH (50 µl) was added on ice to neutralize the mixture, which was then stirred and centrifuged. 50 µl of the supernatant (∿ 10,000 cpm) was spotted on Whatman WA-2 ion-exchange chromatography paper (2.5 cm wide strip) in 5 µl aliquots, blow-drying between each application. The chromatograph was run using 0.1M acetic acid (pH 4.8) as solvent and the solvent front moved about 10 cm per hour. Chromatographs were dried overnight at room temperature after the front had moved 20 cm, sliced into 0.5 cm strips, eluted with 0.2 ml 1N HCl and neutralized with 0.3 ml 1M Tris. Activity was determined by counting in a toluene based scintillation cocktail. In this chromatographic system thymine monomer has an R_f of 0.43, thymine dimer R_f 0.65, and thymine-uracil dimer (deamination product of thymine-cytosine dimer) R_f 0.70 (53).

Results

Pyrimidine dimer induction was measured in rat skin at four doses of near UV and four doses of far UV. It was first established by autoradiographic studies that prelabelling with (methyl-^{3}H)thymidine, labelled only basal cells of the epidermis as expected.

Figure 19 shows a control radiochromatogram of hydrolyzed DNA labelled with ^{3}H-TdR. The thymine monomer migrates with an R_f of 0.42. Figure 20 shows the radiochromatogram of hydrolyzed DNA from animals exposed to 6×10^5 ergs/mm^2 of 275-375 mm UV.

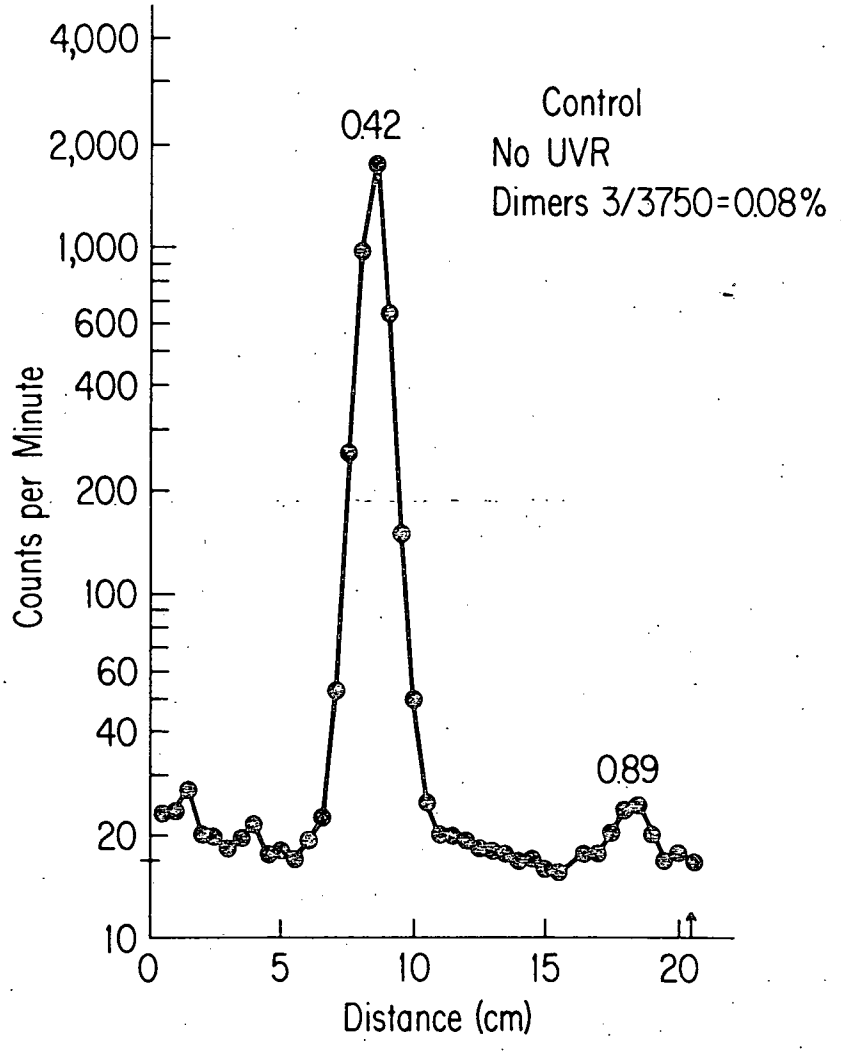

Figure 19. Control (no UV) radiochromatogram of hydrolyzed DNA labelled with ^{3}H-TdR. Thymine monomer: R_f 0.42; thymidine mono-phosphate (see text): R_f 0.89; total counts per minute: 3750. Whatman WA-2 ion-exchange chromatography paper. Solvent 0.1M acetic acid (pH 4.8).

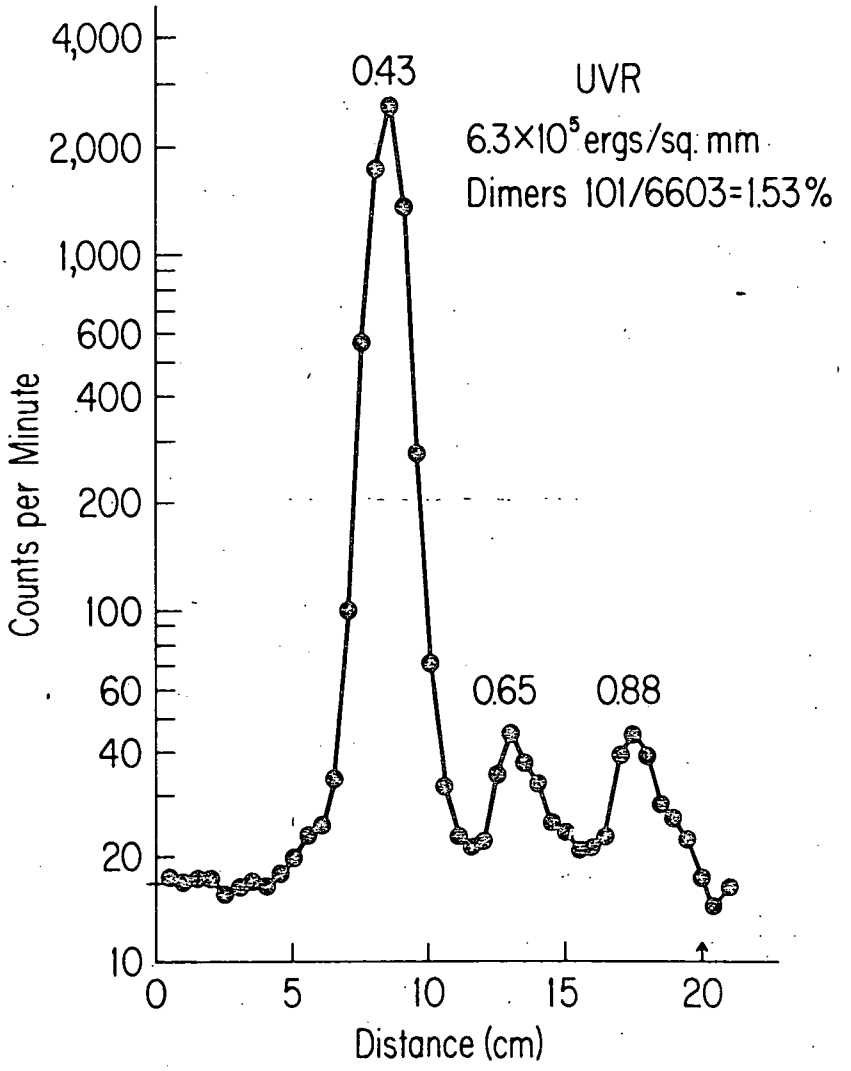

Figure 20. Radiochromatogram of hydrolyzed DNA from epidermis exposed to 6.3 x 10^5 ergs/mm^2 of near UV. Thymine monomer: R_f 0.43; thymine dimer: R_f 0.65; thymidine mono-phosphate (see text): R_f 0.88; total counts per minute: 6603. Whatman WA-2 ion-exchange chromatography paper. Solvent 0.1M acetic acid (pH 4.8).

The thymine dimer migrates with an R_f of 0.65 and was always observed within the range 0.63-0.68. Several investigators have confirmed the identity of this peak by photoreversal of the dimers with short wavelength ($\sim$ 250 nm) UV (53,50). No evidence of a cytosine-thymine dimer peak ($R_f \sim 0.70$) was observed, however, a small peak would be difficult to resolve from the thymine peak at $R_f = 0.65$. Another peak at $R_f = 0.85$-0.89 appeared in all chromatograms, including controls, and was not dose dependent. The R_f of this peak corresponds to that of thymine-monophosphate (5'-TMP), however, this identification was not confirmed. An identical peak has been observed by other investigators using the same chromatography system (54).

The results of the thymine-containing dimer experiments were expressed as the percentage of radioactivity associated with thymine-containing dimers vs. the amount of radioactivity associated with thymine. Error bars are Poisson confidence intervals associated with 10 minute counts. Thymine-containing dimer yields for controls (no UV) were consistently very low (average yield $\sim$ 0.03%). The dimer levels as a function of dose are presented in Figure 21. The 275-375 UV was more efficient per unit fluence than the 254 UV in producing pyrimidine dimers.

The slopes of the dimer versus dose data are 0.18% dimers

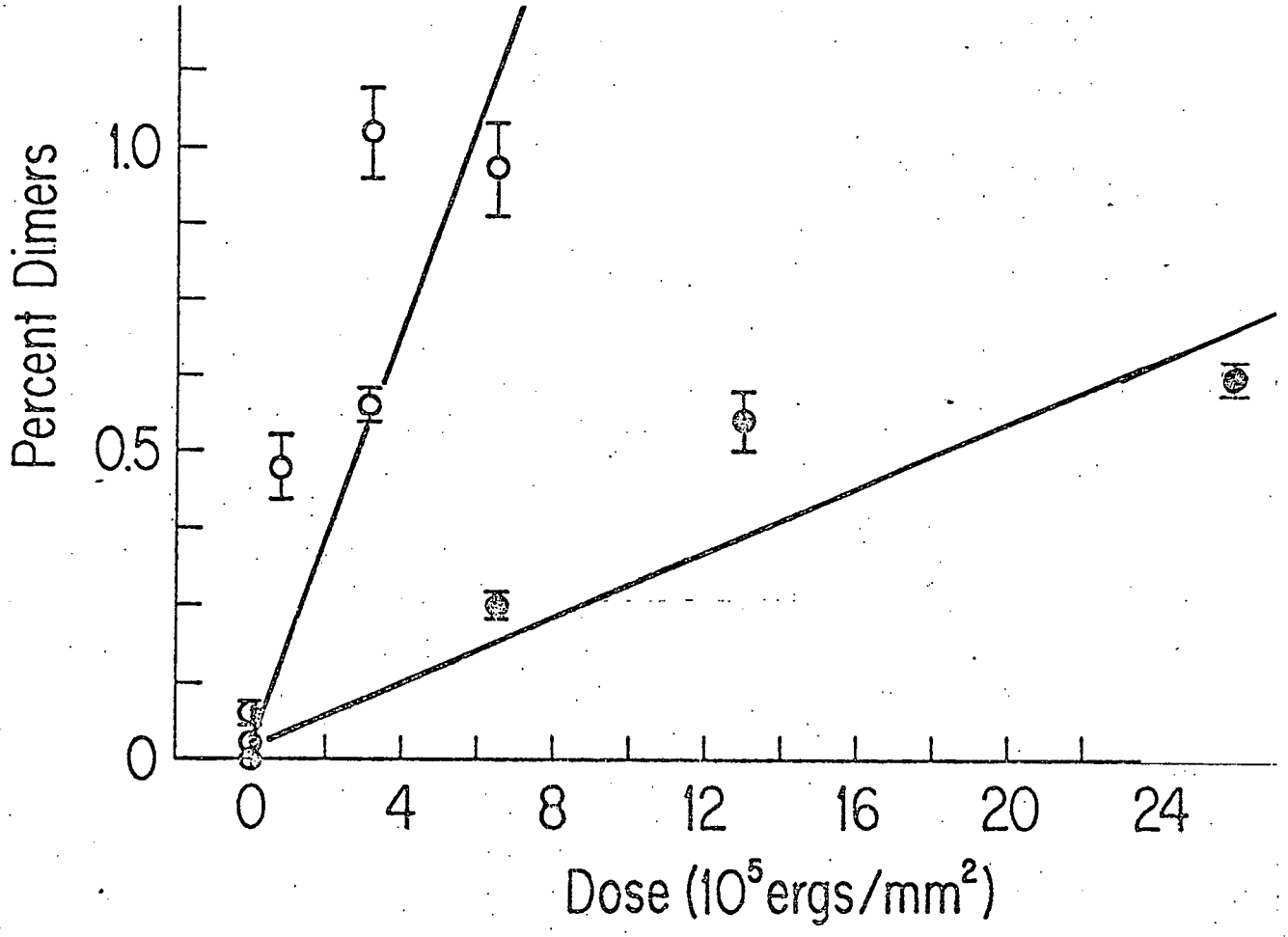

Figure 21. Percentage of thymine-containing pyrimidine dimers detected in epidermis as a function of incident dose. Upper curve: 275-375 nm UV; low curve: 254 nm UV.

per 10^5 ergs/mm^2 for 275-375 UV and 0.03% dimers per 10^5 ergs/mm^2 for 254 UV. The highest 254 UV dose point (50 x 10^5 ergs/mm^2) indicates possible saturation of response.

A reduction in extractability of DNA was noted when an even higher dose of 275-375 UV was used (26 x 10^5 ergs/mm^2),

prohibiting measurement of pyrimidine dimerization at this dose. A decrease in the amount of extractable DNA after UV exposure has been observed in a number of cell systems, and this effect is usually attributed to DNA-protein cross-linking (55).

Discussion

For the same amount of ultraviolet exposure, pyrimidine dimerization produced by 275-375 nm UV (0.18% dimers per 10^5 ergs/mm^2) was greater than that produced by far 254 nm UV (0.03% dimers per 10^5 ergs/mm^2). This observation is in agreement with a previous *in vivo* study (5) in the guinea pig. The amount of dimerization by 275-375 nm UV is similar to that reported recently (56) for cultured, excised mouse skin (0.20% dimers per 10^5 ergs/mm^2).

These results are different from results obtained in cultured mammalian cell systems where 254 nm UV is more effective than 275-375 nm UV in producing dimerization. Elkind (57) has reported dimerization rates for Chinese hamster cells of 0.9% per 10^5 ergs/mm^2 for 275-375 nm UV and 26.2% per 10^5 ergs/mm^2 for 254 nm UV where the two radiation sources used were identical to the sources used in the present experiments. Other investigators have reported values between 10 and 30% dimers per 10^5 ergs/mm^2 for 254 nm UV (58).

The discrepancy between *in vivo* and *in vitro* results is

probably associated with differential UV absorption in the superficial layers of the epidermis which greatly modifies the dose to the basal cell layer for the same incident energy. Th UV transmission through the epidermis was measured in a separate experiment (48). The in vivo dimerization data in the present study can be corrected for epidermal attenuation by dividing the observed dimer percentages by the fraction of UV transmitted to the basal cell layer. The correction for the 275-375 nm UV exposure is made using the transmission at 300 nm because this is the wavelength of maximum dimer production by the near UV light source (57):

$$\frac{0.18\% \text{ dimers per } 10^5}{0.15 \text{ UV transmitted}} = 1.2\% \text{ dimers per } 10^5 \text{ ergs/mm}^2$$

The correction for the 254 nm UV exposure is made using the transmission at 254 nm:

$$\frac{0.03\% \text{ dimers per } 10^5}{0.03 \text{ UV transmitted}} = 1\% \text{ dimers per } 10^5 \text{ ergs/mm}^2$$

It is somewhat surprising that the two wavelengths produce very similar levels of corrected dimerization in view of the fact that in vitro results show 254 nm UV to be approximately 10-30X more effective for dimerization. The transmission corrected amount of dimerization measured in this study for 275-375 nm UV is similar to that amount measured in vitro (1.2% vs. 0.9% dimers per 10^5 ergs/mm^2). However, comparison of the 254 nm UV data with in vitro results indicates an inconsistency (1% vs.

10-30% dimers per 10^5 ergs/mm^2). Thus, differential epidermal attenuation accounts for the difference observed between *in vivo* and *in vitro* results with 275-375 nm UV, but only partially accounts for the difference observed with 254 nm UV.

There are several reasons why one would expect more dimerization in cell culture than in whole epidermis. First, the cell culture system causes cells to be in a flat geometrical configuration which is quite dissimilar from the *in vivo* configuration. This question has been discussed in detail by Rauth (58). In culture the cells spread out, during attachment to the culture plate, to a very thin, flat state in which the nucleus is also spread flat, thus presenting a much thinner target to the incident beam than the nuclei *in vivo* which are more rounded. Mammalian cells in culture typically have a diameter of 15-30 μ and a thickness of 1-3 μ whereas epidermal basal cells are normally 6-10 μ in diameter and thickness. At normal nuclear densities of DNA, the half value of 254 nm UV is only a few microns, and a "shadowing effect" is likely to occur in the nuclei of cells irradiation *in vivo* because these nuclei are more or less spherical in shape with diameter of 4-6 μ.

In addition, certain extranuclear molecules (particularly RNA) absorb strongly at 254 nm. Since the extranuclear material in cultured cells is not evenly distributed around the nucleus

as in the case for basal cell *in vivo*, absorption by cellular constituents directly above the nucleus is decreased in cell culture. Thus, the DNA is afforded some protection from radiation *in vivo*, and this protection is lost with the *in vitro* geometry.

Variable cell cycle sensitivity is also relevant to the question of *in vivo* and *in vitro* dimerization rates. Sensitivity to UV induced pyrimidine dimers with respect to cell cycle, as well as several other endpoints have been studied. The S-phase (DNA synthesis) is the most sensitive phase of cell growth for UV induced pyrimidine dimers (1.3 times more sensitive than G_1); cell lethality (3 times more sensitive than G_1); and chromosome damage in a number of cell lines including Chinese hamster cells (58, 57). Cultured cells exhibit a large percentage of cells in S-phase (up to 70%, whereas rat skin basal cells *in vivo* have only about 5% S-phase cells, the majority of cells being in G_1 phase. Thus, cells irradiated in cell culture are predominately S-phase, the most sensitive phase for pyrimidine dimerization, while the *in vivo* cell population in question was irradiated predominately in G_1 phase.

A comparison of the dose and spectral response of UV induced tumors with the dose and spectral response of pyrimidine dimers suggests a correlation between these two endpoints. The percent dimers were plotted as a function of tumor yield at 70 weeks

postirradiation for equivalent UV doses. The linear regression analysis indicates a linear correlation coefficient of r = 0.89.

While proportionality between biological endpoints produced by UV does not necessarily imply a mechanistic connection, the existence of proportionality in two spectral regions strengthens support for a positive connection. The production of pyrimidine dimers by UV can be used as an indicator of UV absorption by DNA and specifically by thymidine. Therefore, any UV induced molecular lesion in DNA with the same action spectrum as pyrimidine dimer formation would also be expected to be proportional to tumor response. The action spectra of most UV induced DNA lesions (with the exception of pyrimidine dimers and single strand breaks) have not as yet been elucidated, however, those lesions that are produced via thymidine photo-activation, e.g., thymidine photohydrates, would be expected to have action spectra similar to the dimerization action spectrum. It is known that the action spectrum for UV induced single strand breaks is different from that for pyrimidine dimer formation. The ratio of dimers to single strand breaks in cells is about 800 for 254 nm UV and about 25 for 313 nm UV (59). Since tumor induction in the present study has the same spectral dependence as dimer formation, tumor formation cannot be correlated with single strand breaks. Thus, while we cannot

rule out the possibility of a mechanistic connection between oncogenesis and lesions with action spectra similar to that of dimerization, the evidence presented does weaken the implication of molecular alterations with action spectra different from that of dimerization, e.g., single strand breaks in DNA, protein aggregate formation, disulfide bond breakage, etc.

Our measurements indicate that a very large number ($\sim 10^6$ per cell) of pyrimidine dimers are formed by oncogenic doses of UV. Although dimer removal from rodent skin has not been definitively demonstrated, it is probable that some forms of repair (excision, photoreactivation, or post-replication) are operating in these cells. As discussed previously, post-replication repair may have mutagenic properties in mammalian cells, whereas excision and photoreactivation repair are believed to be error-free. Thus, the consequences of dimer removal from skin after UV exposure may be beneficial or detrimental to the animal.

An investigation of dimer repair in mouse skin suggests that repair systems may saturate or be inactivated by high doses (60). A large proportion of dimers were removed following a low dose (2×10^4 ergs/mm^2) whereas no removal was observed following a dose of 8×10^4 ergs/mm^2. Thus, the relatively high doses used in tumor induction studies may produce more damage than repair mechanisms can handle.

In conclusion, pyrimidine dimer formation was also measured in rat skin epidermis following exposure to UV in the oncogenic dose range. These data allow for the first time a direct comparison between tumor induction and dimer formation in the same model system. The amount of pyrimidine dimerization in rat epidermal DNA was shown to be proportional to tumor yield following exposure to either UV source. This correlation supports the concept that UV absorption by DNA is an early event in UV oncogenesis.

4.2.5 DNA Strand Breaks and Their Repair in Electron Irradiated Rat Epidermis

Rat skin has been found to be a useful system for the study of both the early and late effects of ionizing radiation. While biological endpoints such as acute ulcerative damage, oncogenesis and tumor-related recovery have been examined, the studies of the effects of ionizing radiation on molecular target have not been performed in this system.

A large body of evidence suggests that DNA is the major target of ionizing radiation in the cell (61). DNA strand breakage (both single and double strand) has been shown to be a principle molecular effect of ionizing radiation (62). Until recently, methods used to study DNA strand breakage and repair in *in vivo* systems have been undesirable. An alternative to these methods has been developed by Rydberg (63). The method involves the use of hydroxyapatite chromatography

following DNA strand separation in alkali. Further modifications of the method using a single strand specific nuclease to resolve single from double stranded DNA have also been developed (64). Studies have been reported, using both the hydroxyapatite chromatography and the S_1 nuclease methods to measure DNA strand breaks and repair of the in vivo exposure to ionizing radiation in mouse intestinal crypt and villous cells (65) and in rat gliosarcoma 96 cells (66), respectively.

We report here studies on the use of the S_1 nuclease alkaline unwinding assay to measure the time and dose kinetics of the production and repair of DNA strand breaks in rat epidermal cells after in vivo treatment with biologically significant doses of electron radiation

Materials and Methods

Male CD rats, 21 days of age, were obtained from Charles River Breeding Farms, Brookline, Massachusetts. The animals were shaved 5 days prior to irradiation in order to determine the phase of the hair growth cycle. Animals found to be in the resting phase were then given two I.P. injections of 250 μCi each of (methyl-^{3}H)thymidine (55 Ci/mmole from Schwartz-Mann, Orangeburg, New York) 48 and 24 hours prior to irradiation. After 24-48 hours the majority of the cells were in the G_1 phase of the cell growth cycle (66).

The animals were anesthetized with an I.P. injection of

30 mg/Kg of sodium pentobarbital prior to irradiation. The dorsal skin (10 cm^2) was irradiated with 0.8 MeV electrons from a linear electron accelerator (HVEC) at a dose rate of 600 rads/min. Dose measurements were made with a parallel plate ionization chamber. Control rats were sham irradiated using the same conditions.

The rats were killed by cervical dislocation and the irradiation skin dissected, stretched on cardboard dermis side down, and frozen in liquid nitrogen. Immediately prior to the assay, the epidermis was removed by scraping with a scalpel. The epidermal tissue was then placed in ice-cold 0.15 M NaCl, stirred for 30 min. in a cold room and filtered through 200 mesh nylon screening in order to obtain a single cell suspension.

Previously used methods of alkaline treatment (67) and S_1 nuclease reaction (64) were adapted for use in this assay. One milliliter of alkaline solution (1.0 M NaCl, 0.02 M Na_2HPO_4; pH 11.35) was added to one milliliter ($\sim 10^6$ cells) of the cell suspension in order to type the cells and unwind the DNA. The cells were treated with alkali for specified times at 23°C in the dark in order to obtain a DNA unwinding rate. The rate of DNA unwinding in alkali has been shown to be directly proportional to the total number of DNA breaks according to the equation:

$$\ln F = \frac{-k}{Mn} t^B$$

where F is the fraction of double stranded DNA remaining after time (t) of alkali treatment, Mn is the number average molecular weight of the DNA between two breaks and B = 1 is an empirically determined constant. A mathematical derivation of the above relationship appears in Rydberg's paper (63).

The fraction (F) was determined by resistance to single strand specific S_1 nuclease. The cell suspension was made acidic by the addition of 2.5 ml of 0.76 M acetic acid. Cell aggregation was then reduced by sonication at setting 4 for 10 seconds with a cell sonifier (Ultrasonics Inc., Model #W185), followed by the addition of 0.1 ml of 5% SDS and incubation at 55°C for 20 min. In order to optimize S_1 nuclease activity, 0.3 ml of 0.1 M zinc acetate and 0.5 ml of a 0.11 mg/ml solution of denatured calf thymus DNA was added. Each sample was separated into two equal volumes, to one of which was added 800 units of S_1 nuclease (Type III, Sigma Chemical Co., St. Louis, Missouri). All samples were then incubated for 1 hour at 40°C.

The samples were precipitated with an equal volume of ice-cold 14% trichloro acetic acid and filtered through 0.45 μm Millipore filters. The filters were collected, dryed, dissolved in 1.0 ml of ethoxy ethanol, and counted in 10 ml of Bioflour (New England Nuclear, Boston, Massachusetts) in a Beckman liquid scintillation counter.

Results

Figure 22 shows a log-linear plot of F, the fraction of double

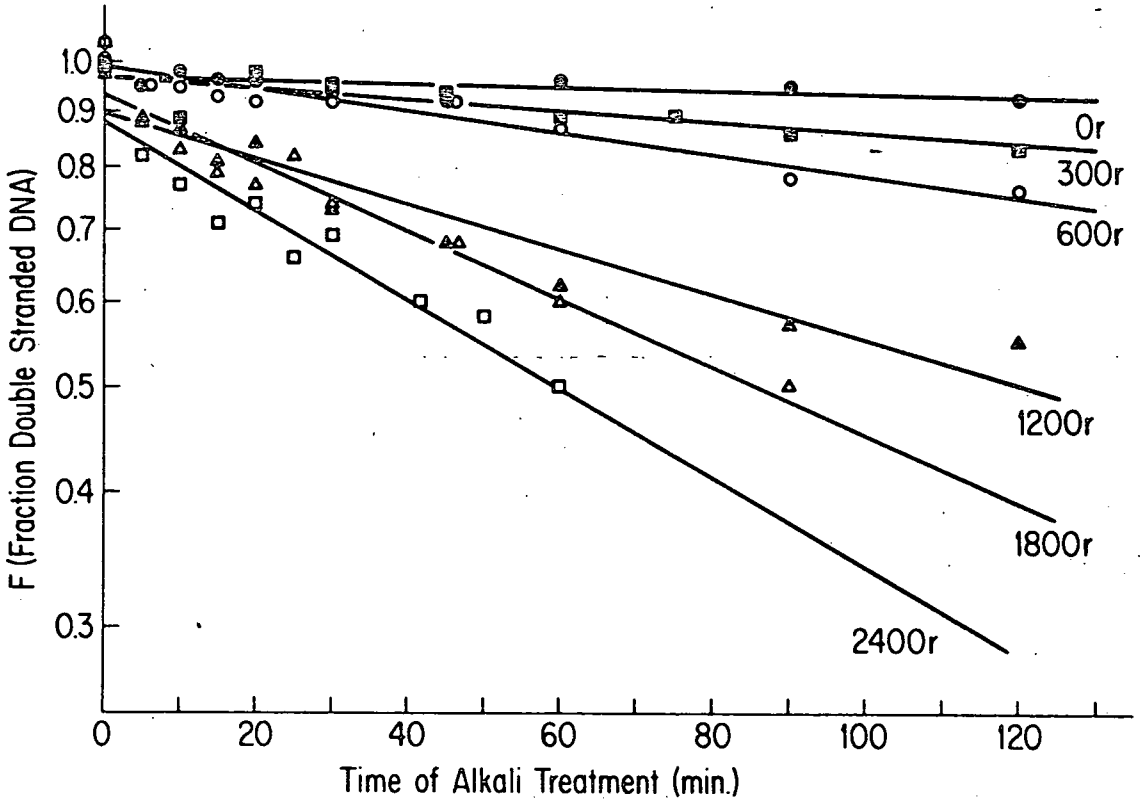

Figure 22. The fraction double stranded DNA of rat epidermis as a function of time in alkali (pH = 11.4) for various doses of electron radiation as indicated.

stranded DNA as a function of alkali treatment for control and electron irradiated rat epidermal cells. A least squares line

was drawn for each set of data and the slopes (K/Mn(o)) were determined. The results show that the slope of the unwinding curve increases as a function of electron dose.

Figure 23 shows that the number of strand breaks per unit length DNA increases linearly with electron dose between 0 and 2400. The number of breaks per unit length is obtained by taking the ratio of slopes of the alkaline winding curves for treated versus control samples.

Figure 24 shows that the fraction (F) increases exponentially with time after irradiation with 1200 rads of electrons. The increasing (F) represents the loss of DNA strand breaks with time, probably due to DNA repair processes. It can be seen that repair is completed within 45 to 60 minutes.

Figure 25 shows that the half-time of repair is 13 minutes. The half-time ($t_{\frac{1}{2}}$) was determined from the first order rate equation:

$$\frac{F_f - F_r}{F_f - F_o} = e^{\frac{-0.693t}{t_{\frac{1}{2}}}}$$

where F_f is the average fraction double stranded DNA reached between 45 and 120 min. after irradiation (the plateau level reached in Figure 24), F_r is the fraction double stranded DNA remaining after time t, and F_o is the initial fraction double stranded DNA.

Because of the rapid rate of repair and the maintenance

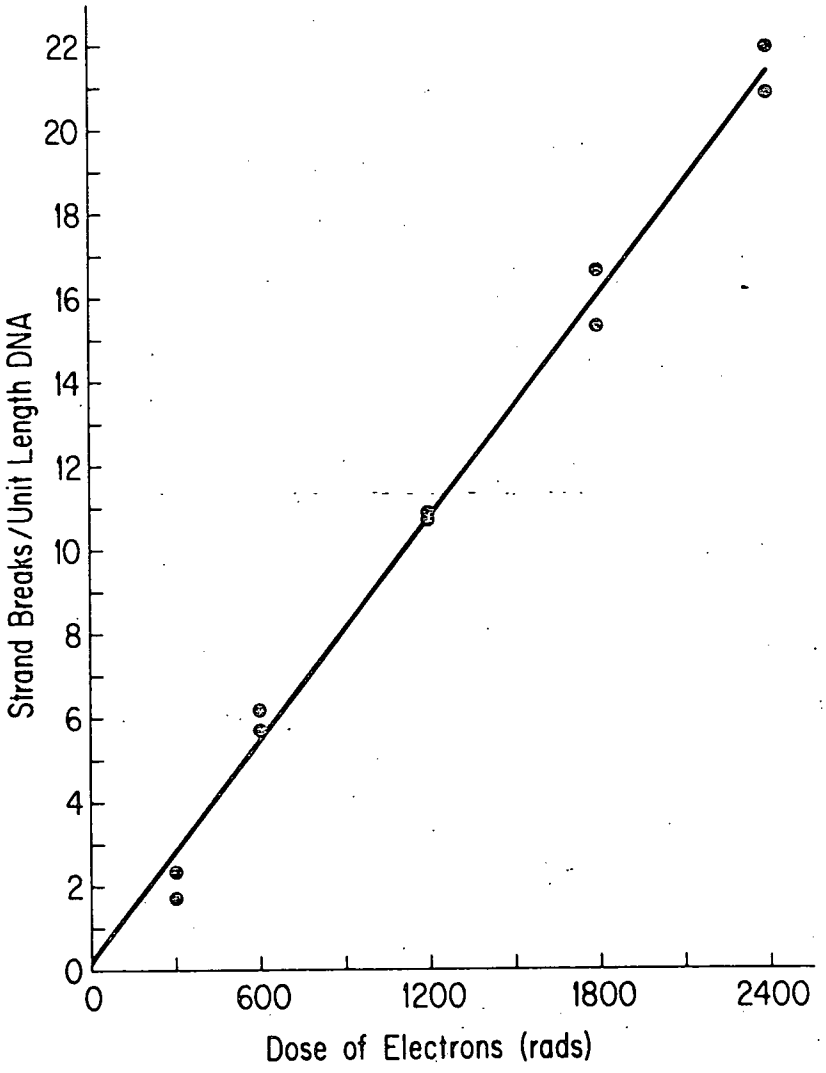

Figure 23. Strands breaks in the epidermal DNA of rats as a function of the dose of electron radiation.

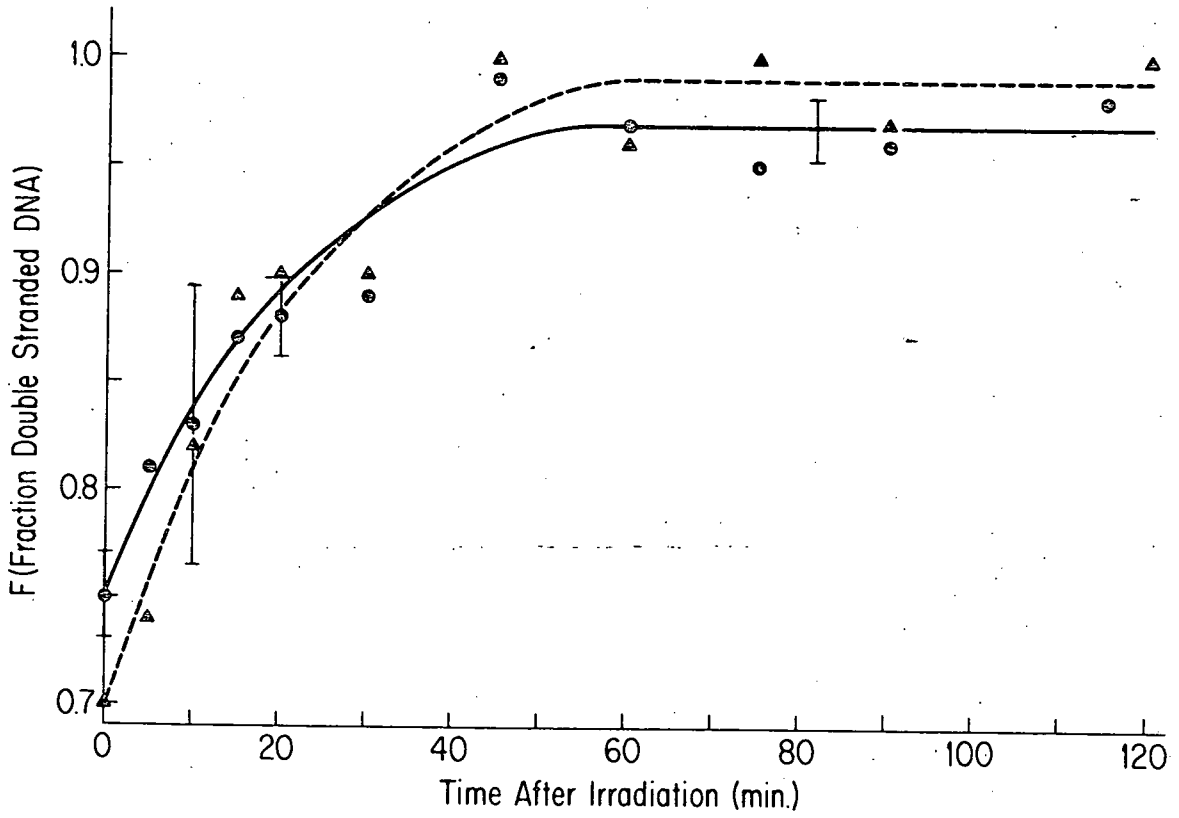

Figure 24. The removal of strand breaks from the DNA of rat epidermis as a function of time after irradiation with 1200 rads of electron radiation.

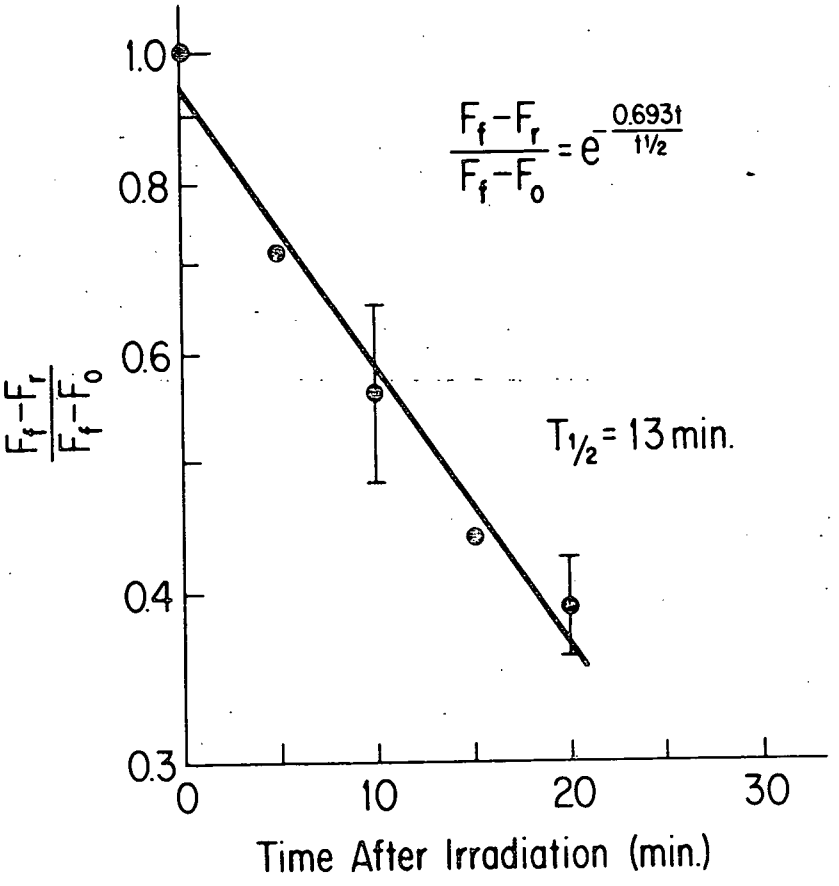

Figure 25. Repair curve for strand breaks in the DNA of rat epidermis. F_f is proportion of double stranded DNA after a long time, F_o is proportion of double stranded DNA at time zero and F_r is the proportion double stranded at intermediate times.

of a dose rate of 600 rads/min. for each dose group, a calculable amount of repair will occur during exposure, depending on total time of exposure. While this repair will increase the slope of the dose response curve, it will not affect its linearity.

Discussion

The results of these experiments show that DNA strand breaks increase as a linear function of dose throughout the dose range of 0 to 2400 rads of electrons and that DNA strand breaks induced by 1200 rads of electrons persisted with a half-time of 13 min. The loss of DNA strand breaks with time is presumably due to repair processes within the epidermal cells, and is in agreement with findings in other experimental systems (63-66).

The procedure used to measure DNA strand breaks is based on the observation that the rate of transformation of double stranded DNA to single stranded DNA is accelerated by a heterogeneous group of alkaline labile DNA lesions, including: single and double strand breaks, DNA adducts, and excision-repair induced gaps. Of these, primary single strand breaks and alkaline labile bonds are the major radiation induced lesions detected by this method (67).

The measurement of the induction and persistence of strand breaks in rat epidermis exposed to electrons enables us to compare these results with those previously obtained using

the rat skin system such as skin tumorigenesis (68, 69) and tumor related recovery (70), the experimental conditions used to generate the dose response curve for electron induced skin tumors, and to study tumor-related recovery were similar to those used in the present experiment. The tumor-response curve was shown to increase approximately as a function of the square of the dose up to 2000 rads, after which it declined due to the acute effect on cell survival. Tumor-related recovery was estimated in rat skin using the split dose technique. Tumor yield was established as a function of dose at 1000 and 1450 rads. Fractionation of these doses resulted in a decrease in tumor yield. The tumor yields declined with half-times of 1.8 hours and 3.9 hours, respectively. This decrease in tumor yield was ascribed to a rapid intracellular repair process. The large difference in repair half-times between tumor recovery and DNA strand break repair and the discrepancy in the shape of the dose response curves for the two endpoints suggests that DNA strand breaks are not the dominant lesion leading to the electron induced tumors.

Tumor Induction by the Combination of Ultraviolet Light and Ionizing Radiation on Rat Skin

Two of the most commonly encountered carcinogens in the human environment are radiations, namely, ionizing radiation and ultraviolet light. Both are known to produce

skin tumors in experimental animals; ionizing radiation having been studied primarily in rats and ultraviolet light having been studied almost exclusively in mice.

An epidemiological study of Tinea capitis patients who had been given depilatory doses of x-irradiation as children, showed an excess incidence of several types of head and neck tumors, including: skin, thyroid, and brain tumors (71). A comparison with the results obtained in rat skin for about the same radiation dose showed approximately equivalent skin tumor incidences at comparable fractions of the respective lifespans. However, many of the human tumors, mostly basal cell carcinoma, were found near the hairline or on the face where exposure to solar ultraviolet light would be expected. Since most basal cell carcinomas on human skin are believed to be associated with exposure to ultraviolet radiation, the excess tumors in the patients could have been associated with an interaction between the two radiations.

The finding that rat skin is susceptible to ultraviolet oncogenesis raised the possibility of testing for an interaction experimentally. Several studies have shown that interactions are sometimes inhibitory, sometimes additive and sometimes synergistic depending on the carcinogen and the test organ. When ultraviolet light is combined with 7,12dimethylbenz(a)anthracene (DMBA) or ionizing radiation on the skin of

hairless mice, tumors are produced as if the agents are additive, i.e., the yield of tumors for combined exposure is the same as would be expected from the summation of yields for the individual exposures. Other studies with mouse skin have shown that ionizing radiation combined with 4-nitroquinoline-1-oxide (4-NQO), or ultraviolet light produce tumors in greater numbers than would be expected from the summation of the effect of individual exposures (72).

The studies described here were aimed at answering two basic questions: (1) whether the tumor yields for ionizing radiation and ultraviolet light are temporarily additive and (2) whether cells that have been transformed by the action of ionizing radiation more readily progress to cancer when exposed to repeated doses of ultraviolet light.

Materials and Methods

Male (CD-1) rats were obtained from Charles River Co., Brookline, Massachusetts. They were housed two per cage and given lab chow (Ralston Purina, St. Louis, Missouri) and water from the tap ad libitum. At 28 days of age the dorsal skin was exposed to a single dose of 0.7 MeV electrons generated by a Van de Graaff accelerator. The beam penetrated to a depth of 1.0 mm and provided a dose rate at the skin surface of 500 rads/min. As described previously, the animals were anesthetized with sodium pentobarbital and placed in small wooden boxes

containing a metal lid with an rectangular opening 2 cm x 5 cm. The hair was removed with clippers and only that part exposed through the opening in the lid of the box received radiation dosage.

At various times after the exposure to electron radiation, the dorsal skin was exposed to single or multiple doses of ultraviolet light. The ultraviolet light was produced by 4 FS20 fluorescent sun lamps (Westinghouse Electric Co.) with a spectral range of 275-375 nm and peak output at 313 nm.

The skin was observed every six weeks and photographs were taken of each lesion when it was first observed and periodically thereafter. The tumor response in each observation interval was calculated as the incidence rate of new tumors in the interval. In any given six week interval, if there were L animals at the start of the interval, N new tumors occurred, and D animals died during the time interval, then the tumor appearance rate was calculated as $N/(L-D/2)$. The cumulative response at a given time after irradiation was the sum of the rates in the preceding intervals. Sketches of tumor location were made from the photographs so that each tumor could be identified, assigned a time of appearance, and examined histologically at the time of death. The experiments were terminated at 80 weeks after the electron irradiation, and all surviving rats were sacrificed for histological samples.

Results

UVR caused erythema within 24-48 hours. The erythema was followed by dry desquamation at about 5 days. The protracted UVR treatments produced hyperplasia, necrosis, and scab formation which subsided 2-4 weeks after treatment ended. As in previous experiments, the protracted UVR treatment produced a more severe acute reaction than a single treatment of equivalent total fluence.

Tumors were first observed at 20-32 weeks and continued to appear throughout the life of the animals. As in previous experiments, the predominant tumor type observed in UVR treated animals was the keratoacanthoma, of which 344 were histologically confirmed. The electron radiation induced predominantly epidermal tumors in agreement with previous results; a total of 311 were histologically confirmed. The percentage of various epidermal tumor types observed was 25% undifferentiation (basal cell), 37% keratinizing (squamous cell component), and 38% keratosebaceous or sebaceous. A small number (39) of sarcomas were also observed.

In Figure 26 the yield of keratoacanthomas as a function of time past four weeks of age is shown for the various UVR treatment schedules. The highest yield of keratoacanthomas appeared in the treatment group receiving a total fluence of 25.2×10^5 ergs/mm^2 in 12 equal weekly fractions beginning at 5 weeks of age. If the same total fluence and fractionation

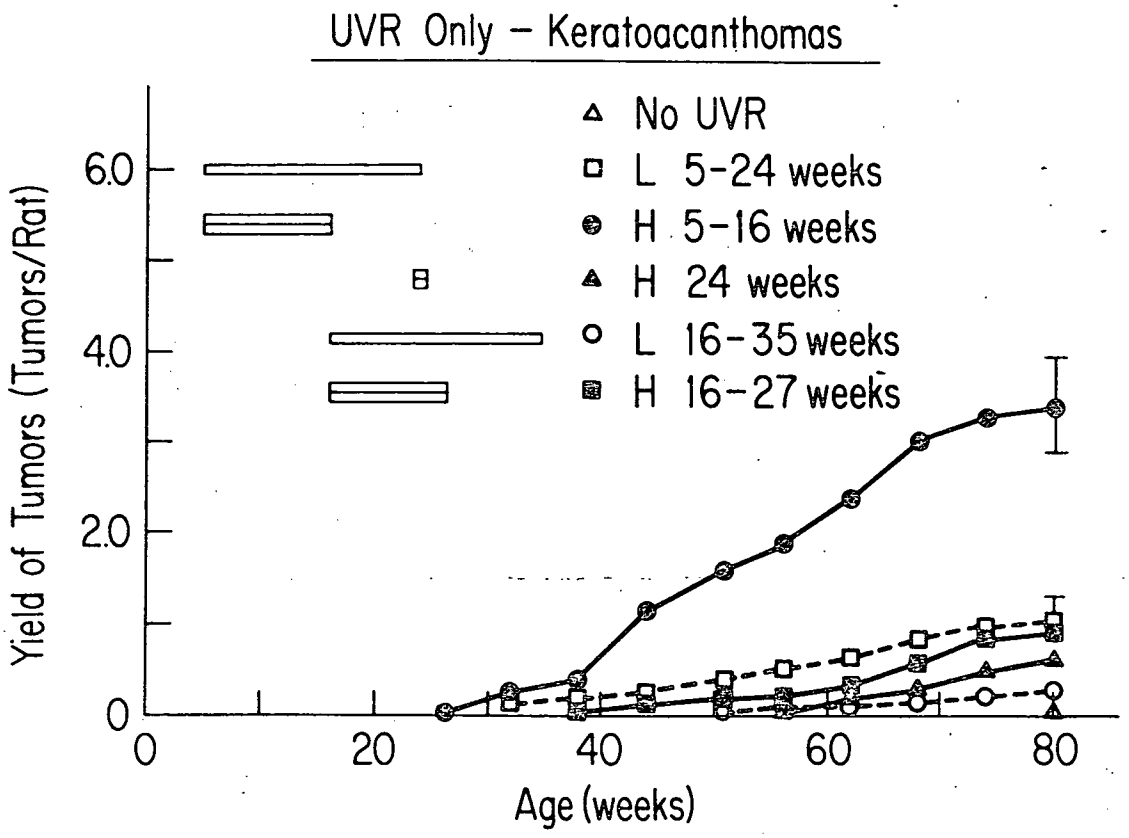

Figure 26. Keratoacanthoma yield as a function of age for rats irradiated with high (H) or low (L) fluences of 275-375 nm UV for various periods of time as indicated by the horizontal bars in the figure.

schedule was used beginning at 16 weeks of age, the tumor yield was reduced by a factor of 3.7 (3.35 vs. 0.90 tumors per rat at 84 weeks). This difference is significant at $p < .0001$. The second highest response occurred in the treatment group

receiving a total of 8.4×10^5 ergs/mm^2 in 20 equal weekly fractions beginning at 5 weeks of age. If the same total fluence and fractionation schedule was initiated at 16 weeks of age, the tumor yield was reduced by a factor of 4.1 (0.99 vs. 0.24 tumors per rat at 84 weeks). This difference is significant at $p = .011$. Thus, the early treatment schedule beginning at 5 weeks of age is much more effective than the late treatment schedule beginning at 16 weeks of age.

The tumor yield observed following a single UVR treatment of 25.2×10^5 ergs/mm^2 at 24 weeks of age was slightly lower than the yield observed following the same total fluence fractionated into 12 weekly treatments beginning at 16 weeks (0.60 vs. 0.90 tumors per rat at 84 weeks). This difference is not significant at $p = .05$.

In Figure 27 the yield of keratoacanthomas at 80 weeks of age is shown as a function of electron dose (skin surface) administered at 4 weeks of age and prior to commencement of UVR treatment. The dependence of yield on UVR fluence is clearly exhibited. No consistent effect of electron treatment on yield of keratoacanthomas is obvious although some anomalies in the data appear, particularly at 1700 rads.

In Figure 28 the yield of epidermal tumors (squamous cell carcinomas, basal cell carcinomas, and keratosebaceous carcinomas) is presented as a function of electron dose for each of the various

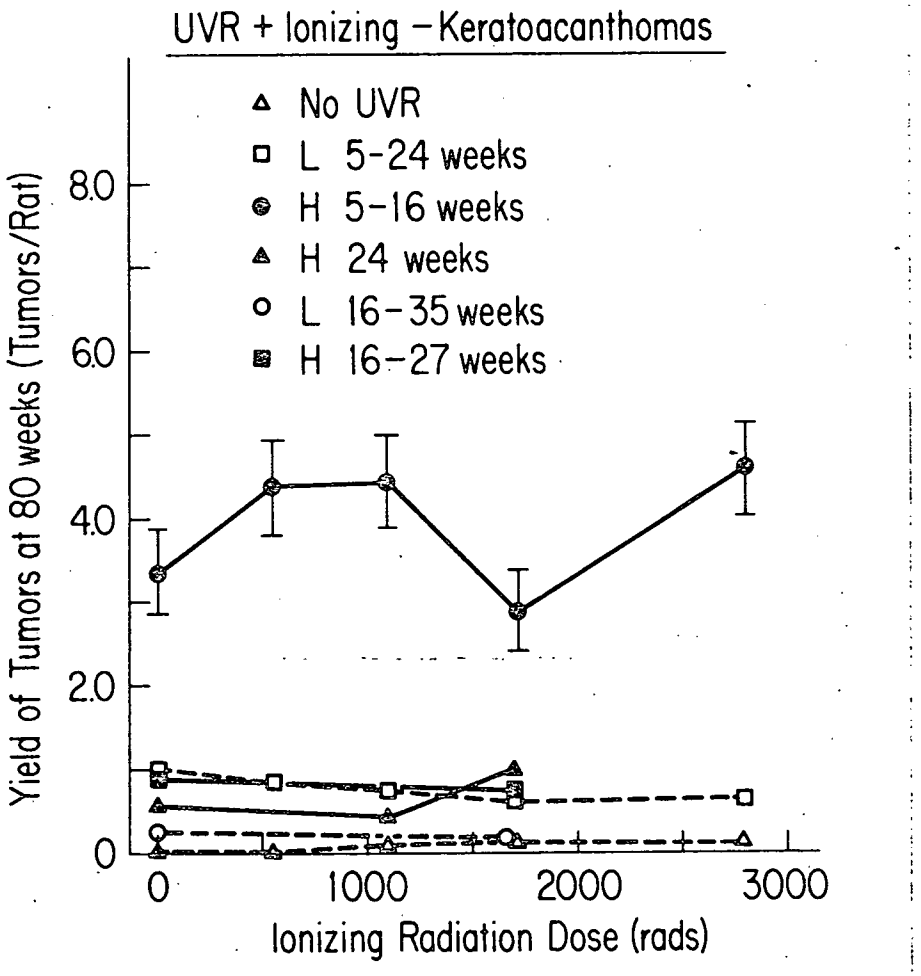

Figure 27. Keratoacanthoma yield at 80 weeks as a function of dose of electron radiation for rats exposed to 275-375 nm UVR for various periods of time and fluences as indicated. High fluence (H) was 25.2 x 10^4 joules/m^2 and low fluence (L) was 8.4 x 10^4 joules/m^2 given in weekly increments.

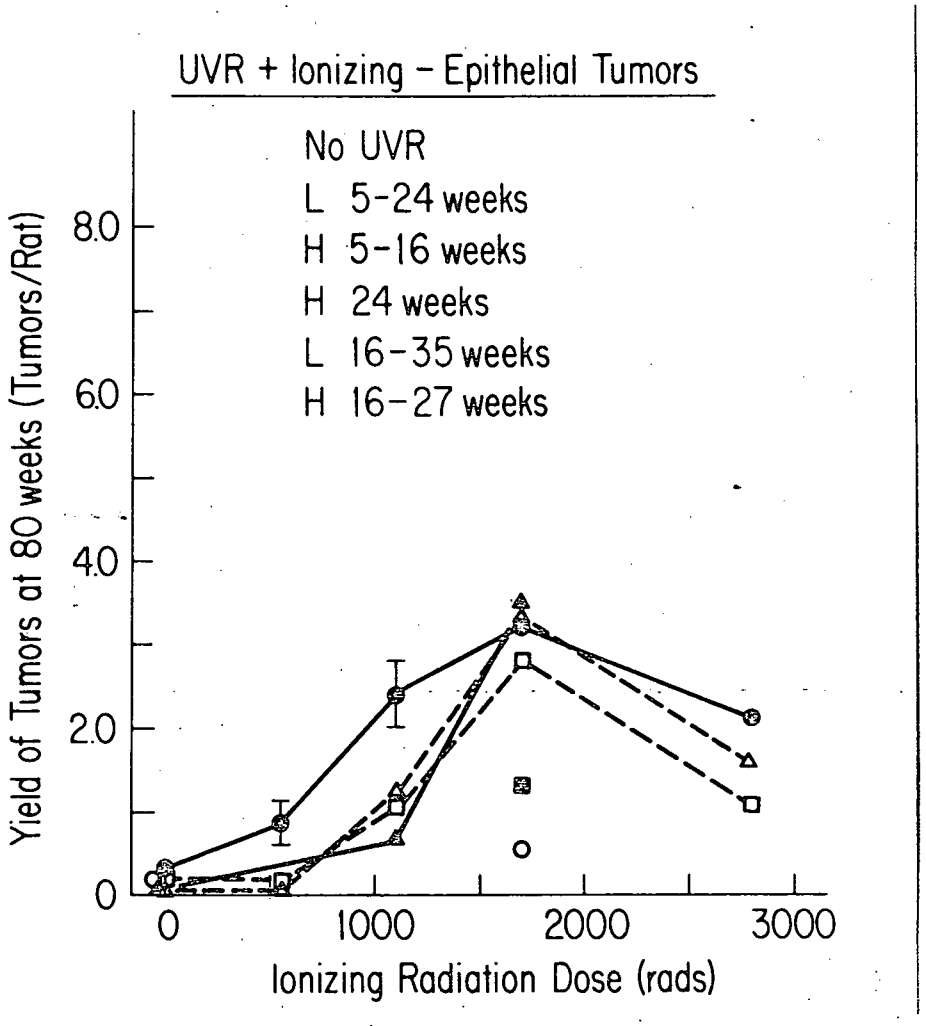

Figure 28. Epithelial skin tumor yield at 80 weeks as a function of dose of electron radiation for rats exposed to 275-375 nm UVR for various periods of time and fluences as indicated. High fluence (H) was 25.2 x 10^4 joules/m^2 and low fluence (L) was 8.4 x 10^4 joules/m^2 given in weekly increments.

UVR treatment schedules. The shape of the electron dose-response relationship (without UVR treatment) is similar to many previous experiments completed in this laboratory and is characterized

by an increase in response between 500 rads and 2000 rads, and a decrease in response at doses greater than 2000 rads. The additional treatment with UVR after electron treatment does not exhibit any consistent influence on the epidermal tumor yields.

One UVR treatment schedule (25.2×10^5 ergs/mm^2 in 12 weekly fractions beginning at week 5) appears to enhance the yields at 550 rads and 1100 rads compared to (no UVR) control groups. However, some of this increase (0.36 tumors per rat) is observed at the zero electron dose group indicating that some epidermal tumors are produced by the UVR treatment alone. Neither of these two slight increases is significant at $p = .05$.

Two UVR treatment groups at 1700 rads exhibit a lower yield than the comparable (no UVR) group. These differences are significant at $p < .0001$. These two groups received protracted UVR treatment beginning at 16 weeks of age in contrast to all other UVR groups which began fractionated treatment early (5 weeks) or received a single treatment (at 24 weeks). Therefore, the two groups with decreased yields received a substantial portion of their UVR treatment during the period when epidermal tumors were beginning to appear (20-32 weeks). This implies that protracted UVR treatment after tumors began appearing may have inhibited their growth.

The results in Figure 29 show the yield of epithelial tumors in rats exposed only to UVR radiation as indicated. The yield

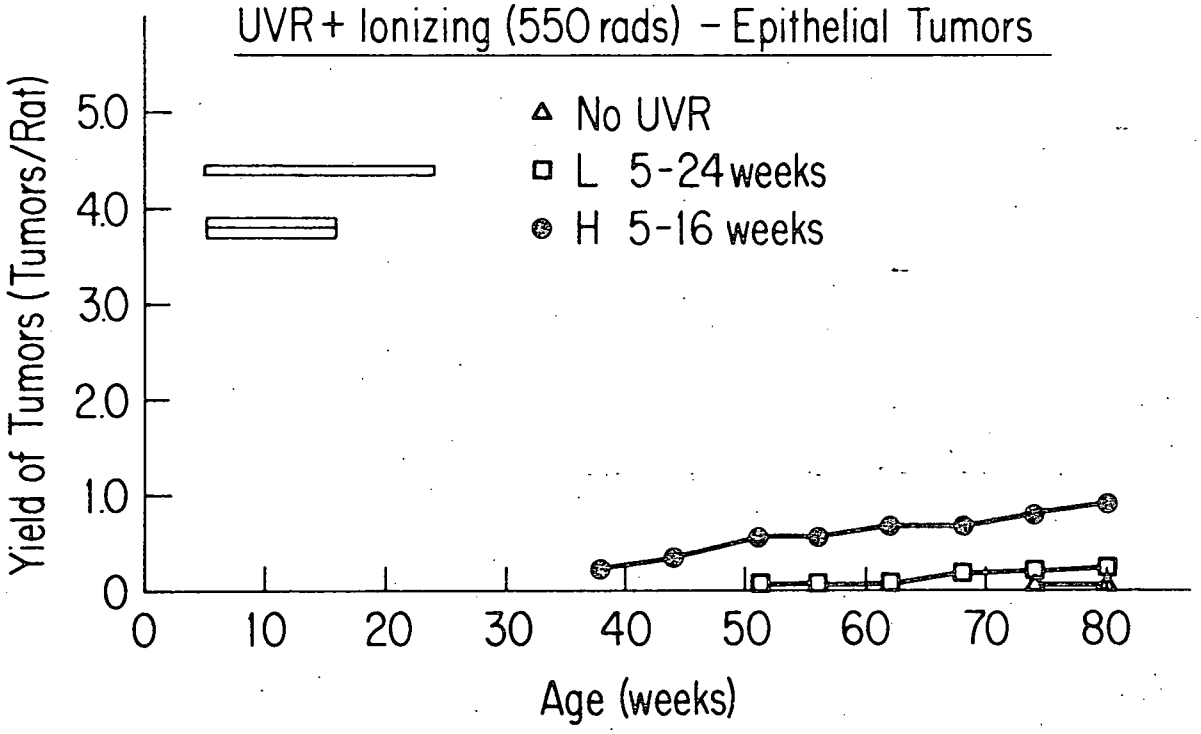

Figure 29. Epithelial tumor yield as a function of age for rats irradiated with high (H) or low (L) fluences of 275-375 nm UVR radiation for various periods of time as indicated by the horizontal bars on the figure.

of tumors was very low at both low and high fluences of UVR radiation. These results indicate that ultraviolet radiation is a very poor inducer of the type of tumors induced by ionizing radiation. The ultraviolet radiation induces mainly

keratoacanthomas, which are benign cystic lesions that are clearly distinguishable from the malignant tumors induced by ionizing radiation.

Figure 30 shows the yield of epithelial tumors as a function

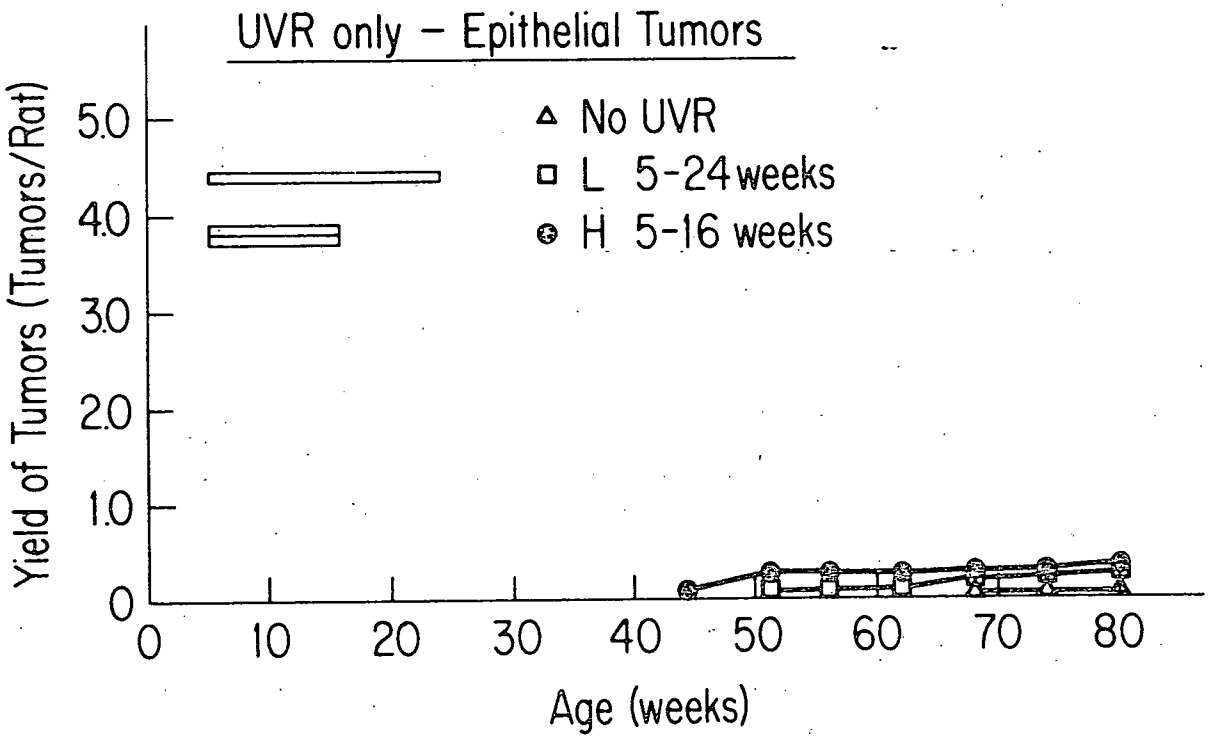

Figure 30. Epithelial skin tumor yield as a function of age for rats irradiated with 550 rads of electron radiation at 4 weeks of age and then with 275-375 nm UVR radiation for various periods of time as indicated by the horizontal bars on the figure. H and L refer to high and low fluence of UVR.

of age in rats that received 550 rads of electron radiation at 4 weeks of age followed by various doses of UVR radiation as indicated. The dose of electrons is low and alone induced very few tumors, however, there was a considerable increase (nearly a factor of 10) in epithelial tumors in rats that received the UVR radiation especially at the higher dose. These results suggest that UVR radiation is capable of enhancing tumors induced by ionizing radiation at the lower doses, although no such enhancement was apparent at the higher doses of ionizing radiation.

Enhancement of epithelial tumor yield was apparent at 1100 rads of electron radiation, especially at the high fluence of UVR radiation (see Figure 31). Nearly twice as many epithelial tumors were present at 80 weeks in the high fluence UVR radiation group as in the group that received only electron radiation. The magnitude of the enhancement was considerably less than for the lower dose of electron radiation but still greater than observed for an even higher dose of electrons.

When the rats were irradiated with 1700 rads of electron radiation, the ultraviolet exposure that produced an enhancement of epithelial tumor yield at the lower electron doses now produced no enhancement (see Figure 32). When the same UVR fluence was extended for a longer period of time the yield of epithelial tumors was decreased as if the UVR had inhibited the growth or

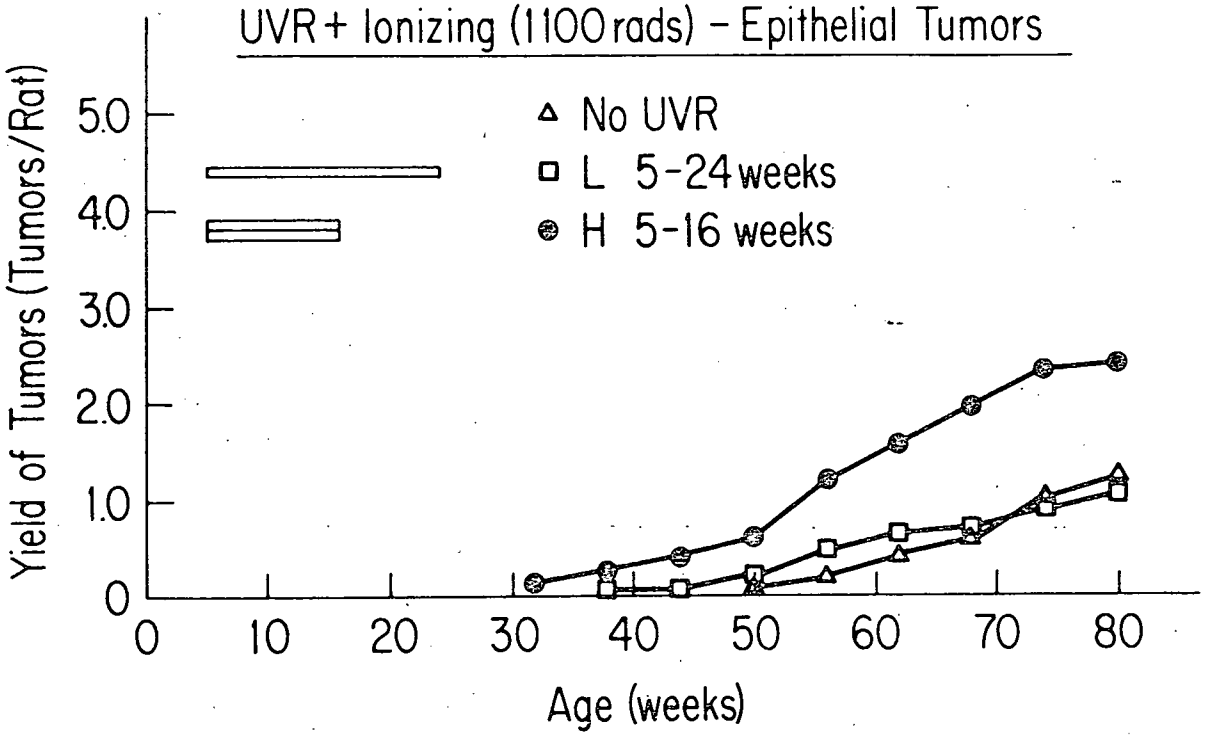

Figure 31. Epithelial skin tumor yield as a function of age for rats irradiated with 1100 rads of electron radiation at 4 weeks of age followed by 275-375 nm UVR radiation for various times as indicated by the horizontal bars on the figure. H and L refer to high and low fluence of UVR.

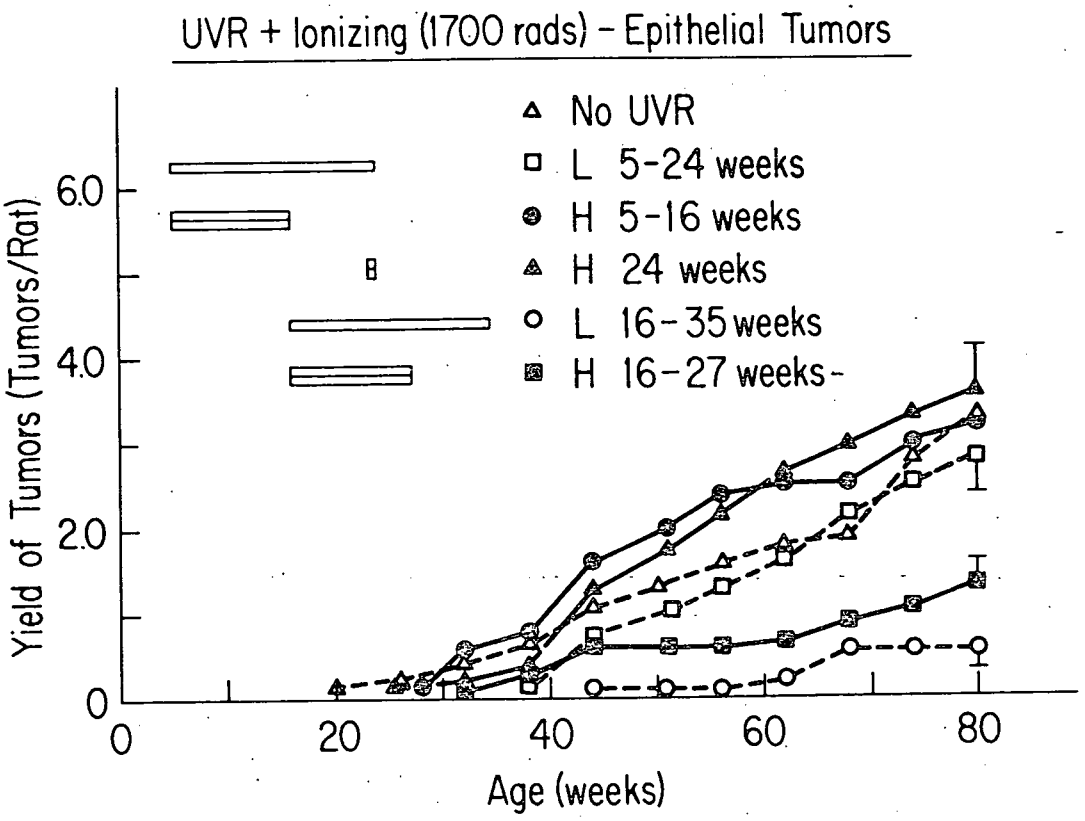

Figure 32. Epithelial skin tumor yield as a function of age for rats irradiated with 1700 rads of electron radiation at 4 weeks of age followed by 275-375 nm UVR radiation for various times as indicated by the horizontal bars on the figure. H and L refer to high and low fluence of UVR.

development of the electron-induced tumors. The inhibition was observed only when the UVR exposures extended into the time when the electron-induced tumors were beginning to appear. These results suggest that the UVR radiation can have an

enhancing effect on tumor development at low doses of ionizing radiation and an inhibitory effect at high doses of ionizing radiation under circumstances where the developing tumor cells are expected to be exposed to the ultraviolet radiation.

A considerable number of keratoacanthomas were induced in rats that received exposure to ultraviolet light as expected (Figure 33), although a few occurred in the group that received

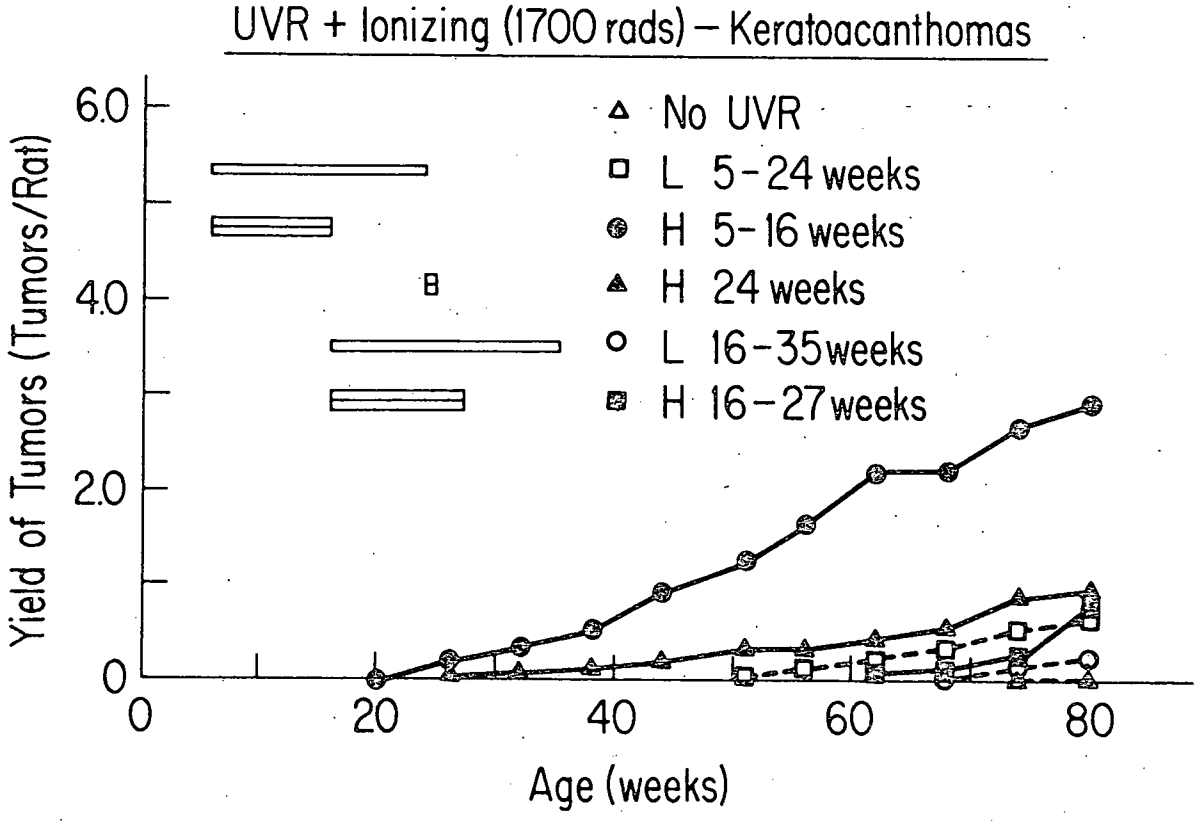

Figure 33. Keratoacanthoma yield as a function of age for rats irradiated with 1700 rads of electron radiation at 4 weeks of age followed by 275-375 nm UVR radiation for various times as indicated by the horizontal bars on the figure. H and L refer to high and low fluence of UVR.

only ionizing radiation. The early exposures to the UVR radiation were considerable more effective in producing keratoacanthomas than the later exposures and a single high exposure at 24 weeks was just about as effective as the same dosage given between 12 and 23 weeks. Similarly at the low UVR fluence the early exposure was more effective than the later exposure.

Discussion

The marked difference in tumor types induced by the two radiations may reflect differences in the oncogenic targets. It is interesting that the UVR induced tumors were exclusively keratinizing acanthomas, whereas the deeply penetrating electron radiation induced undifferentiated and sebaceous tumors. Thus, the cell population at risk may be different for these two radiations. If this is true, then the independent tumorigenic action of these agents may not be unexpected.

We did not observe the "summation" effect observed by other investigators in which non-oncogenic doses of two agents induced tumors when administered together in a combined treatment schedule.

An age effect was observed for keratoacanthoma induction with protracted UVR treatment. When weekly UVR exposures began at 5 weeks of age, the tumor yield was 3.7-4.1 times as great as when identical UVR treatments began at 16 weeks of age. The enhanced resistance to oncogenic insult with age is consistent

with previous studies in this laboratory with ionizing radiation in rat skin.

The absence of oncogenic interaction between UVR and electrons suggests that cellular or molecular changes leading to oncogenic transformation caused by either radiation do not affect analogous changes caused by the other radiation. For example, if we assume that single strand breaks in DNA caused by electrons result in transformed cells and pyrimidine dimers in DNA caused by UVR result in transformed cells; then the presence of DNA single strand breaks does not appear to alter production of pyrimidine dimers by subsequent UVR exposure.

Recovery and Dose Rate in Radiation Carcinogenesis of Rat Skin

Estimates of the risks of leukemia and other cancers from exposure to relatively high doses and dose rates of ionizing radiation are available from epidemiological studies of various exposed populations, such as, the Japanese A-bomb survivors, patients irradiated for ankylosing spondylitis, etc. (73, 74). However, most occupational and environmental exposures occur at much lower doses and dose rates, and at the present time no generally accepted rationale exists for extrapolating risks from relatively high doses to low doses where the data is either very poor or nonexistent (75). For making such extrapolations, not only must the dependence of tumor induction on dose be known, but also there must be information on possible effects

of dose rate when exposures are extended over long periods of time.

Dose rate could significantly affect tumor induction because of the occurrence of recovery which tends to reduce the biological effectiveness of certain types of ionizing radiation (76). Quantitative effects of recovery on tumor induction have not been clearly established in epidemiological studies, although there is evidence from experiments with animals that low dose rates are less effective in producing tumors than high dose rates (77, 78). As irradiation controls improve, opportunities for epidemiological studies diminish and we must rely on experiments with animals for establishing the importance of dose rate, age, etc. on the induction of tumors. Ultimately the applicability of the animal data to the estimation of human risks will have to be established through an understanding of the general principles that apply to different species.

An initial attempt to explain the role of recovery in tumor induction in rat skin has been made by postulating a two-stage model where one of the stages is reversible. The dose-response function derived from the model consists of the sum of linear and quadratic terms and is in reasonable agreement with tumor induction data. In the model, the dose rate effect on tumor induction depends on the recovery constant which can be measured experimentally by means of a split dose protocol.

The elements of the model are illustrated in Figure 34. Radiation may convert normal cells (designated S_1)

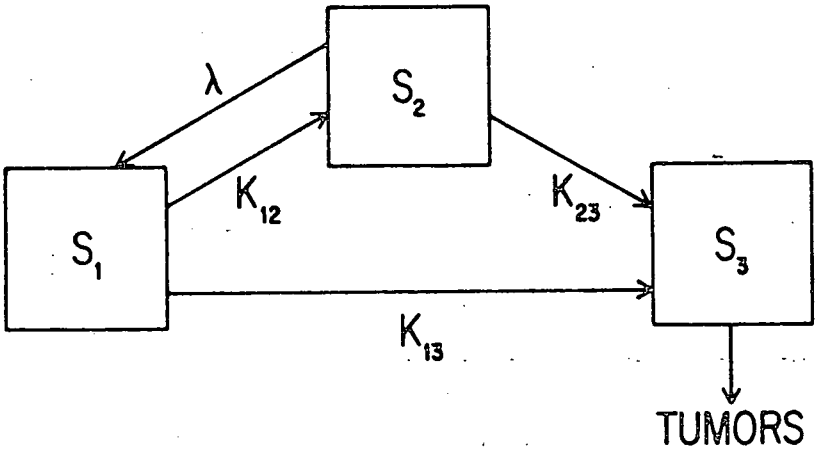

S_1: Initial state of unirradiated cells
S_2: State of reversible, suboncogenically damaged cells
S_3: State of irreversibly damaged, potential tumor cells
K_{ij}: Transition constant of cells from state i to j under the influence of radiation (rad^{-1})
λ: Recovery rate constant of reversibly damaged cells (h^{-1}).

Figure 34. A model for the induction of tumors by radiation. Initially all cells are in state S_1, and as the result of irradiation are induced to state S_3, tumor precursor cells.

to potentially neoplastic cells (designated S_3) by one of two routes, either a two step route with a reversible first step (designated S_2) or a route involving a single irreversible step. Each step is assumed to occur in proportion to dose in single cells, but the identity of the change and its site of occurrence within the cell need not be specified. If cells are converted to S_2 they may either revert back to S_1 or an equivalent state or be converted by further radiation action to S_3. The following differential equations describe these various transitions:

(1) $\frac{dS_2}{dt} = S_1K_{12}r - S_2(\lambda + K_{23}r)$

(2) $\frac{dS_3}{dt} = K_{23}rS_2(t) + K_{13}rS_1(t)$,

where S represents the number of cells in the respective states, the K's are proportionality constants, λ is the recovery rate constant and r and t are the dose rate and exposure times, respectively. Since the production of a few cancer cells is not expected to deplete significantly the relatively large population of normal cells, S_1 can be taken as constant. The exact solution for S_3 is somewhat complicated but can be simplified by considering certain limits. When the exposure time t is very short in comparison to the mean time cells spend in S_2, i.e., the exposure is 'acute' and $t << 1/(\lambda + K_{23}r)$ the solution is:

(3) $S_{3a}(d) = S(K_{13}D + \frac{K_{12}K_{23}}{2} D^2)$

where the subscript 'a' indicates acute exposure. Equation 3

s a special case of the general form $S_{3a} = AD + BD^2$, i.e., a linear term plus a quadratic term.

Another limit exists when the dose rate is so low that $K_{23}r << \lambda$ and $t >> 1/\lambda$, i.e., cells enter S_2 much more slowly than they leave, and the exposure time is much longer than the reciprocal of λ. Within the above limits the solution is:

(4) $S_{3p}(D) = S(K_{13}D + \frac{K_{12}K_{23}}{\lambda} rD)$

where 'p' indicates protracted exposure. In equation 4, S_{3p} is linear with total dose for a given dose rate and with dose rate for a given dose.

The model postulates an S_3 population which unfortunately cannot be detected directly but must be inferred by the presence of tumors. The relationship between tumor yield (y) and S_3 is assumed to be a simple proportionality, i.e., $y = CS_3$. Since C must be independent of dose, it is assumed that events intervening between the formation of S_3 cells and their eventual expression as tumors are not influenced by radiation.

The quantitative expression of tumor yield may differ for different organs and types of tumors. Skin tumors tend to occur at a constant rate, I, after an initial tumor-free interval, and these rates were utilized as time-independent measures of yield. The measurable quantity, I, was substituted

for S_3 in equations 3 and 4.

An initial question that needs to be answered is whether the general form of equation 3 is consistent with the experimental dose-response data, i.e., can the coefficients of the linear and quadratic terms in equation 3 be evaluated? This is best done by plotting the tumor response per unit dose versus dose, because in such a plot the data should be linear with a slope of B and an y axis intercept of A. Such data for the induction of tumors in rat skin with electrons, protons and alpha particles are shown in Figure 35. The data for electron and proton radiation indicate that if a linear term exists it must be very small and probably does not contribute more than about 10% to the total response. A measurable linear term does exist for alpha particles which have a mean LET value considerably higher than for electrons or protons.

The expected dependence of tumor response on dose rate is contained in equation 4 and can be expressed in terms of the response at high dose rates by defining a dose rate factor (DRF) as the ratio of dose (D_p) at low dose rate to dose (D_a) at high dose rate for the same tumor response. The DRF may be calculated by equating equations 3 and 4 and solving for D_a/D_p. The result is:

(5) $DRF = 1-R(1-2r/\lambda\ D_a)$

Equation 5 specifies that the effect of dose rate, r, on tumor

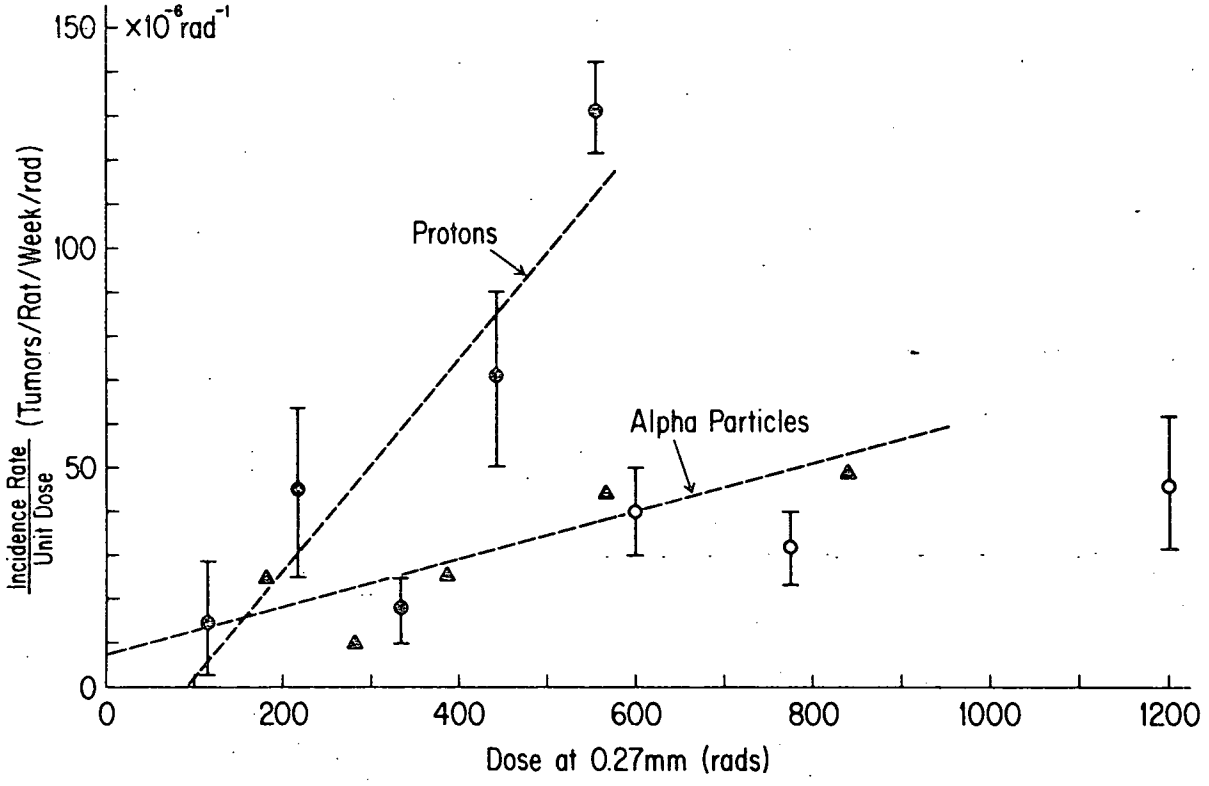

Figure 35: Tumor yield per unit dose as a function of dose for single exposures to protons 10 Kev/μ or alpha particles (40 Kev/μ).

induction can be calculated for any given equivalent acute dose, D_a, provided values can be assigned to λ and R. The general form of R is the ratio of the effect produced solely by the two step mode to the total effect, i.e.,

$$(6)\quad R = \frac{A_2 D_a^2}{A_1 D_a + A_2 D_a^2}$$

In principle, A_1 and A_2 would be determined from the dose-response curve, but as already noted, A_1 was too small to measure for electron radiation. If A_1 were in fact zero, R would equal 1 and the expression for DRF would be:

$$(7)\quad DRF = \frac{2r}{\lambda D_a}$$

Equation 7 indicates a progressively decreasing effectiveness with declining dose rate. For various mixtures of linear and quadratic terms the dose rate effect would occur in accordance with the relative magnitude of the quadratic term. If even a very tiny linear term exists, the DRF would approach a plateau of 1-R at low dose rates. The data in Figure 35 indicate that R for electrons is probably greater than 90%. On the basis of a model derived by Rossi and Kellerer from biophysical considerations, the K could be as high as 98% (79).

A value must be obtained for λ, the recovery constant, in order that DRF functions can be calculated numerically. Experiments were undertaken to measure λ for tumor induction on the basis of the rationale that after a given dose D_1 at high dose rate the persistence of S_2 cells would be indicated by the response to a second dose given at same later time, t. It can be calculated that S_2 cells ought to persist in accordance with the equation:

(8) $S'_2(t) = S_2(0)e^{-\lambda t}$

Equation 8 indicates that eventually the entire population of S_2 cells will be depleted. Nevertheless, D_1 itself will produce a response in accordance with equation 3.

For the measurement of λ, equation 8 must be expressed in terms of measurable quantities. A general expression for the amount of unrecovered effect, i.e., in the model the proportion S_2 cells still remaining, can be derived as follows. If I represents tumor yield, the difference in response between split and single doses can be represented by $I(D_1,D_2,0)-I(D_1,D_2,t)$ where $D_1 + D_2 = D$ is the total dose between fractions. The zero in the first term indicates no time between exposures which is equivalent to a single dose of multiple D. Since recovery is detectible by the difference in response between single and fractionated doses, it would be natural to express recovery quantitatively as the actual difference in response as a fraction of the maximum possible difference. Since the maximum difference in response would be expected if t were very long or effectively infinite, recovery (R_e) can be expressed as follows:

(9) $$R_e = \frac{I(D,0) - I(D_1,D_2,t)}{I(D,0) - I(D_1,D_2,\infty)}$$

Accordingly, the amount of effect not recovered (p) is given by:

$$(10)\quad p = 1-R_e = \frac{I(D_1,D_2,t) - I(D_1,D_2,\infty)}{I(D,O) - I(D_1,D_2,\infty)}$$

which can be shown mathematically to be equivalent to $e^{-\lambda t}$ in equation 8. Hence, equation 10 provides an experimental basis for the measurement of λ.

Procedures and Materials Used

Male (CD strain) rats obtained from Charles River Co., Brookline, Massachusetts, were housed two per cage and fed Purina Laboratory Chow (Ralston Purina, St. Louis, Missouri) and water ad libitum. The rats were irradiated at 28 days of age on a 2 x 5 cm area approximately centered on the dorsal skin surface. Three days prior to irradiation the hair was clipped and animals exhibiting hair regrowth within 7 days of irradiation were eliminated from the experiment in order to insure that all the animals were in the telogen (resting) phase of the hair growth at the time of irradiation.

Irradiations were performed on the Van de Graaff accelerator at the Union Carbide Research Laboratory in Tuxedo, N.Y. The beam consisted of 0.7 Mev electrons at a current of 200 μA. The primary beam was far too intense for the direct exposure of the rats, and the dose rate was reduced by passing the beam through a 0.6 cm diameter orifice in a large (100 cm x 100 cm) lucite shield (0.6 cm in thickness) and by placing the rats as far as possible (130 cm) from the end of the beam pipe. The above configuration produced a radiation field with less than

10% dose variation sufficiently large to irradiate about 20 rats simultaneously.

Dose measurements were made with a 1.0 mm gap, parallel-plate ionization chamber. The electrons penetrated about 1.0 mm and results were expressed in terms of the dose at about 0.3 mm which has been found previously to correlate best with the tumor response. In the beam the dose rate was about 120 rads per min. The protocol of the experiment consisted of 9 single doses in order to establish the shape of the dose-response curve, and at three doses the exposures were split into two equal doses spaced at intervals of 15 min., 1 hr., 3.2 hrs. and 6.3 hrs. The irradiated area was outlined with a felt tipped pen to indicate the skin actually exposed to the radiation in order to insure proper alignment during reirradiation. About 5 min. prior to irradiation the rats were anesthetized with intraperitoneal injections of 30 mg/kg Nembutal (sodium pentobarbital) Abbott Laboratories, North Chicago, Ill.

Notations were made of the skin response every 6 or 8 weeks and photographs were made of each lesion when it was first observed and periodically thereafter. The tumor response in each observation interval was obtained as the average appearance rate of new tumors in the interval, and the cumulative response from the time of irradiation to the midpoint of any later interval was the sum of appearance rates in preceding intervals.

Specifically, if n were the number of new tumors in an interval, L the numbers of animals at the start of the interval and d the number of deaths in the interval, appearance rate was $n/(L-d/2)$. Sketches were made from the photographs in order that each tumor could be identified, assigned a time of occurrence, and examined histologically at the time of death. Only histologically-confirmed tumors were included in the analysis. The experiment was terminated at either 52 weeks or 64 weeks and all rats surviving to these times were killed in order to obtain histological samples of the tumors.

Results

For single doses the tumor appearance rates were generally constant after tumor-free intervals that ranged from 10 to 20 weeks. Mean rates and standard errors are shown in Figure 36 as a function of dose. The 'peaked' shape is typical of dose-response curves observed previously for rat skin and, as already indicated, the ascending limb is consistent with a dose-squared function.

Mean tumor appearance rates as a function of time between split doses are shown in Figure 37. For the lowest dose the data are somewhat variable, however, a general decline in tumor yield with time between doses was apparent. No residual effect of the first dose was detectible at 6 hours. Similarly for the intermediate dose, a declining trend with time between exposures

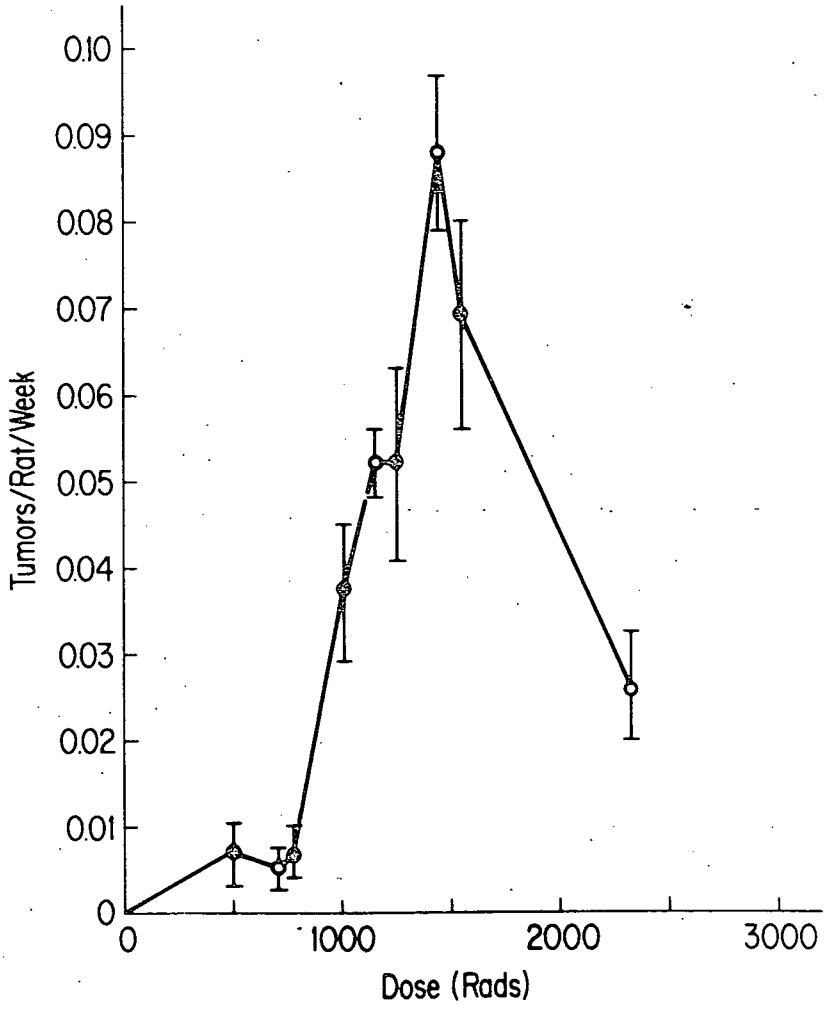

Figure 36. The tumor response curve for single doses of electrons. The rate of new tumor appearance increases up to a peak tumor yield dose at about 1400 rads.

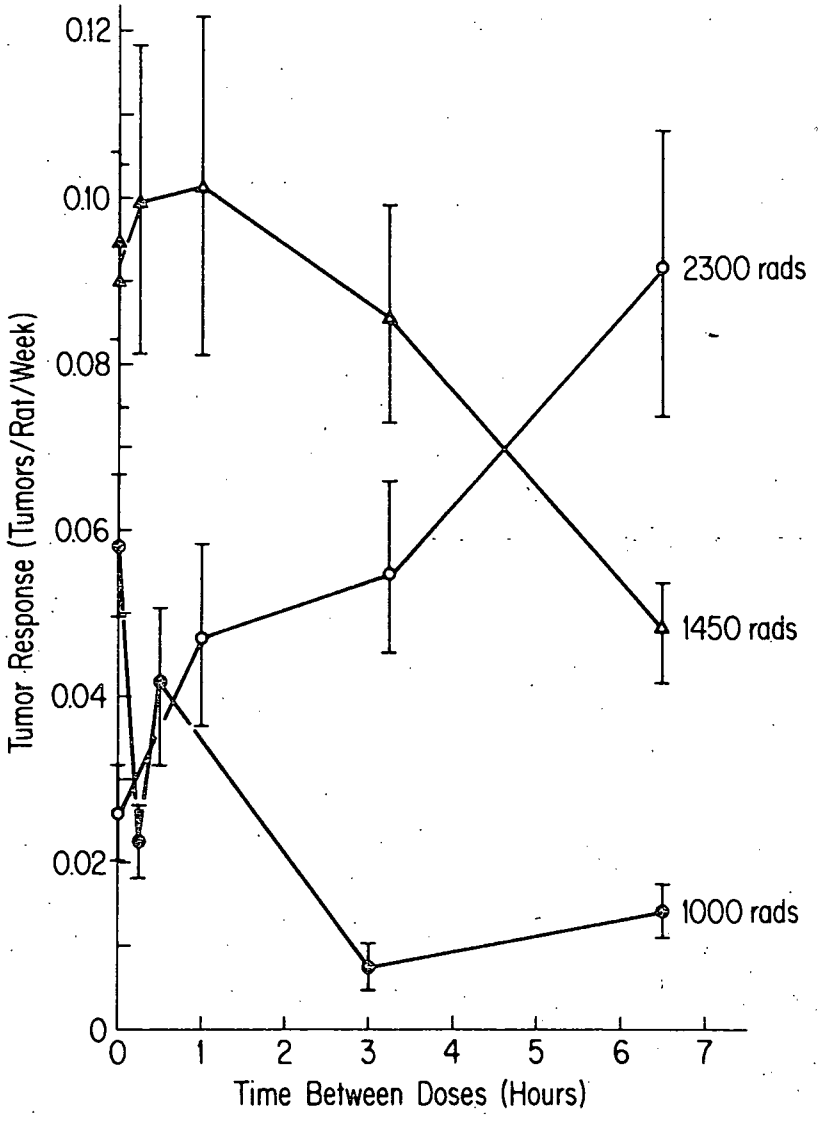

Figure 37. The mean tumor appearance rates following total doses of 1000, 1450, or 2300 rads given in two equal dose fractions as a function of time between the doses.

was apparent. The increasing trend for the highest dose was also consistent with the occurrence of recovery in the sense that on the descending limbs of the response curve a shift to lower effective doses would be expected to increase the yield.

Discussion

The tumor induction data expressed in accordance with equation 10 and plotted against time between exposures are shown in Figure 38. The data from the highest dose was not included because it occurred on the descending limb of the dose-response curve where cell lethality was severe. The intermediate dose was in the vicinity of the tumor peak and a modest correction for lethality was made by dividing the tumor yield by the fraction of surviving hair follicles. The best fitting straight line on the basis of a least squares analysis provides an estimate of $\lambda = 0.4$ hr.$^{-1}$ which is roughly equivalent to a recovery half-time of 3.5 hrs.

With $\lambda = 0.4$ hr.$^{-1}$ the DRF functions for tumor induction are shown in Figure 39 for several doses. If there were no linear term in the dose-response curve, the curve labeled R = 1 would be expected. The curve labeled R = .925 would be expected if the linear term were .075% of the response and the curve labeled R = 0.999 would be expected if the linear term were .1% of the response. Only through additional experimentation can the appropriate curve be determined, but clearly in the dose

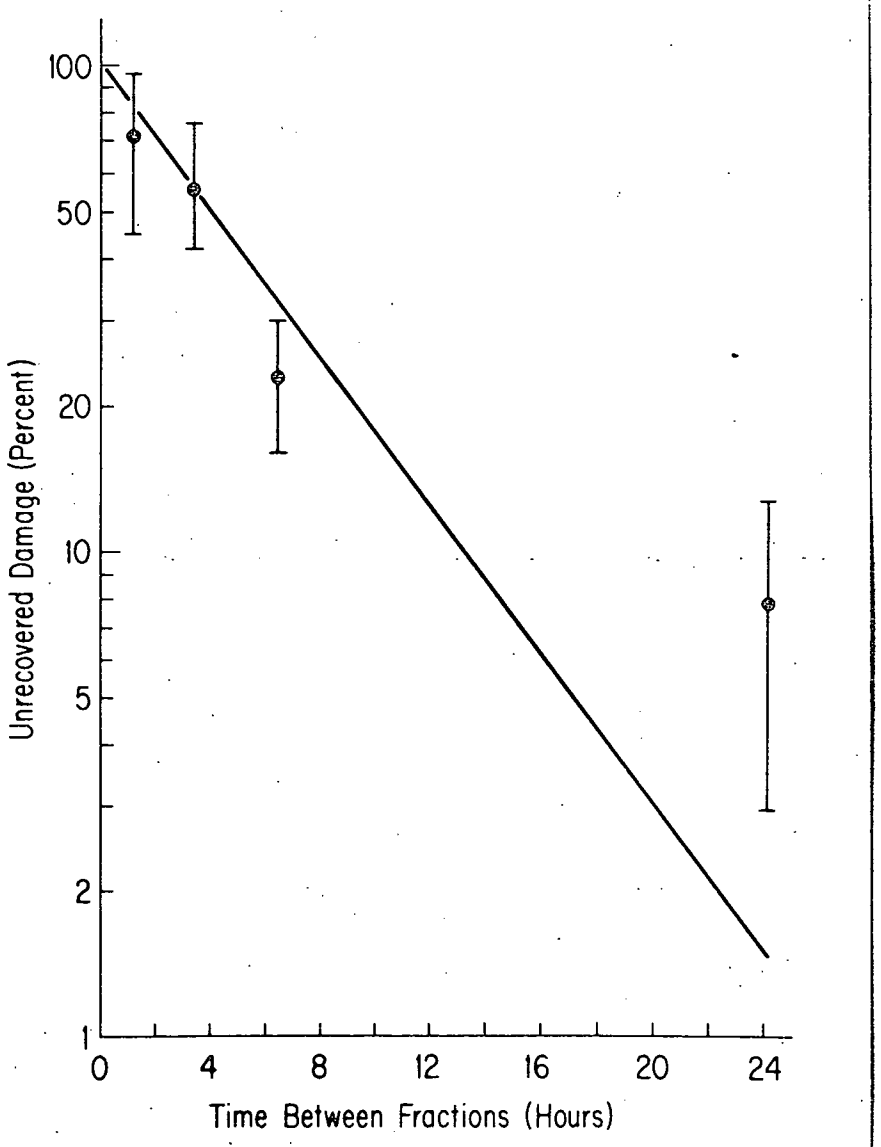

Figure 38. The fraction of unrecovered oncogenic injury remaining as a function of time between dose fractions.

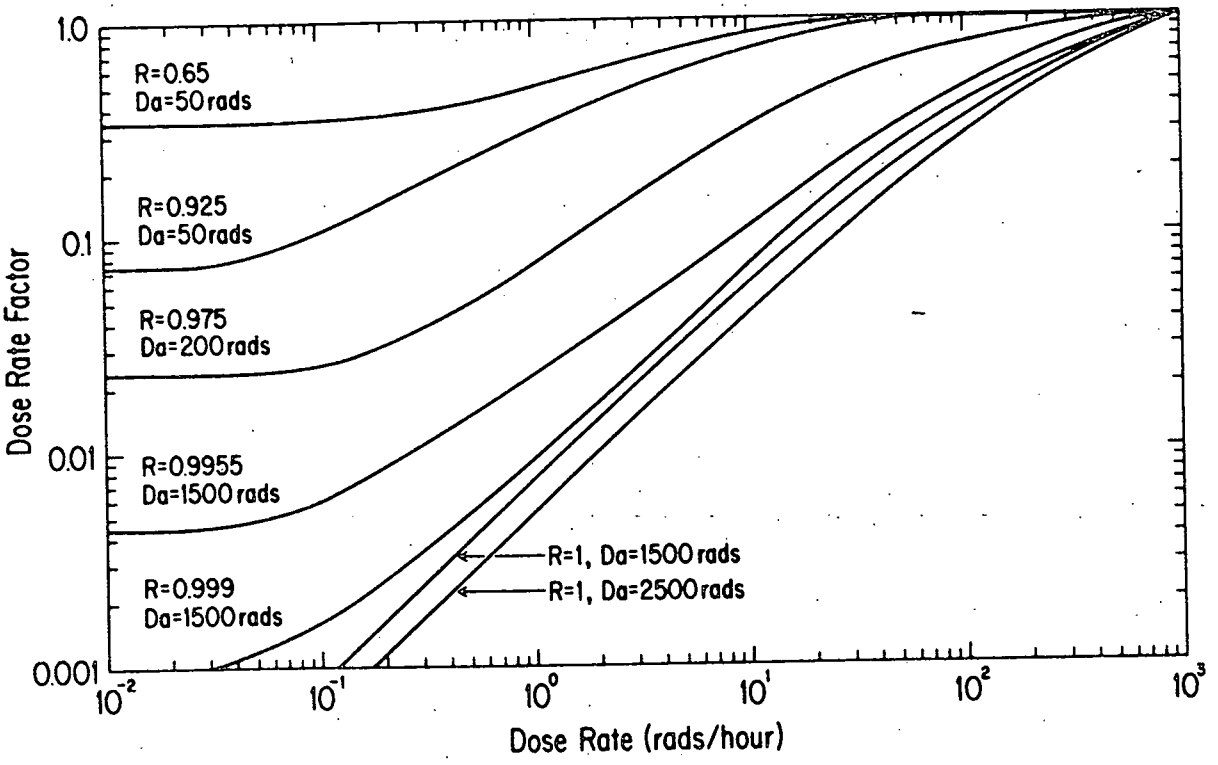

Figure 39. The Dose Rate Factor (DRF) as a function of dose rate for several doses and values for constants in the model.

rate range from 0.01 to 1.0 rads/hr. DRF values may range from 0.001 to 0.1 depending upon assumptions made about the nature of the dose-response curve.

For a given A_1 and A_2 values the value of R tends to decline as the dose declines and correspondingly the DRF value

rises, such that, as the dose approaches the dose of background radiation, i.e., in the range from 0.1 to 10 rads, the DRF becomes very nearly 1.0, and the effect of a dose given in minutes would be about equivalent to the effect of the same dose extended over a period of months or years.

The general features of the DRF functions in Figure 39 may apply to other types of radiation provided that split-dose recovery can be demonstrated and λ values are comparable to values observed for electrons. So far the evidence suggests that for 24 hr. fractionation intervals, protons and X-rays exhibit considerable recovery although λ values are not available (80). Other types of radiation, such as, alpha particles, remain to be tested for recovery, although the possibility of a substantial linear term in the dose-response curve for alpha particles would tend to minimize the effect of recovery on dose rate.

The implication of these results and calculations is that dose rate could be an important determinant of the carcinogenic effect of radiation, especially in the intermediate ranges of dose and dose rate, such as might be encountered in certain occupational exposures. On the other hand, at very low doses the dose rate effect would be effectively abolished if the dose-response function contained even a very small linear term and at dose levels approaching background doses prudence would lead

to the exclusion of dose rate effects on risk estimation.

Comparison of the Incidence and Time Patterns of Radiation-Induced Skin Cancer in Humans and Rats

Extensive use is being made of animal models for the purpose of assessing carcinogenic risks to humans from physical and chemical agents in the environment. Consequently, there is a critical need to obtain as much information as possible on the comparative carcinogenic responses of humans and animals. Extensive studies have been done at the Institute of Environmental Medicine during the past decade on the oncogenic response of rat skin to various types of ionizing radiation and on the pattern of skin tumor occurrence in the scalps of about 2200 patients who were given therapeutic X-ray treatments for Tinea capitis (ringworm) as children (81, 82, 83). These data provide an opportunity to compare tumor responses between human and rat in a comparable tissue under comparable conditions of exposure.

Materials and Methods

A group of 2213 individuals who were irradiated for Tinea capitis and a group of 1396 controls who were treated by some other means for Tinea capitis have been located and surveys have been made of their health status in 1967, 1972 and most recently in 1977. These individuals were treated at the NYU Hospital Skin and Cancer Unit between the years 1940 and 1959. The

irradiated and control groups are closely matched for age at time of treatment, race, years of education and elapsed time since treatment. When an individual indicated by questionnaire that a tumor had occurred, the time of occurrence, type of tumor and treatment were ascertained from the patient and appropriate physicians or health officials.

The dosimetry of the so-called, Adamson-Kienbock procedure has been extensively documented. The X-ray beam was nominally 100 KVP with only the inherent filtration of the X-ray tube. The head was irradiated in 5 separate exposures of approximately equal duration as follows: front, back, left, right and top. The entire procedure usually required about 1 hour. Lead plaques were placed over the eyes and ears for all but the back irradiation and a lead sheet was placed over the face almost up to the hairline for all but the back irradiation. Average doses measured in a phantom were as follows: scalp - 650 rads, brain - 140 rads, eyes - 50 rads, thyroid - 6 rads and internal ear - 70 rads.

Skin tumors were noted in relation to elapsed time since exposure for each individual and cumulated by means of standard statistical procedures. The ages of the irradiated and control groups were comparable at the time of treatment.

The rats (males only) were irradiated on their dorsal skin (24 cm^2) at 8 weeks of age with 30 KVP X-rays. These X-rays

penetrated with an half value layer of about 0.5 mm so that the internal organs received virtually no dose. The dose to the skin surface was 1100 rads given at a dose rate of about 300 rads/min. in a single exposure. Subsequent to irradiation the rats were observed every 6 weeks for 60 weeks. Tumors were scored when first observed but only if they persisted at the time of death or sacrifice. The method of analysis was the same as for the human tumors.

Results and Discussion

The temporal pattern of skin tumor onset as tumors per person (upper curve) and proportion of people with tumors (lower curve) is shown on log-log coordinates in Figure 40. The slope gives the exponent of the best-fitting power function, i.e., $P \sim t^{5.4}$, where P is either response and t is elapsed time since treatment. If the tumors were randomly distributed the two curves should be essentially identical since multiple tumors should be rare for values below 0.1 per person. The separation of the curves indicates that the tumors were not distributed randomly. In fact, closer inspection revealed 4 individuals having 33 tumors and the remaining 25 individuals having 37 tumors. It should be noted that the temporal trend in the upper curve where the 4 high responders were disproportionately represented is the same as in the lower curve where the high responders were relatively insignificant. The similarity in the trends indicates that

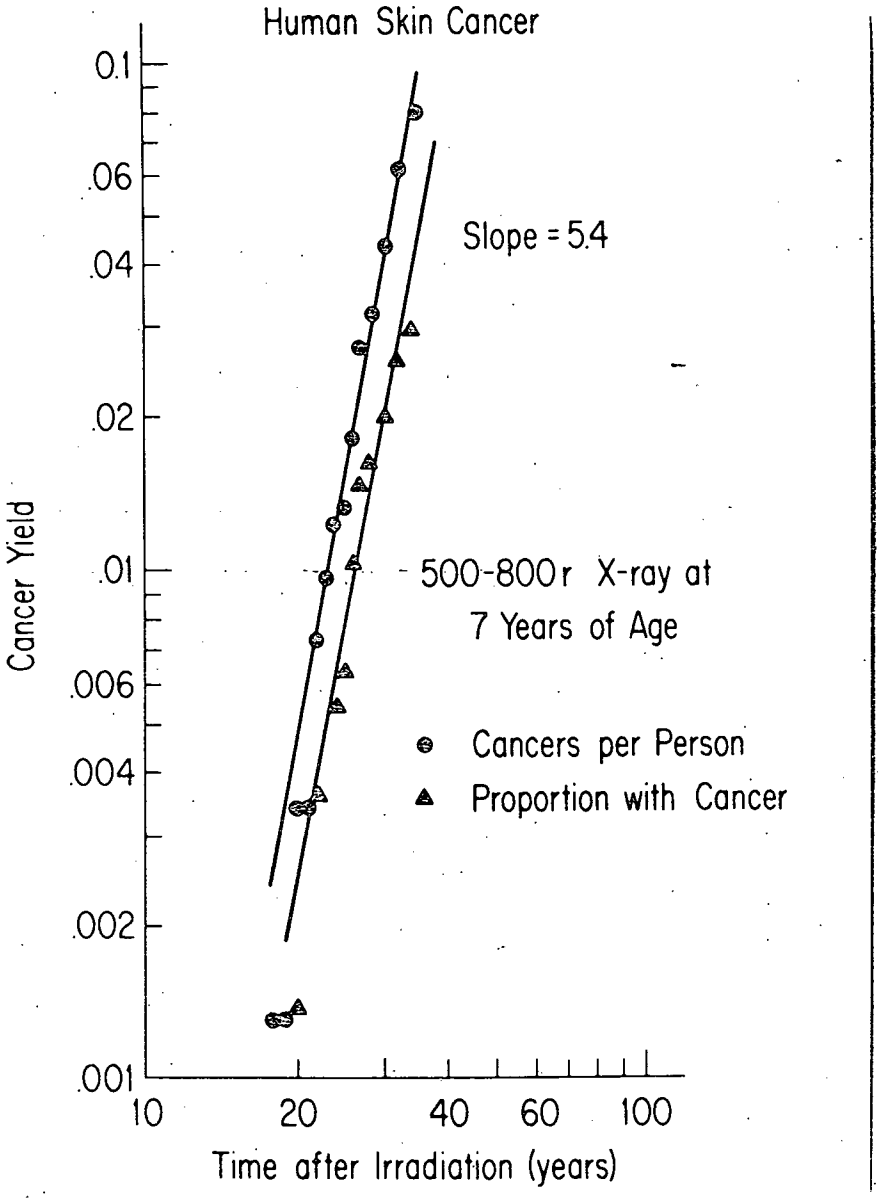

Figure 40. A log-log plot of skin cancers of the face and scalp among irradiated Tinea capitis patients as a function of time after irradiation. The lines shown have a slope of 5.4 which means that yield was proportional to $(\text{time})^{5.4}$. The tumors were exclusively basal cell carcinomas.

the temporal pattern was unaffected by the sensitivity of the individuals at risk.

Figure 41 shows the spatial distribution of the 64 skin tumors so far detected, excised and confirmed in the irradiated group. About half of these tumors occurred on skin that might have been exposed to ultraviolet light because of lack of hair cover. Such tumors could, of course, have been induced in part by the ultraviolet light. However, the lack of a substantial number of tumors in the controls, who were presumably as likely as the irradiated group to be exposed to ultraviolet light, suggests that the substantial numbers of tumors on the face, ears and neck were produced at least in part by the X-rays.

On the other hand, it is interesting that none of the non-white individuals (about 24% of the total) in the irradiated group have yet developed any skin tumors where about 8 cases would be expected in a comparable group of whites. The lack of tumors among nonwhites suggests that ultraviolet light may be a factor in producing the tumors observed in whites because the skin pigmentation in nonwhites would provide an effective screen against ultraviolet light without significantly affecting the X-ray dose. On the other hand, the lack of tumors among nonwhites may reflect a lower sensitivity of their skin to X-rays.

The temporal pattern of tumor response for the rat skin is

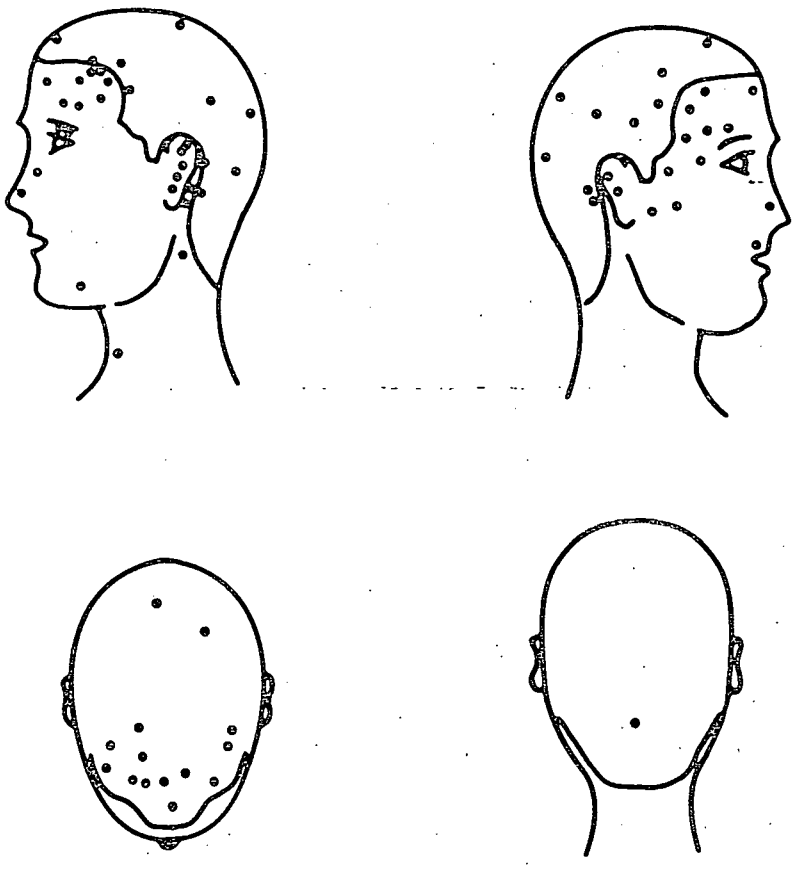

Figure 41. A scatter diagram showing the location of each of 64 cancers diagnosed and confirmed in the x-irradiated group.

shown in Figure 42 on the same log-log coordinates as for the

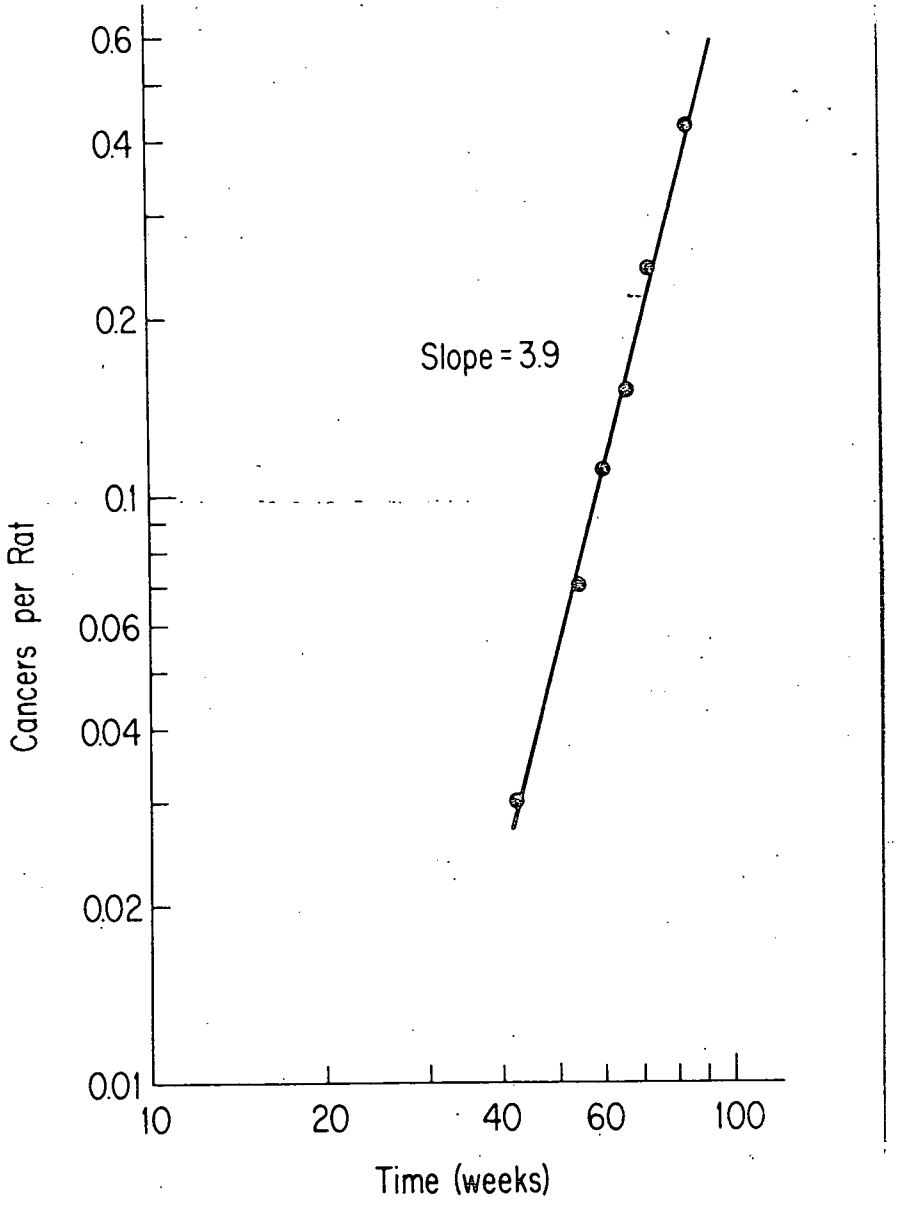

Figure 42. Cancers per rat as a function of time after exposure to a single 30 KVP X-ray dose of 1100 rads. The tumors were predominantly basal cell carcinomas and sebaceous cell tumors. There were 33 male rats in the group, and about 24 cm^2 of dorsal skin surface was irradiated on each rat.

human data. The power function exponent was 3.9 for the rat data, but the level of response was necessarily much higher in rats than in humans because of the relatively small number (33) of rats per group.

The same data as in Figures 41 and 42 are shown in Figure 43 on linear coordinates with a time scale ratio of 37.1 as

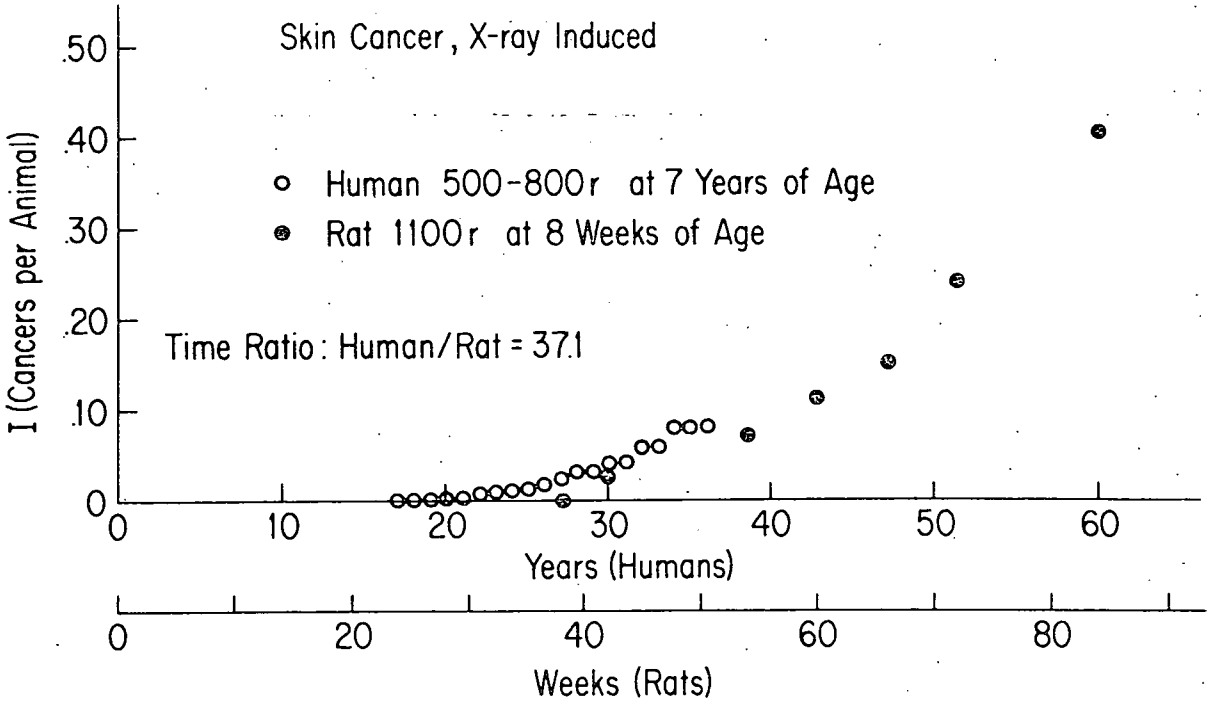

Figure 43. The cumulative number of cancers per animal for rats and humans are plotted on linear coordinates. The dose to human skin was about 500-800 rads and the dose to rat skin was 1100 rads. The time scale was shifted by a factor of 37.1 in order to approximately superimpose the two sets of data.

indicated. The scale factor was chosen to make the data as consistent as possible in the region where they overlap. If the human data were to continue following a power law with an exponent of 5.4, it would rise above the rat data in a relatively short time; certainly by 5 years. On the other hand, the human data could bend and follow the rat data at the higher incidence levels. Only a longer follow-up will resolve this issue.

These results suggest that human and rat skin are about equally susceptible to the carcinogenic action of x-irradiation under comparable conditions of exposure when allowance is made for the different times for expression of tumor development in the two species. That the time ratio is similar to the ratio of life spans is interesting and may mean that life span ratio provides a useful approximation for comparing temporal responses in different species.

Carcinogenesis in Rat Skin with 7,12-Dimethylbenz(a)anthracene and Ionizing Radiation

Carcinogenesis experiments were performed in order to determine whether prior irradiation would alter the susceptibility of rat skin to polycyclic hydrocarbons, and to establish the dose and temporal response of rat skin to chemical carcinogens.

The dorsal skins of 28 day male CD rats were irradiated with various doses (0, 500, 1000, 1500 and 2500) of

0.8 MeV electrons. One week after irradiation weekly doses of DMBA (7,12 dimethylbenz(a,h)anthracene) (20 µg, 100 µg or 500 µg) were applied topically in 1.0 ml of acetone to the irradiated area. Twenty animals were assigned to each dose group. Animals were autopsied at 76 weeks after the irradiation dose; tumors were excised and diagnosed histologically. Tumor yield was caclulated using standard life table analysis.

Figure 44 shows a log-log plot of tumor yield in tumors per rat versus time of weekly topical applications of DMBA at the doses indicated. The results show that the first appearance of DMBA induced tumors was dose-dependent and that tumor yield increased approximately as the 7th power of time and the 2.5nd power of dose. The tumor yield for DMBA were consistent with Blum-Druckrey reciprocity formula, i.e., $dt_{1.0}^{n}$ = constant, where d was DMBA dose rate, time was time to reach 1.0 tumors per rat, and n was empirically determined to be 2.8. Figure 45 shows the tumor yield in tumors per rat at 76 weeks as a function of radiation dose and DMBA treatment. It can be seen that the number of tumors (30-40/rat) induced by 100 µg/week. DMBA completely overwhelms the 1-4 tumors per rat induced by the radiation in animals exposed to both agents. The histological types of tumors produced by the DMBA were similar to those produced by the radiation. Figures 46 and 47 show the tumor yield as a function of time for animals receiving weekly

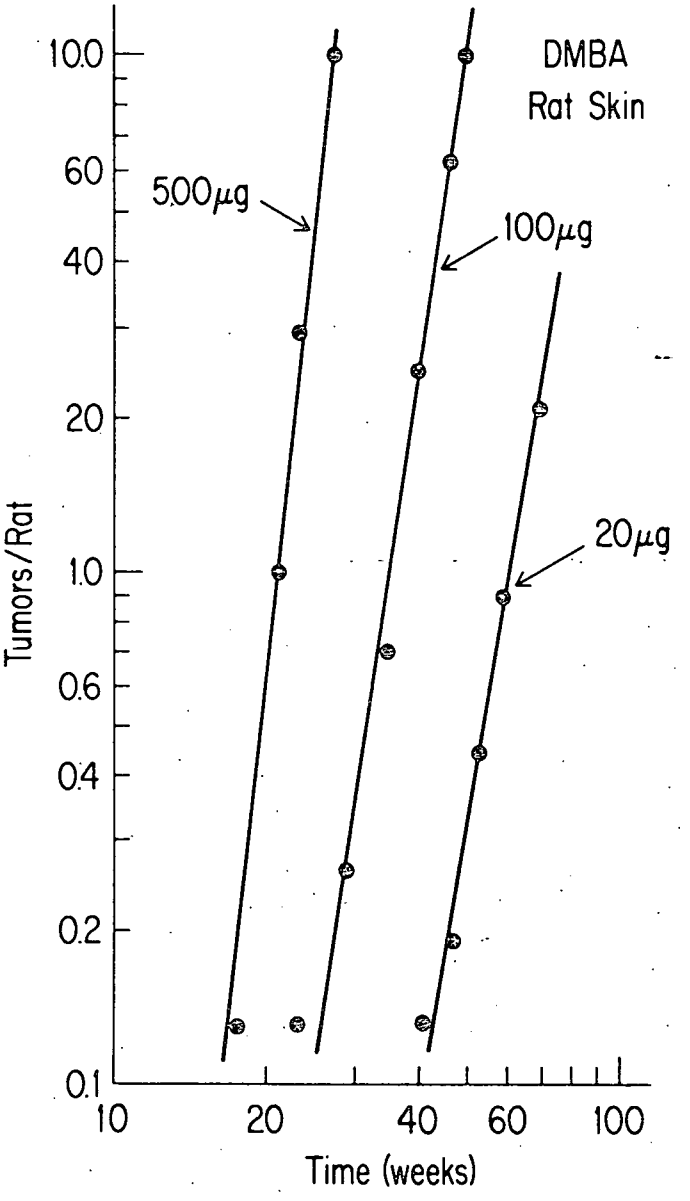

Figure 44. Log-log plot of tumor yield in tumors per rat as a function of time for weekly topical applications of DMBA doses as indicated.

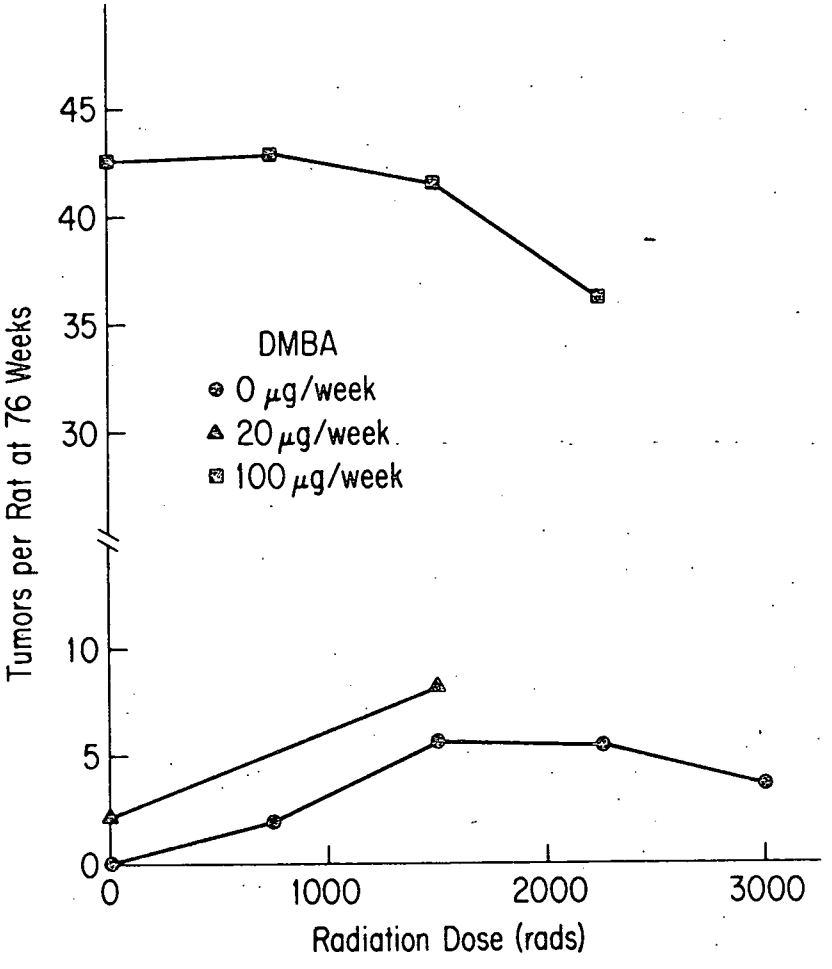

Figure 45. Tumor yield in tumors per rat at 76 weeks of age as a function of electron dose and DMBA treatment.

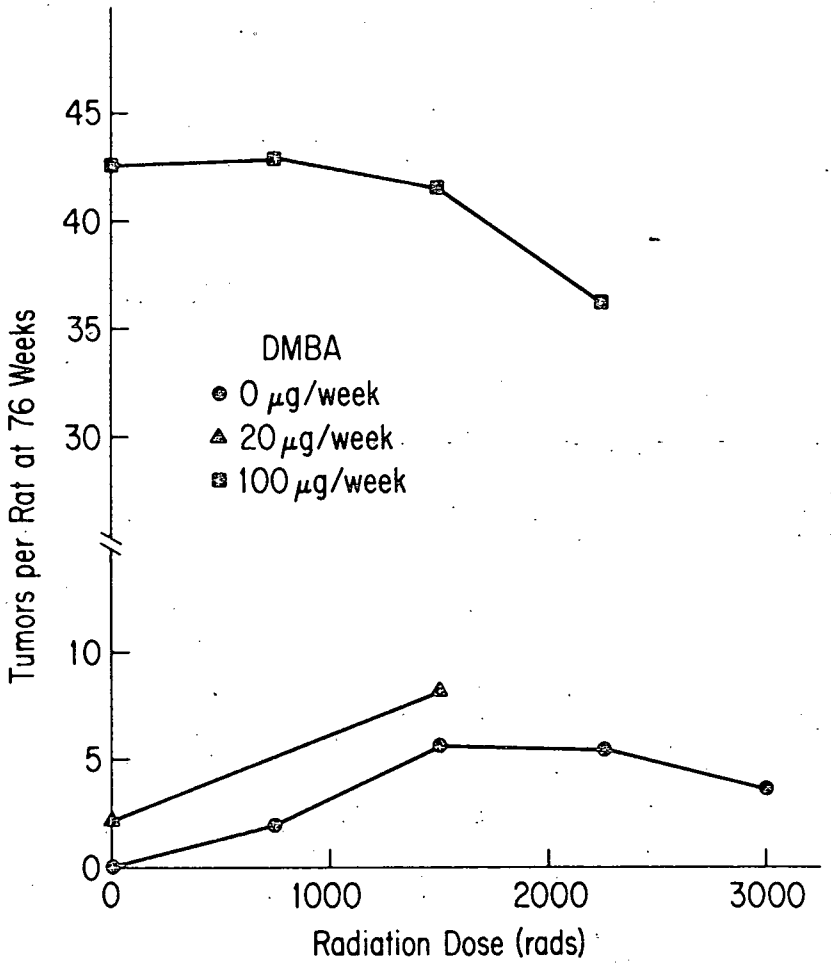

Figure 45. Tumor yield in tumors per rat at 76 weeks of age as a function of electron dose and DMBA treatment.

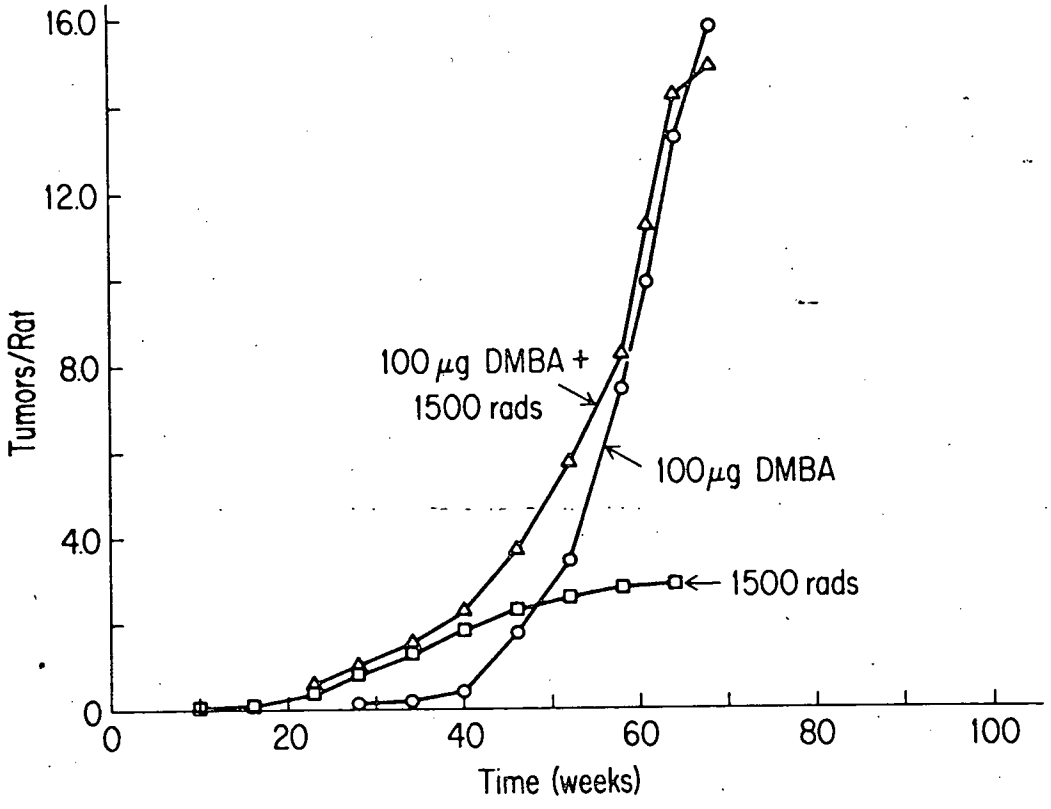

Figure 46. Tumor yield in tumors per rat as a function of time for animals given 1500 rads of 0.8 MeV electrons followed by weekly topical applications of 100 μg DMBA.

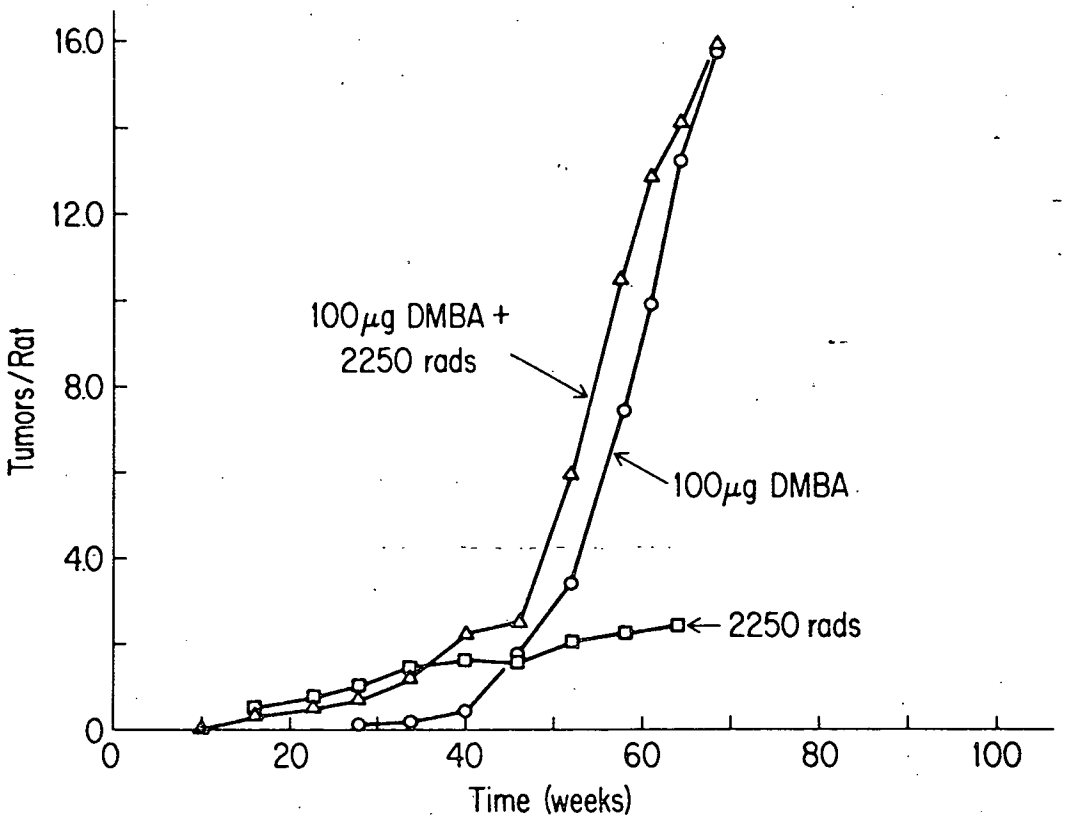

Figure 47. Tumor yield in tumors per rat as a function of time for animals given 2250 rads of 0.8 MeV electrons followed by weekly topical applications of 100 μg DMBA.

treatments of 100 μg DMBA and 1500 rads or 2250 rads, respectively, of electrons. The radiation-induced tumors began to appear by 15 weeks and tumor yield thereafter increased in approximate

proportion to elapsed time. It can be seen that the combined treatment with DMBA and either electron dose resulted in tumor yields which were approximately equal to the sum of the tumor yields induced by the separate treatments. Prior irradiation therefore did not alter the susceptibility of rat skin to DMBA carcinogenesis.

Dose-Response for Rat Skin Tumors Induced by Single and Split Doses of Argon Ions

Considerable attention has been given to establishing the dose-response for induction of tumors by low linear energy transfer (LET) radiations, such as, X-rays and electrons. It is firmly established that skin and other organs are capable of repairing part of the damage that eventually leads to induction of tumors if the radiation is low LET.

It is reasonable to expect on the basis of whole body irradiation with neutrons that oncogenic damage induced by high LET radiation is such that the tissue cannot recover. Certainly numerous studies have shown cells are incapable of repairing the lethal damage produced by high LET radiation. These lethality studies showed that the LET with the greatest biological effectiveness (RBE) was about 125 kev/μ above which the energy density becomes so great that energy is wasted and efficiency declines.

With the availability of the argon ion beam at Bevalac facility at Lawrence Radiation Laboratory, Berkeley,

California, it became feasible to study repair or recovery at the LET of maximum biological effectiveness. The plateau region of the Bragg ionization curve has an LET of about 12.5 kev/μ. The existence of extensive data on the dose-response curve for skin tumor induction in rat skin made this an ideal system for studying the RBE and repair at high LET values in a specific organ where whole body irradiation can be avoided.

Male CD strain rats (Charles River, Wilmington, Massachusetts) were arranged in small boxes in such a way that the skin could be drawn up through the top of the box and the beam passed through double thickness flaps of 20 rats simultaneously. The total skin thickness was about 6 cm in comparison to the 16 cm range of the argon ion beam in water. The area irradiated was about 12 cm^2.

The rats were irradiated with various doses in a matter of a few minutes. As seen in Figure 48, tumors began to appear by about 10 weeks in the higher dose groups and continued to appear more or less steadily until the end of the experiment at 99 weeks when overall survival was about 70%.

Similarly, when the dose was fractionated the tumors began to appear at 10 weeks and continued to appear throughout the experiment (Figure 49) at both doses. The fractionated exposures rather than reducing the yield of tumors as for fractionated electron radiation actually produced a slight

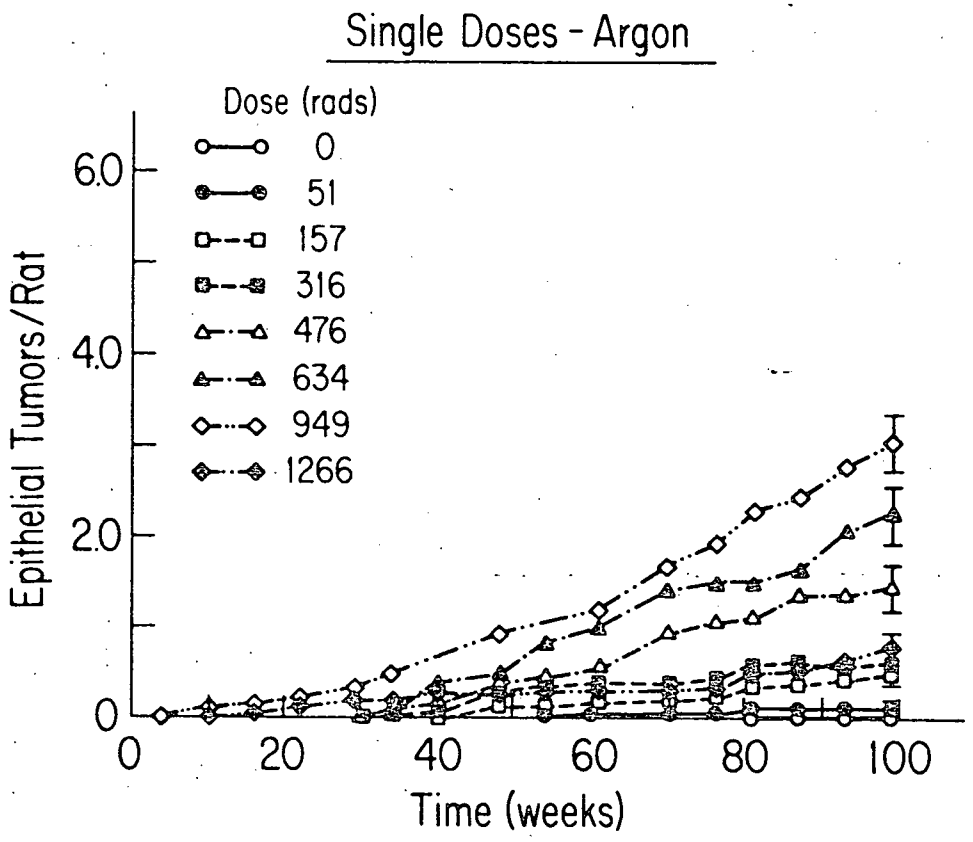

Figure 48. Epithelial tumors in rat skin irradiated with various single doses of argon ions as indicated. There were 20 rats per group except at 51 and 157 rads where there were 60 rats per group. Time zero was the day of irradiation.

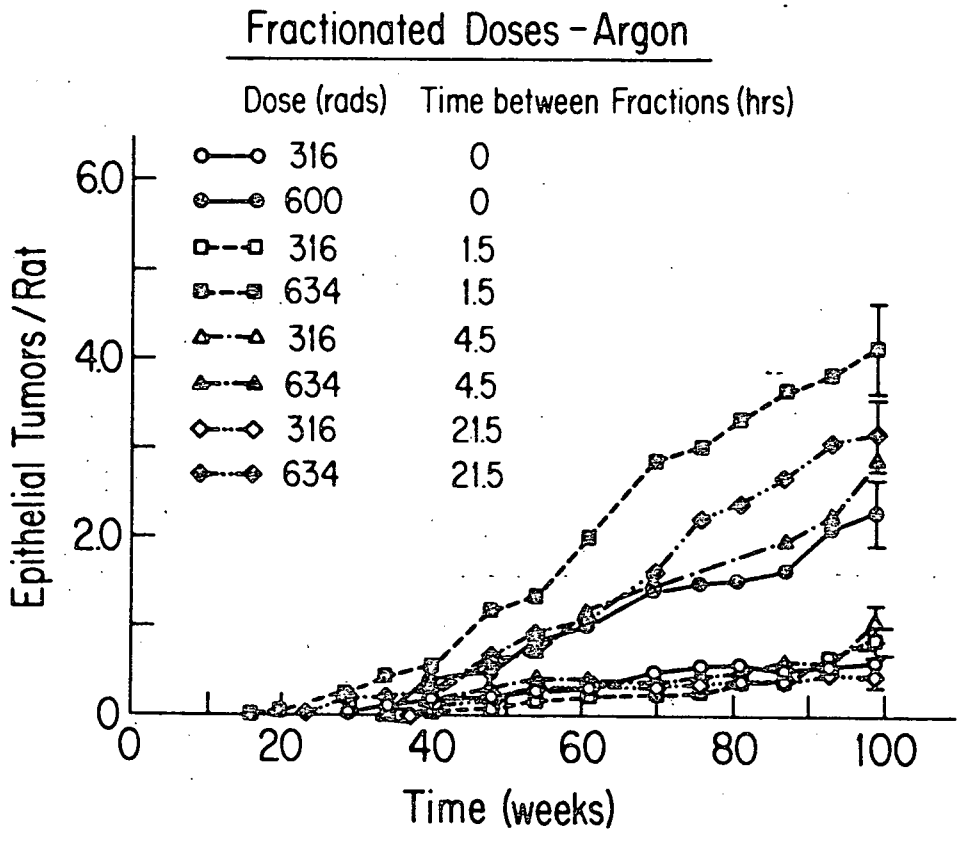

Figure 49. Epithelial tumors in rat skin irradiated with one dose or two equal doses split by various periods of time as indicated. Time zero was the day of irradiation and there were 20 rats per dose group.

increase in tumor yield, especially at 1.5 hrs. The meaning of this slight increase in tumor yield is not clear.

The dose response for all epithelial tumors at 49 weeks is shown in Figure 50. The tumor yield was

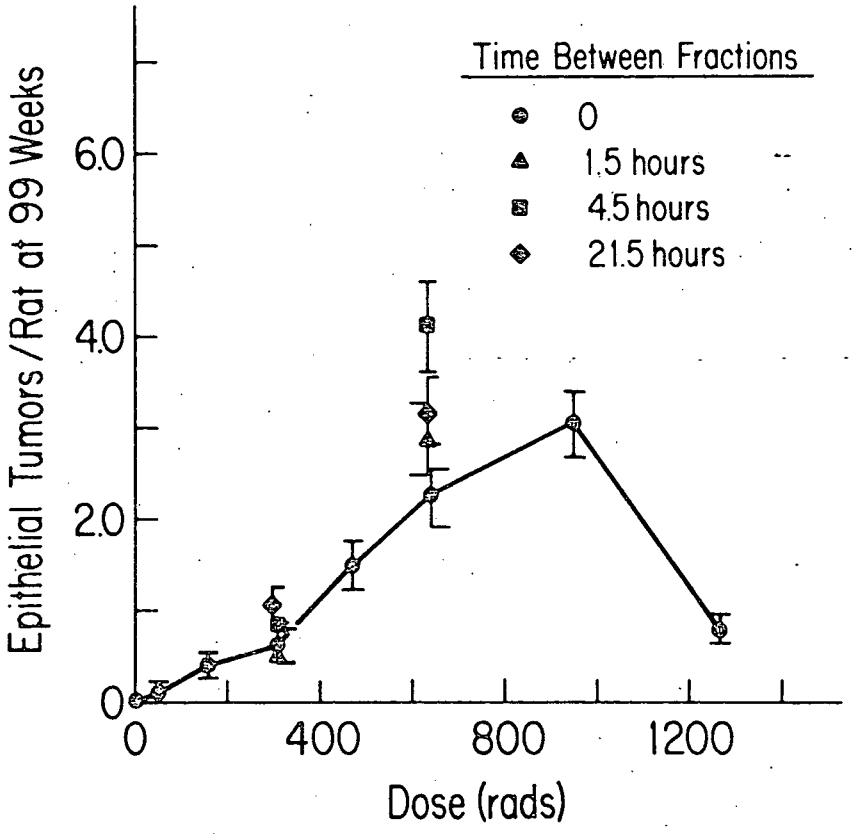

Figure 50. The dose response at 99 weeks for epithelial skin tumors induced by one dose or two equal dose of argon ions as indicated. The error bars are standard deviations derived from the square root of the total number of tumors in each treatment group.

essentially linear with dose throughout the range up to about 1000 rads. In no instance were the fractionated exposures less oncogenic than corresponding single exposures, and in several cases fractionation actually enhanced the tumor yield slightly at the higher dose. No enhancement was observed at the lower dose which raises a question about its validity at the higher dose. Not even a suggestion of recovery or repair is apparent in these data.

When the epithelial tumors were classified into various subtypes, the overall pattern for each was about the same as for the epithelial tumors as a whole (Figure 51). There seems to be a departure from linearity at low doses for the miscellaneous category, but the yield of tumors in this category was comparatively small and statistical variability was correspondingly large. No evidence for recovery or repair was found in any of the subtypes.

Comparatively large numbers of connective tissue were found in the present experiment probably because the straight through irradiation technique meant that a greater proportion of the dermal cells were irradiated than in earlier experiments with electrons where the penetration was limited. The dose response for fibromas (benign connective tissue tumors) is shown in Figure 52. The curve appears to be linear at lower doses, although the maximum tumor yield occurs at a considerably

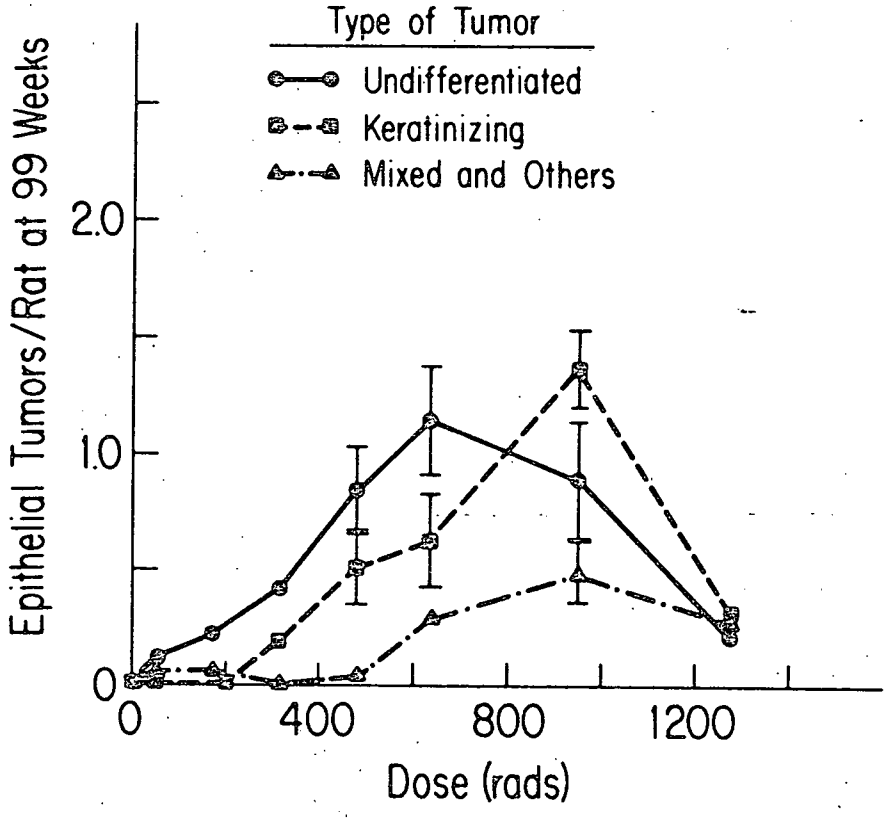

Figure 51. The dose-response at 99 weeks for various types of epithelial skin tumors induced by single doses of argon ions as indicated. Error bars are standard deviations based on the square root of the total number of tumors in each treatment group.

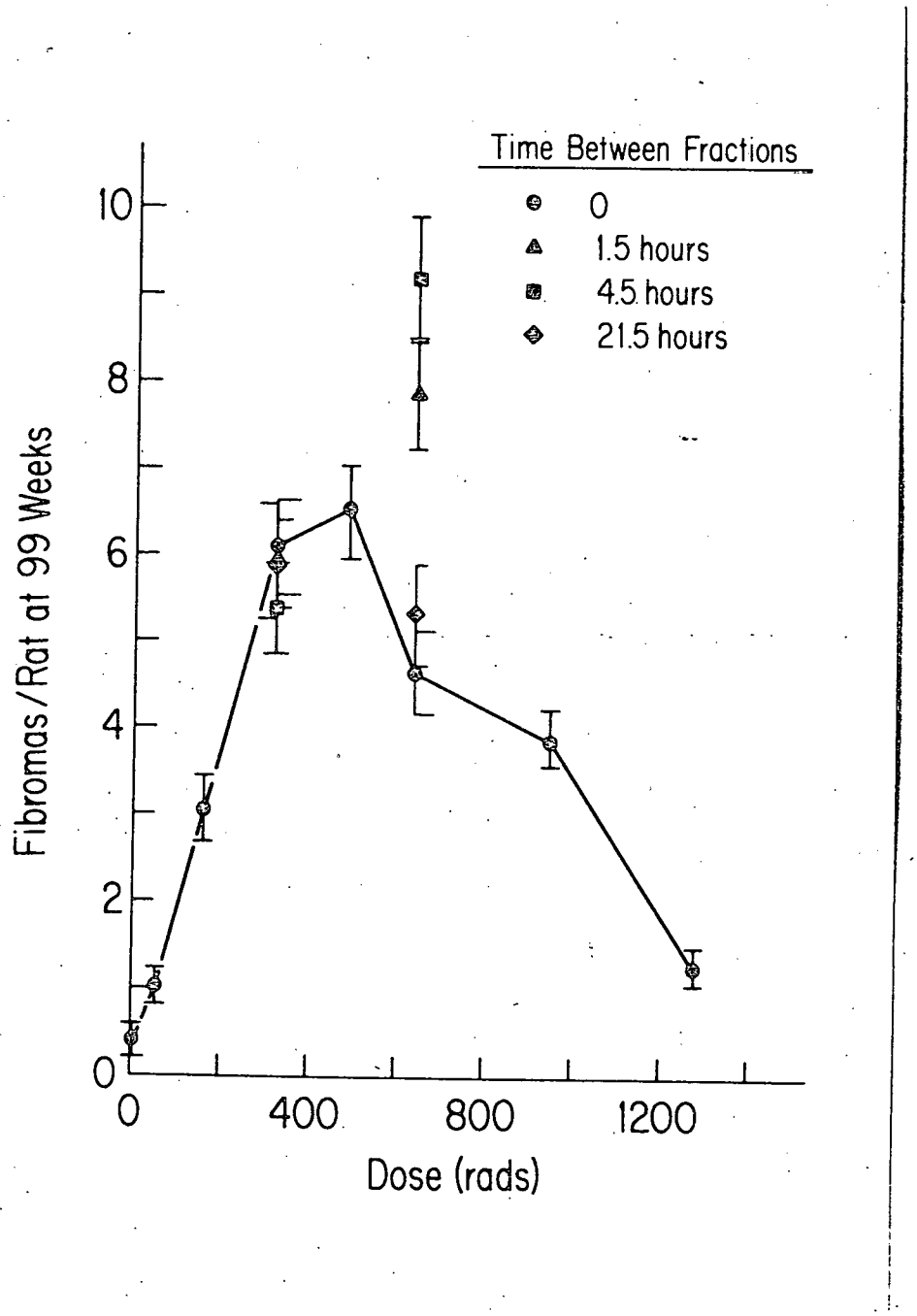

Figure 52. The dose response at 99 weeks for fibromas induced by one or two equal doses of argon ions as indicated. Error bars are standard deviations based on the square root of the total number of tumors in each treatment group.

lower dose than the peak for epithelial tumors. The fractionated doses showed no evidence for recovery or repair.. There was enhancement of the fibroma yield for fractionation intervals of 1.5 and 4.5 hrs. but not for 21.5 hrs. The fibromas were the most numerous type of tumor in the middle dose regions.

Sarcomas were seen more frequently than in previous experiments with elecrrons. The sarcoma data is shown in Figure 53. The error bars are comparatively large but the data are consistent with a linear dependence of tumor yield on dose and no evidence of repair or split dose recovery.

Tumor induction in rat skin by argon ions is strikingly similar in dose response and amount of recovery to cell lethality produced in tissue culture by the same radiation beam. It is intriguing that for yet another endpoint high LET radiation produces an effect that is approximately linear with dose and from which the tissue is unable to recover. There may have been a slight enhancement in the yield of tumors but this remains to be confirmed.

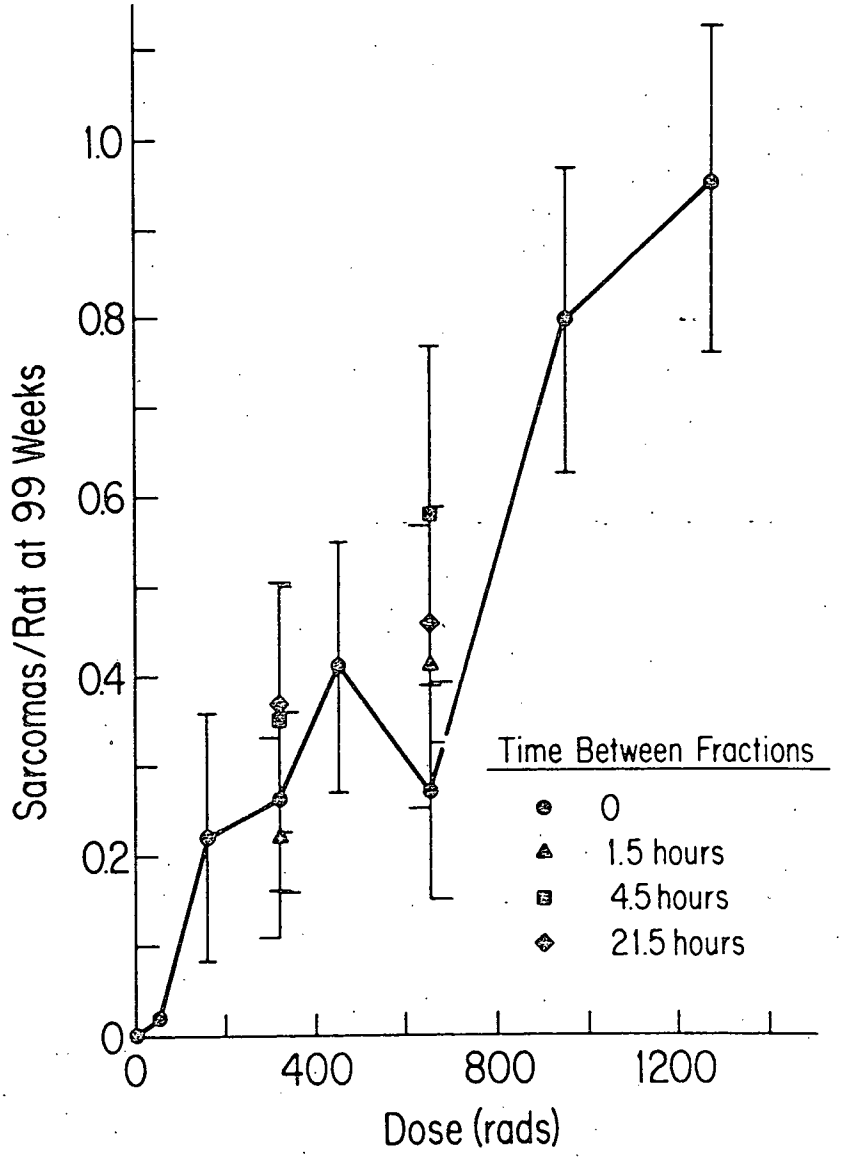

Figure 53. The dose response at 99 weeks for sarcomas induced in rat skin by one or two equal doses of argon ions as indicated. The error bars are standard deviations based on the square root of the total number of tumors.

Sensitization of Skin to Tumor Induction

The presence of 5-bromodeoxyuridine (BUdR) in DNA sensitizes cells to ionizing radiation and ultraviolet light (84, 85, 86). Sensitization has been measured as increased cellular lethality (87), DNA strand breaks (88) and chromosomal aberrations and transformation (89). Most such experiments have been carried out on cells in tissue culture and we initiated some preliminary experiments to determine the most favorable conditions for incorporating sufficient quantities of BUdR into epidermal DNA of the rat in order to produce measurable sensitization. In these experiments the effect of BUdR incorporation on DNA strand breaks induced by electron radiation was determined.

Male CD rats, 28 days of age, were given a single intraperitoneal injection of ^{3}H-thymidine in order to label the DNA. Thirty minutes after the ^{3}H-thymidine injection, half the animals were given 1.2 mg of BUdR intraperitoneally. The injections were given every 30 min. thereafter for 4 hrs., resulting in a total dose of 96 mg/animal. This dose regimen has been shown in previous studies to result in approximately 2% BUdR incorporation. In order to examine the combined effects of ionizing radiation and BUdR on cells in the S phase, animals were irradiated 30 min. after the final BUdR injection. The replicative phase of rat epidermal cells is approximately

65 hrs. long, therefore, in order to examine cells in the G_1 phase, animals were irradiated 48 hrs. after the ^3H-thymidine and BUdR treatment. Animals were irradiated with 1200 rads of 0.7 Mev electrons at a dose rate of 600 rads/min., in order to introduce breaks into the DNA. The DNA strand breaks were measured by using the alkaline unwinding assay of Rydberg.

Figures 54 and 55 show semilog plots of the fraction of double strand DNA (F) as a function of time of alkali treatment. Figure 54 shows F versus time for cells irradiated in the G_1 phase of the cell cycle and Figure 55 for cells irradiated in the S phase. The slopes of the unwinding curves were determined by a least squares fit and are proportional to the number of DNA strand breaks. G_1 phase DNA unwound very little in 2 hrs. of alkali treatment in comparison to DNA of G_1 phase cells irradiated with 1200 rads of electrons or treated with BUdR. The combined treatment of BUdR and 1200 rads of electrons produced an enhanced DNA unwinding rate in comparison to 1200 rads of electrons alone. However, when irradiation occurred in S phase BUdR did not produce a significantly greater rate of DNA unwinding than in the corresponding control or irradiated group (Figure 55).

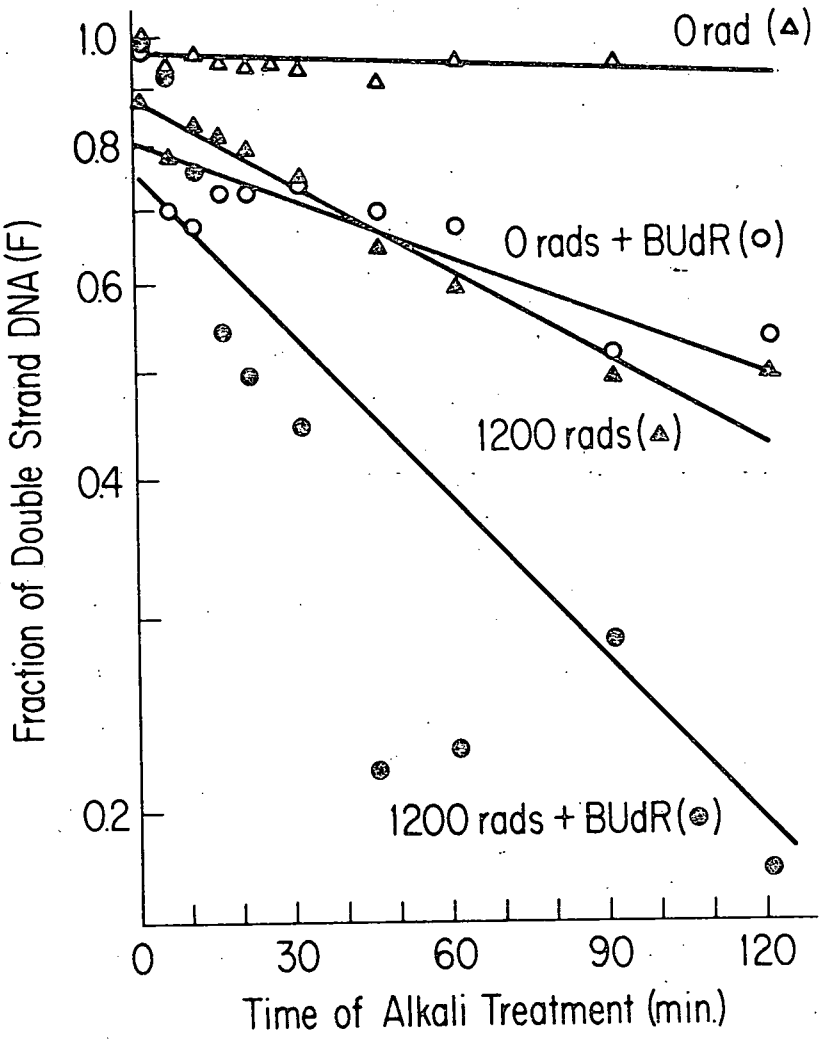

Figure 54. Log-linear plot of fraction of double strand DNA (F) versus time of alkali weight as a function of BUdR substitution and electron dose. The ^{3}H-thymidine labelled cells are in the G_1 phase of the cell cycle at time of irradiation.

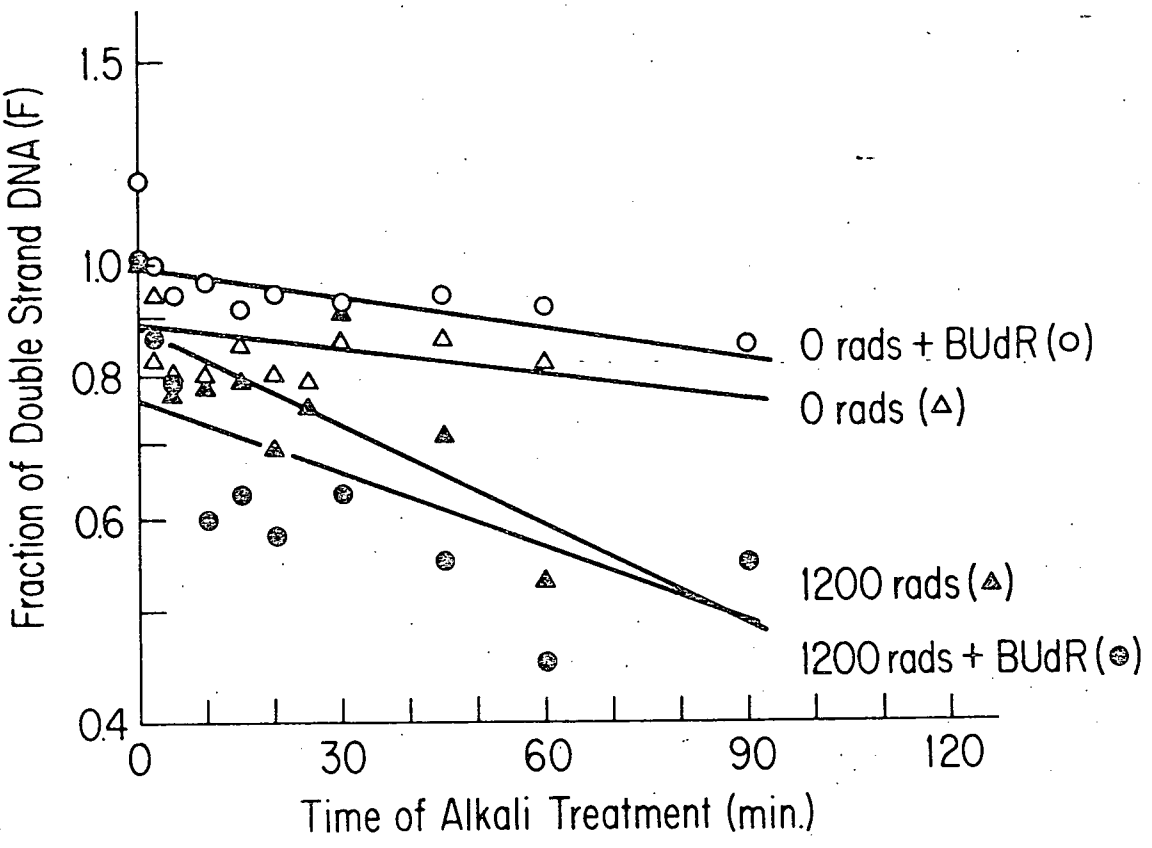

Figure 55. Log-linear plot of fraction of double strand DNA (F) versus time of alkali weight as a function of BUdR substitution and electron. The ^{3}H-thymidine labelled cells are in the S phase of the cell cycle at the time of irradiation.

References

1. Albert, R. E. W. Newman and B. Altshuler. The Dose Response Relationships of Beta-Ray Induced Skin Tumors in the Rat. Radiation. Res. 15:410, (1961).

2. Albert, R. E., F. J. Burns and R. D. Heimbach. Skin Damage and Tumor Formation from Grid and Sieve Patterns of Electron and Beta Radiation in the Rat. Radiat. Res. 30:525-540, (1967).

3. Albert, R. E., F. J. Burns and R. D. Heimbach. The Effect of Penetration Depth of Electron Radiation on Skin Tumor Formation in the Rat. Radiat. Res. 30:515-524, (1967).

4. Albert, R. E. and F. J. Burns. Tumor and Injury Responses of Rat Skin After Sieve Pattern X-Irradiation. Radiat. Res. 67:142-148, (1976).

5. Burns, F. J., R. E. Albert, I. P. Sinclair and P. Bennett. The Effect of Fractionation on Tumor Induction and Hair Follicle Damage in Rat Skin. Radiat. Res. 53:235-240, (1973).

6. Burns, F. J., R. E. Albert and I. P. Sinclair. The Effect of a 24-Hour Fractionation Interval on the Induction of Rat Skin Tumors by Electron Radiation. Radiat. Res. 62:478-487, (1975).

7. Burns, F. J., R. E. Albert and R. D. Heimbach. The RBE for Skin Tumors and Hair Follicle Damage in the Rat Following Irradiation with Alpha Particles and Electrons. Radiat. Res. 36:225-241, (1968).

8. Burns, F. J., R. E. Albert, M. Vanderlaan and P. Strickland. The Dose-Response Curve for Tumor Induction with Single and Split Doses of 10 Mev Protons. Radiat. Res. 62:598, (1975).

9. Burns, F. J., R. E. Albert, P. Bennett and I. P. Sinclair. Tumor Incidence in Rat Skin Following Proton Irradiation in a Sieve Pattern. Radiat. Res. 50:181-190, (1972).

10. Albert, R. E., F. J. Burns and P. Bennett. Radiation-Induced Hair Follicle Damage and Tumor Formation in Mouse and Rat Skin. J. Natl. Cancer Inst. 49:1131-1137, (1972)

11. Albert, R. E., F. J. Burns and R. D. Heimbach. The Association between Chronic Radiation Damage of the Hair Follicles and Tumor Formation in the Rat. Radiat. Res. 30:590-599, (1967).

12. Vanderlaan, M., F. J. Burns and R. E. Albert. A Model Describing the Effects of Dose and Dose Rate on Tumor Induction by Radiation in Rat Skin. Conference Report--Presented to International Atomic Energy Agency (IAEA), November, 1975.

13. Burns, F. J. and M. Vanderlaan. Split Dose Recovery for Radiation Induced Tumors in Rat Skin. Inter. J. Radiat. Biol. 32(2):135-144, (1977).

14. Burns, F. J., I. P. Sinclair, R. E. Albert and M. Vanderlaan. Tumor Induction and Hair Follicle Damage for Different Electron Penetrations in Rat Skin. Radiat. Res. 67:474-481, (1976).

15. Laird, A. K. Dynamics of Tumor Growth: Comparison of Growth Rates and Extrapolation of Growth Curve to One Cell. Brit. J. Cancer 19:278-291, (1965).

16. Simpson-Herren, L. and H. H. Lloyd. Kinetic Parameters and Growth Curves for Experimental Tumor Systems. Cancer Chemotherapy Reports Part I 54/3:143-174, (1970)

17. McCredie, J. A., W. R. Inch and J. Kruuv and T. A. Watson. The Rate of Tumor Growth in Animals. Growth 29:331-347, (1965).

18. Ishimaru, T., T. Heshino, M. Ichimaru, et. al. Leukemia in Atomic Bomb Survivors, Hiroshima and Nagasaki. Radiat. Res. 45:216-233, (1971).

19. Jablou, S., K. Tachikawa, J. Belsky, et al. Cancer in Japanese Exposed as Children to Atomic Bombs. Lancet 1:927-932, (1971).

20. Lindop, P. J. and G. A. Sacher (eds.). Radiation and Ageing. Taylor and Francis, Ltd., London, 1966.

21. Upton, A. C., T. T. Odell and E. P. Sniffen. Influence of Age at Time of Irradiation on Induction of Leukemia and Ovarian Tumors in RF Mice. Proc. Exp. Biol. Med. 104:769-772, (1960).

22. Toth, B., H. Rappaport and P. Shubik. Influence of Dose and Age on the Induction of Malignant Lymphomas and Other Tumors by 7,12Dimethlybenz(a)anthracene in Swiss Mice. JNCI 30:723-737, (1963).

23. Heranze, D. R., M. Gruenstein and M. B. Shimkin. Effect of Age and Sex on the Development of Neoplasms in Wistar Rats Receiving a Single Intragastric Instillation of 7,12 Dimethylbenz(a)anthracene. Int. J. Cancer 4:480-486, (1969).

24. Whitmire, C. E., R. A. Salerno, V. A. Merold and L. S. Robstein. Effect of Age at Treatment and Dose of 3-Methyl-cholanthracene on Development of Leukemia and Sarcoma in AKR Mice. JNCI 49:1411-1415, (1972).

25. Ebbesen, P. Papilloma Induction in Different Aged Skin Grafts to Young Recipients. Nature 241:280-281, (1973).

26. Ebbesen, P. Aging Increases Susceptibility of Mouse Skin to DMBA Carcinogenesis Independent of General Immune Status. Science 183:217-218, (1974).

27. Ebbesen, P. Effect of Age of Non-Skin Tissues on Susceptibility of Skin Grafts to 7,12Dimethylbenz(a)anthracene (DMBA) Carcinogenesis in BALB/c Mice, and the Effect of Age of Skin Graft on Susceptibility of Surrounding Skin to DMBA. JNCI 58:1057-1060, (1977).

28. Van Duuren, B. L., A. Sivak, C. Katz, I. Seidman and S. Melchionne. The Effect of Aging and Interval Between Primary and Secondary Treatment in Two-Stage Carcinogenesis on Mouse Skin. Cancer Res. 35:502-505, (1975).

29. Condry, E. V. and V. Suntzeff. Influence of Age on Epidermal Carcinogenesis Induced by Methylcholanthrene in Mice. Yale J. Biol. Med. 17:47-58, (1944).

30. Peto, R., F. J. C. Roe, P. N. Lee, L. Levy and J. Clack. Cancer and Ageing in Mice and Men. Br. J. Cancer 32:411-416, (1975).

31. Adelman, R. C. Impaired Hormonal Regulation of Enzyme Activity During Aging. Fed. Proc. 34:179-182, (1975).

32. Albert, R. E., M. E. Phillips, P. Bennett, F. Burns and R. Heimbach. The Morphology and Growth Characteristics of Radiation Induced Epithelial Skin Tumors in the Rat. Cancer Res. 29:658--68, (1969).

33. Orentreich, N. and V. J. Selmanowitz. Levels of Biological Functions with Aging. Trans. N.Y. Acad. Sci. Series # 31:992-1012, (1969)

34. Blum, H. F. Carcinogenesis by Ultraviolet Light. Princeton University Press, Princeton, N. J., 1959.

35. Epstein, J. H. In: Photophysiology, Vol. 5. (A. C. Giese, Ed.), Academic Press, N. Y., 1970, pg. 235.

36. Kelner, A. and E. B. Taft. Cancer Res. 16:860-866, (1965).

37. Winkelmann, R. K., E. J. Baldes and P. E. Zollman. J. Invest. Dermatol. 34:131-138.

38. Epstein, J. H. and W. L. Epstein. J. Invest. Derm. 41:463-473, (1963).

39. Epstein, J. H. W. L. Epstein and T. Nakai. J. Natl. Cancer Inst. 38:19-20, (1967).

40. Epstein, J. H. In: Advances in Biology of Skin, Vol. VII: Carcinogenesis. (W. Montagna and R. L. Dobson, Eds.), Chapter 13, Pergamon Press, N. Y., 1966.

41. Pound, S. W. Induced Cell Proliferation and the Initiation of Skin Tumor Formation in Mice by UV Light. Path. 2:269-275, (1970).

42. Findlay, G. M. Cutaneous Papillomata in Rat Following Exposure to UV Light. Lancet 2:1229, (1930).

43. Hsu, J., P. D. Forbes, L. C. Harber and E. Lakow. Induction of Skin Tumors in Hairless Mice by a Single Exposure to UV Radiation. Photochem. Photobiol. 21(3):185-188, (1975).

44. Marrs, J. M. and J. J. Voorhees. A Method for Bioassay of an Epidermal Chalone-Like Inhibitor. J. Invest. Derm. 56:174-181, (1971).

45. Smith, K. C. Physical and Chemical Changes Induced in Nucleic Acids by UVL. Radiat. Res. Suppl. 6:54, (1966).

46. Setlow, R. B. and R. W. Hart. Direct Evidence That Damaged DNA Results in Neoplastic Transformation. In: Radiation Research: Biomedical, Chemical and Physical Perspectives. (O. F. Nygaard, H. I. Adler and W. K. Sinclair, Eds.), Academic Press, New York, 1975, pg. 879.

79. Kellerer, A. M. and H. H. Rossi. The Theory of Dual Radiation Action. Curr. Top. Radiat. Res. Q. 8:85-158, (1972).

80. Burns, F. J. and M. Vanderlaan. Split Dose Recovery for Radiation Induced Tumors in Rat Skin. Internat. J. Radiat. Biol. 32:135-144, (1977).

81. Albert, R. E. and A. R. Omran. Follow-up Study of Patients Treated by X-Ray Epilation for Tinea Capitis. Arch. Environ. Health 17:899, (1968).

82. Albert, R. E. and F. J. Burns. Tumor and Injury Responses of Rat Skin After Sieve Pattern X-Irradiation. Radiat. Res. 67:142, (1976).

83. Schulz, R. J. and R. E. Albert. Dose to Organs of the Head from the X-Ray Treatment of Tinea Capitis. Arch. Environ. Health 17:935, (1968).

84. Cleaver, J. E. Repair Replication and Degradation of Bromouracil-Substituted DNA in Mammalian Cells After Irradiation with Ultraviolet Light. Biophys. J. 8:775-791, (1968).

85. Puck, T. T. and F. Kae. Genetics of Somatic Mammalian Cells. V. Treatment with 5-Bromodeoxyuridine and Visible Light for Isolation of Nutritionally Deficient Mutants. Proc. Natl. Acad. Sci. 58:1227-1233, (1967).

86. Shipley, W. W., M. M. Elkind and W. B. Prather. Potentiation of X-Ray Killing by 5-Bromodeoxyuridine in Chinese Hamster Cells: A Reduction in Capacity for Sublethal Damage Accumulation. Radiat. Res. 47:437-449, (1971).

87. Dewey, W. C., L. E. Stone, H. H. Miller and R. E. Giblak. Radiosensitization with 5-Bromodeoxyuridine of Chinese Hamster Cells X-Irradiated During Different Phases of the Cell Cycle. Radiat. Res. 47:672-688, (1971).

88. Shipley, W. U. and M. M. Elkind. DNA Damage and Repair Following Irradiation: The Effect of 5-Bromodeoxyuridine in Cultured Chinese Hamster Cells. Radiat. Res. 48:86-94, (1971).

89. Barrett, J. C., T. Tsutsui and P. O. P. Ts'o. Neoplastic Transformation Induced by a Direct Perturbation of DNA. Nature 274:229-232, (1978).

47. Cleaver, J. E. Xeroderma Pigmentosum: Variants with Normal DNA Repair and Normal Sensitivity to UV Light. J. Invest. Dermatol. 58:124, (1972).

48. Albert, R. E., F. J. Burns and P. Bennett. Radiation-Induced Hair Follicle Damage and Tumor Formation in Mouse and Rat Skin. JNCI 49:1131, (1972).

49. Everett, M. A., E. Yeargers, R. M. Sayre and R. L. Olson. Penetration of Epidermis by Ultraviolet Rays. Photochem. Photobiol. 5:533, (1966).

50. Pathak, M. A., D. M. Kramer and U. Gungerich. Formation of Thymine Dimers in Mammalian Skin by UVR in vivo. Photochem. Photobiol. 15:177, (1972).

51. Freedberg, I. M. and H. P. Baden. Studies of Epidermal Protein Metabolism. J. Invest. Dermatol. 39:339, (1962).

52. Marmour, J., W. F. Anderson, L. Matthews, K. Berns, E. Gajewska, D. Lane and P. Doty. The Effects of UVL on the Biological and Physical Chemical Properties of DNA. J. Cell Comp. Physiol. 58(Suppl. 1):33, (1961).

53. Brown, R. D. and C. E. Holt. Rapid Separation of Thymine Dimers and Pyrimidines on Ion-Exchange Paper. Anal. Biochem. 20:358, (1967).

54. Kittler, L. and G. Lober. Photochemistry of the Nucleic Acids. Photochem. Photobiol. Revs. 2:39, (1977).

55. Smith, K. C. Dose-Dependent Decreases in Extractability of DNA from Bacteria Following Irradiation with UVL or with Visible Light Plus Dye. Biochem. Biophys. Res. Comm. 8:157, (1962).

56. Ley, R. D., D. D. Grube and R. J. M. Fry. Photosensitizing Effects of 8-Methoxypsoralen on the Skin of Hairless Mice. Photochem. Photobiol. 25:265, (1977).

57. Elkind, M. M., A. Han and C. Chang-Liu. Sunlight Induced Mammalian Cell Killing. Photochem. Photobiol. (In press, 1978).

58. Rauth, A. M. Effects of UV Light on Mammalian Cells in Culture. Current Topics in Radiat. Res. 6:195, (1970).

59. Webb, R. B. Lethal and Mutagenic Effects of Near-UV Radiation. Photochem. Photobiol. Revs. 2:169, (1977).

60. Cooke, A. and B. E. Johnson. Dose Response, Wavelength Dependence and Rate of Excision of Ultraviolet Radiation Induced Pyrimidine Dimers in Mouse Skin DNA. Biochim. Biophys. Acta 517:24, (1978).

61. Chadwick, K. H. and H. P. Leenhouts. A Molecular Theory of Cell Survival. Phys. Med. Biol. 18:78-87, (1973).

62. Ormerod, M. G. Radiation-Induced Strand Breaks in the DNA of Mammalian Cells. In: Biology of Radiation Carcinogenesis. (J. M. Yuhas, R. W. Tennant and J. D. Regan, Eds.), Raven Press, New York, 1976, pp. 67-92.

63. Rydberg, B. The Rate of Strand Separation in Alkali of DNA of Irradiated Mammalian Cells. Radiat. Res. 61:274-282, (1975).

64. Sheridan, R. B. and P. C. Huang. Single Strand Breakage and Repair in Eukaryotic DNA as Assayed by S_1 Nuclease. Nucl. Acids Res. 4:301-348, (1977).

65. Rydberg, B. and K. J. Johanson. Radiation-Induced DNA Strand Breaks and Their Rejoining in Crypt and Villous Cells of the Small Intestine of the Mouse. Radiat. Res. 64:281-292, (1975).

66. Gutin, P. H., J. Hilton, V. J. Fein, A. E. Allen and M. D. Walker. S_1 Nuclease from Aspergillus Oryzae for the Detection of DNA Damage and Repair in the Gamma Irradiated Intracerebral Rat Gliosarcoma 9L. Radiat. Res. 72:100-106, (1977).

67. Teoule, R. and J. Cadet. Radiation-Induced Degradation of the Base Component in DNA and Related Substances-Final Products. In: Effects of Ionizing Radiation on DNA. (J. Huttermann, W. Kohnlein and R. Teoule, Eds.), Springer-Verlag, Berlin, 1978, pp. 171-202.

68. Albert, R. E., F. J. Burns and R. D. Heimbach. The Effect of Penetration Depth of Electron Radiation on Skin Tumor Formation in the Rat. Radiat. Res. 30:515-524, (1967).

69. Albert, R. E., F. J. Burns and R. D. Heimbach. The Association Between Chronic Radiation Damage of the Hair Follicles and Tumor Formation in the Rat. Radiat. Res. 30:590-599, (1967).

70. Burns, F. J., R. E. Albert, I. P. Sinclair and M. Vanderlaan. The Effect of a 24-Hour Fractionation Interval on the Induction of Rat Skin Tumors by Electron Radiation. Radiat. Res. 62:478-487, (1975).

71. Shore, R. E., R. E. Albert and B. Pasternack. Follow-up Study of Patients Treated by X-ray Epilation for Tinea Capitis: Resurvey of Post Treatment Illness and Mortality Experience. Arch. Environ. Health 31:17, (1976).

72. Hoshino, H. and H. Tanooka. Interval Effect of β-Irradiation and Subsequent 4-Nitroquinoline-1-oxide Painting on Skin Tumor Induction in Mice. Cancer Res. 35:3663, (1975).

73. Beebe, G. W., H. Kato and C. D. Land. JNIH-ABCC Life-Span Study, Hiroshima-Nagasaki. Report 5: Mortality and Radiation Dose, October 1950-September 1966. ABCC-TR 11-70, (1970).

74. Court Brown, W. M. and R. Doll. Mortality from Cancer and Other Causes After Radiotherapy for Ankylosing Spondylitis. Brit. Med. J. ii:1327-1332, (1965).

75. Report of the United Nations Scientific Committee on the Effects of Atomic Radiation. (1972). Ionizing Radiation: Levels and Effects.

76. Elkind, M. M. and G. F. Whitmore. The Radiobiology of Cultured Mammalian Cells. Gordon and Breach, Inc., New York, 1967.

77. Upton, A. E., M. L. Randolph and J. W. Conklin. Late Effects of Fast Neutrons and γ-Rays in Mice as Influenced by the Dose Rate of Irradiation: Induction of Neoplasia. Radiat. Res. 41:467-491., (1970).

78. Yuhas, J. M. Recovery from Radiation-Carcinogenic Injury to the Mouse Ovary. Radiat. Res. 60:321-332, (1974).